



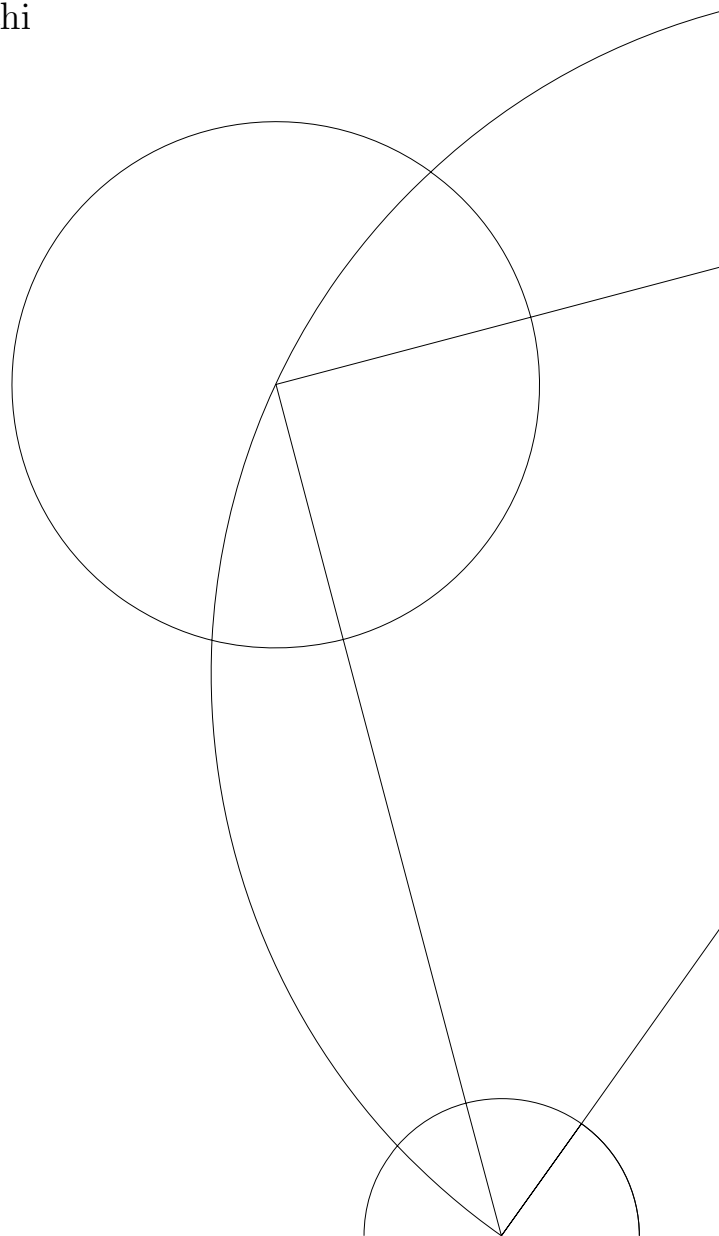
Master's thesis
Electro-mechanical properties of lipid
membranes at their phase transition

Karis Amata Zecchi

Supervisor:
Thomas Heimburg

Niels Bohr Institute
University of Copenhagen

Submitted: May 31, 2013



Abstract

Lipid membranes in physiological conditions sustain significant transmembrane voltages. The effect of such voltages on the thermodynamical properties of the system, however, is not fully understood. Furthermore, couplings between the electrical and mechanical properties of lipid bilayers have been observed and well documented in literature. Both these properties are known to undergo significant changes in the lipid melting. In this thesis, the effect of the lipid phase transition on the electro-mechanical properties of the system is analysed theoretically, with a special focus on the coupling between the membrane curvature and the electric polarization, phenomenon known as *flexoelectricity*. The effect of flexoelectricity on the melting properties of the membrane is also analysed.

Curved membranes are here shown to display transmembrane potentials that depend on the geometry of the system. This offset potential can induce asymmetry in the electrical properties of the membranes. This asymmetry has been investigated in the experimental part of the thesis through experiments on membrane patches formed using a new instrument. It is also proposed how electrical measurement on lipid patches can be interpreted in the light of the theoretical predictions, and how further experiments can be performed to test the predictions.

Finally, a simple experimental method to measure the temperature dependence of the relative permittivity of lipid membranes is here proposed. It can, in principle, give important information, that together with the theoretical considerations made in the first part of the thesis, could allow for a better understanding of the dielectric properties of lipid membranes at the phase transition.

Dansk Resumé

Ved fysiologiske betingelser er der fundet betydelige spændingsforskelle hen over cellers lipidmembraner. Denne spændingsforskel påvirker de lipidmembranernes termodynamiske egenskaber, men effekten er ikke fuldt ud forstået. Det er veldokumenteret at lipidmembraners elektriske og mekaniske egenskaber er koblet. Når membraner smelter ændres både elektriske og mekaniske egenskaber drastisk. I dette speciale beskrives faseovergangens på lipidmembranernes mekaniske og elektriske egenskaber. Effekten er analyseret teoretisk med fokus på koblingen mellem krumning af membraner og elektrisk polarisering, et fænomen kaldet flexoelektricitet. Effekten af flexoelektricitet på lipidfaseovergangen er også blevet analyseret.

Det er påvises at membranens krumning skaber en elektrisk spænding over membraner, som kaldes "afsætspændingen". Afsætspændingen forårsager asymmetri i membranens elektriske egenskaber. Denne asymmetri er blevet undersøgt i den eksperimentelle del af specialet, på lipidmembranpatches, som er blevet lavet ved hjælp af en ny teknik. I specialet foreslås det yderligere, hvordan elektriske målinger på membranpatches kan blive analyseret ud fra de teoretiske forudsigelser, og hvordan yderligere eksperimenter kan blive udføres for at teste disse forudsigelser.

Endelig foreslås en eksperimentel metode til at måle temperatur afhængigheden af lipid membraners relative permittivitet . Dette kan give vigtig information vedrørende de termodynamiske overvejelser beskrevet i den første del af specialet, hvilket kan udvide forståelsen af de dielektriske egenskaber af lipidmembraner vedrørende lipidfaseovergangen.

Contents

| | | |
|----------|--|-----------|
| 1 | Introduction | 1 |
| 1.1 | Motivation | 1 |
| 1.2 | Biological Membranes | 2 |
| 1.2.1 | Phospholipids | 3 |
| 1.2.2 | Lipid bilayers | 5 |
| 1.3 | Equivalent circuit of membranes | 6 |
| 1.4 | Outline | 8 |
| 2 | Background Theory | 9 |
| 2.1 | Thermodynamics of lipid membranes | 9 |
| 2.1.1 | Phase transition in lipid membranes | 13 |
| 2.2 | Electrical properties | 23 |
| 2.2.1 | Membrane capacitance | 23 |
| 2.2.2 | Polarization | 34 |
| | Flexoelectricity | 37 |
| 2.3 | Permeability | 45 |
| 2.3.1 | Protein ion channels | 45 |
| 2.3.2 | Lipid ion channels | 47 |
| 3 | Materials and Methods | 53 |
| 3.1 | Materials | 53 |
| 3.1.1 | Sample preparation | 54 |
| 3.2 | Methods | 55 |
| 3.2.1 | Calorimetry | 56 |
| 3.2.2 | Summary of permeability experimental technique | 57 |
| 3.2.3 | Ionovation Bilayer Explorer | 60 |
| 4 | Results and Discussion | 69 |
| 4.1 | Theory | 70 |
| 4.1.1 | Dielectric effects | 71 |
| 4.1.2 | Flexoelectric effects | 78 |

| | | |
|-------|---|------------|
| 4.2 | Experiments | 88 |
| 4.2.1 | State dependence of the relative permittivity | 88 |
| 4.2.2 | Calorimetry | 91 |
| 4.2.3 | Permeability | 94 |
| 4.2.4 | Discussion | 103 |
| | Conclusions | 107 |

Chapter 1

Introduction

1.1 Motivation

Biomembranes are ubiquitous in biology. Every eukaryotic and prokaryotic cell is surrounded by a plasma membrane, which defines the cell from the surrounding environment. Furthermore, organelles (such as chloroplasts, mitochondria or the endoplasmatic reticulum) inside the cell are enclosed in biological membranes.

A number of important functions in the cell are performed by biomembranes. They provide structural organisation to the cell and to the cell compartments, securing the entrance of nutrient elements and the release of waste products [1]. In this sense they act as a selective semipermeable wall, regulating transport processes inside the cell. Furthermore, they enable communication with the environment and cell-to-cell signalling.

Most of these functions are attributed to specific proteins embedded in a lipid matrix, the latter being often considered as a mere structural support for them. Nevertheless, lipid bilayers themselves represent an extremely interesting physical system, because of their peculiar mechanical, electrical and thermodynamical properties.

In every living cell, biomembranes maintain non-equilibrium ion distributions across themselves, which create potential differences between the interior of the cell and the environment (the interior being more negative) [2]. In the case of excitable cells (like nerve tissues, or neuronal cells), transmembrane voltages reach values of the order of 100 mV [1, 3]. Such potentials are used as an energy source for the cell. In neurons, they are essential for the generation and propagation of the nerve pulse. In this respect, the lipid matrix is believed to provide electrical insulation to the cell, all the action being attributed to specific protein channels. However, a voltage of 100 mV

results in a large electric field (on the order of $10^7 V/m$) on the nanoscale of the membrane thickness. This is very unlikely to leave the lipid matrix totally unaffected.

The motivation of this thesis lies in the lack of understanding of the effects of voltage on the lipid membrane. Despite its biological relevance, the topic has received little attention by the biomembrane community, which has devoted most of its efforts in understanding the structure and function of the specific membrane proteins.

1.2 Biological Membranes

Biomembranes are macroscopic ensembles consisting mainly of lipids and proteins [4]. Lipids are organised in a double layer (with a thickness on the order of $5 - 8 nm$) where proteins are embedded.

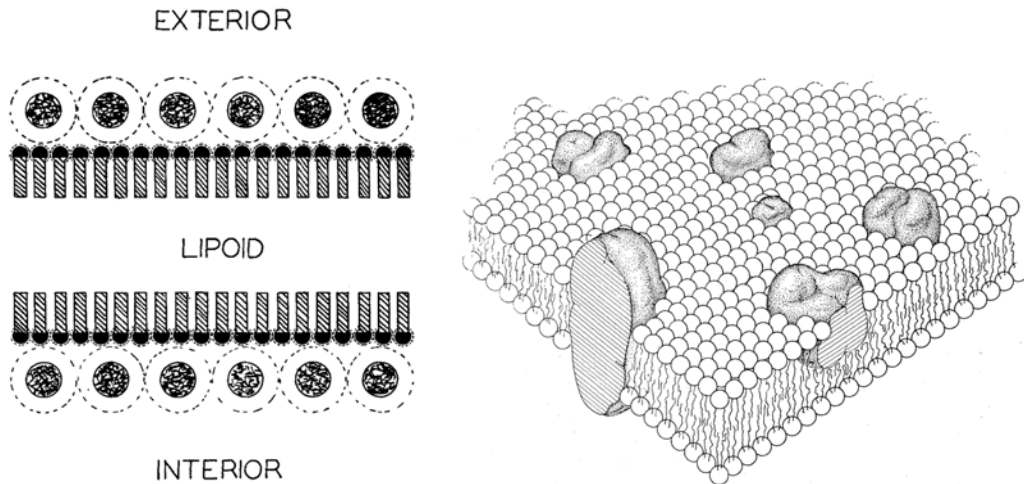


Figure 1.1: Models of biological membranes. *Left*: biomembranes according to the model of Danielli and Davson. The interior of the membrane is made of a lipid bilayer, to which a protein layer is associated (the circles, having a hydrophobic interior and a hydrophilic shell), [5]. *Right*: the fluid mosaic model proposed by Singer and Nicolson. Globular proteins (either integral or peripheral) are distributed inhomogeneously in the fluid environment provided by the lipid bilayer, [6].

The bimolecular structure of the cell membrane was first postulated in 1925 by Gorter and Grendel [7]. They found that the surface area of lipids extracted from red blood cells was double the surface area of the cell itself. They concluded that cell membranes are made of two lipid layers organised

in the form of a bilayer. Their model didn't consider the presence of proteins, which were later included by Danielli and Davson in 1935 [5] (see fig.1.1). The most accepted model of membrane structure originates from the so called *fluid mosaic model*, proposed by Singer and Nicolson in 1972 [6], and shown in fig. 1.1. In their model, the lipid bilayer is considered as a homogeneous fluid in which globular protein molecules diffuse in two dimensions. Nowadays, biomembranes are believed to be heterogeneous structures where lipids can exist in different states and form domains, and interact dynamically with the proteins (see fig. 1.2).

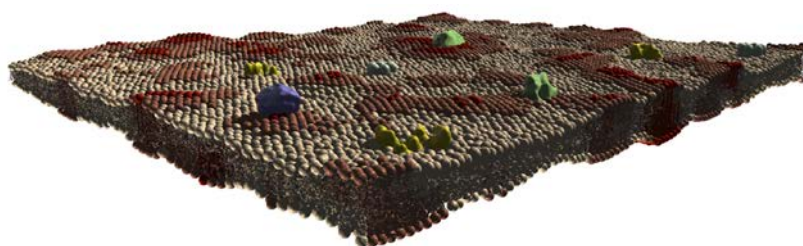


Figure 1.2: Modern view of biological membranes. Membrane proteins and lipids of different species and states are distributed inhomogeneously in the membrane plane. Picture taken from [8].

The mass (or volume) ratio between proteins and lipids varies from 0.25 to 4, the typical value being 1 [9]. This includes also the extra-membrane domains of the proteins. Thus, even in densely crowded biological membranes, the in-plane membrane area is mainly occupied by lipids [10].

Throughout this thesis, pure lipid bilayers will be considered. Being the major constituent of biomembranes, any result concerning the lipid double layer, has an immediate biological relevance.

1.2.1 Phospholipids

As mentioned before, lipids are the major constituent of biological membranes. They can be divided in three main classes: glycolipids, phospholipids and sterols. Phospholipids are the most abundant class in biomembranes [1]. The identification of the first phospholipid in biological tissues dates back to 1847, when Theodore Nicolas Gobley, a French chemist and pharmacist, isolated lecithin (phosphatidylcholine) in egg yolk. His discovery arrived after almost 130 years of investigations on the chemical composition of brain tissues [11].

Phospholipid molecules are made of three parts: a hydrophilic head group and a hydrophobic hydrocarbon tail which are connected by a backbone, most

commonly made of glycerol. Being constituted by a polar hydrophilic part and a non polar hydrophobic tail, phospholipids are amphiphilic molecules. The name phospholipid is due to the presence of a negatively charged phosphate group (PO_4) in the head group. Differences in head group and tail result in the different species of phospholipids.

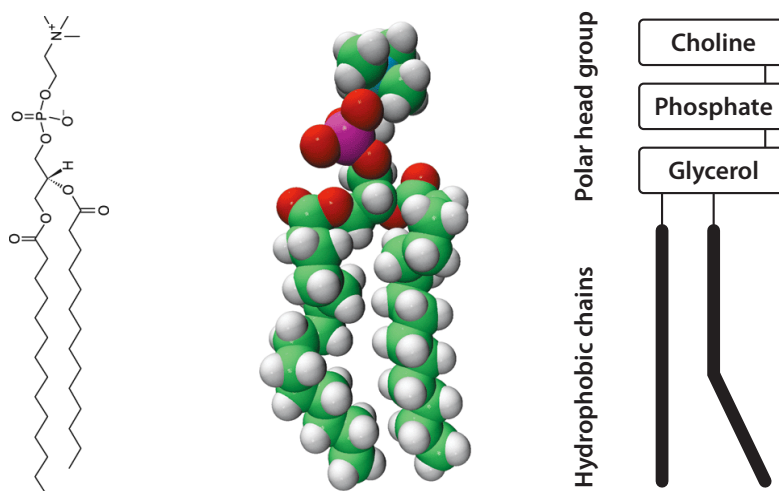


Figure 1.3: Chemical structure and schematic representation of a molecule of dimyristoyl phosphatidylcholine (DMPC), showing the hydrophilic head group and the hydrophobic tail. The picture on the right is adapted from [1]. The left and center are taken from the website of Avanti Polar [12].

Head group Head groups may differ in size, polarity and charge, depending on the organic compound that is bound to the phosphate group. The most common are choline, ethanolamine (both positively charged), serine and glycerol (both uncharged). The resulting head groups are called phosphatidylcholine (PC), phosphatidylethanolamine (PE), phosphatidylserine (PS) and phosphatidylglycerol (PG). PC and PE are zwitterionic, while PS and PG are negatively charged. There is no evidence of positively charged headgroups in biological membranes [4]. Between 10 and 20% of lipids in biomembranes are charged, but their concentration can increase up to the 40% as in the case of mitochondria [4]. The relative abundance of different head groups in biomembranes can influence their phase behaviour as well as electrical properties or their interaction with proteins or drug, being the main binding site for them.

Hydrophobic tails Hydrophobic tails are basically hydrocarbon chains which can differ in number, length and saturation. A phospholipid molecule

can have between one and three chains attached to the glycerol backbone, two being the most common case [13]. The length of the chains is determined by the number of carbons which can oscillate between 12 and 24 depending on the particular fatty acid. Saturation means the number of double bonds between the carbon atoms in the chain, and can affect the hydrocarbon chain mobility.

1.2.2 Lipid bilayers

Lipid bilayers are self assembling structures formed of lipid molecules in an aqueous environment [1].

This is not the only configuration that they assume when placed in water. Lipid polymorphism is a well documented phenomenon [14, 15]. Different structures can form depending on the packing constraints for the lipid molecules and their concentration (see fig.1.4). The common feature is that they aggregate exposing their polar heads to the water, thus shielding the hydrophobic tails which strongly repel water. This corresponds to the most energetically and entropically favoured configuration [4]. The ability of self assembling is the result of a balance between attractive forces that minimise the hydrophobic effect and repulsive (steric or electrostatic) forces between the molecules [13].

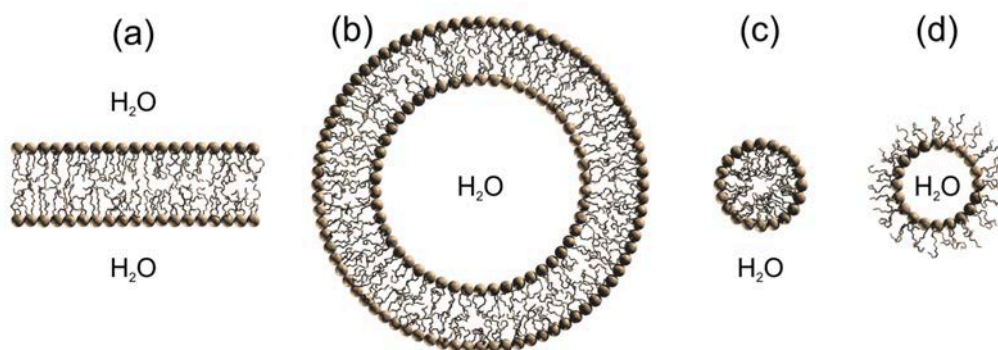


Figure 1.4: Polymorphism of lipids in aqueous environment. (a): bilayer, (b): vesicle, (c): micelle, (d): inverse micelle. Picture taken from [8]. In organic solvents, like chloroform, they are in their monomeric form (fig. 1.3).

Lipid molecules can display three types of movement inside the bilayer: rotation around their axis, lateral diffusion and flip-flop. Flip-flop is a slow uncatalyzed transbilayer movement. Transbilayer movements of lipids are energetically unfavoured, since they require the passage of the polar head

through the hydrophobic region and the consequent transient exposure of the non polar tail to the polar environment. Nevertheless, flip-flop is observed, with typical time scales between 3 and 27 hours in the case of PC. In the case of PE, instead, flip-flop is catalysed by an ATP dependent enzyme (flippase), which reduces the time scale to about 30 minutes [1].

From a structural point of view, lipid bilayers are inhomogeneous and highly anisotropic systems. This distinctive feature makes them similar to liquid crystals of smectic type. Their peculiar behaviour in solvents resemble properties of lyotropic liquid crystal. Many of their properties can indeed be understood with the aid of liquid crystal physics [1, 16]

1.3 Equivalent circuit of membranes

When studying electrical phenomena in excitable cells, the biological membrane is usually represented as an electrical circuit, like the one shown in fig. 1.5.

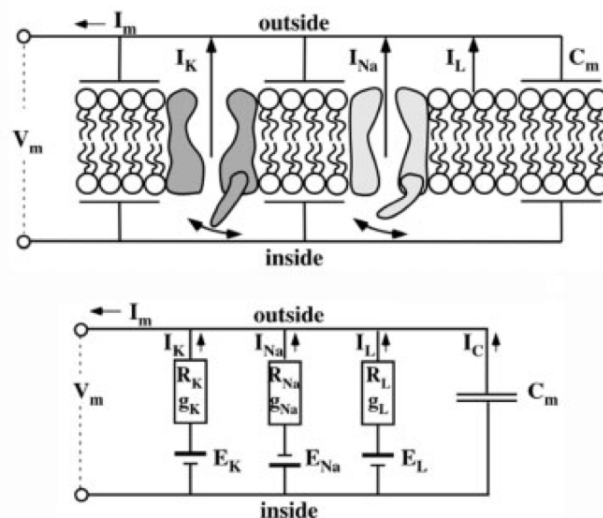


Figure 1.5: *Top*: schematic representation of the membrane. The lipid bilayer behaves as a capacitor, while the protein channels provide a passage for the ionic currents (I_K , potassium, I_{Na} , sodium and I_L , leak current). *Bottom*: from an electrical point of view, the biomembrane is believed to be equivalent to an electric circuit, where the proteins are substituted by resistors of variable conductance and the lipid bilayer by a capacitor of constant capacitance C_m . The current flowing through the membrane is a sum of the ionic and capacitive contributions. The picture is taken from [4].

Such representation was first proposed by Hodgkin and Huxley in the context of nerve pulse propagation [17]. A complete description of the mechanism of nerve pulse propagation is beyond the purposes of this thesis. However, their assumptions about the electrical behaviour of membranes, have become the most accepted model ever since. In the model, the generation and transmission of an action potential¹ along the membranes of nerve cells is attributed to ionic currents (mainly of sodium and potassium), flowing through transmembrane protein called protein channels. Such protein channels can open and close in a complex time and voltage dependent manner, thus enhancing selective conduction of different ions. When a channel is open, ions can permeate in and out of the membrane following their electrochemical potential gradient. The transmembrane potential regulates the opening of the channels, which, in turn, can alter the potential through ionic currents. These currents are measured in voltage-clamp experiments, where the voltage is clamped at a fix value and currents resulting from a sudden voltage change are recorded [18].

In the Hodgkin and Huxley model, the lipid bilayer doesn't play any active role. Because of its hydrophobic interior, it is assumed to behave like an insulator.

In fig.1.5, protein channels are substituted by resistors, whose conductance is time and voltage dependent, and the membrane is considered as a capacitor of fixed capacitance. The current (I_m) through a membrane containing Na^+ (sodium) and K^+ (potassium) channels is the sum of the capacitive and ionic currents and it is described by:

$$I_m = C_m \frac{dV}{dt} + g_K(V, t)(V - E_K) + g_{Na}(V, t)(V - E_{Na}) \quad (1.1)$$

Here, C_m is the membrane capacitance, V is the transmembrane voltage, g_K and g_{Na} are the conductances of the potassium and sodium channel, respectively, and $E_K \simeq -70 \text{ mV}$ and $E_{Na} \simeq +30 \text{ mV}$ are the resting potentials for potassium and sodium. They correspond to the voltage at which no net flow of the correspondent ion is observed through the membrane. Once the explicit dependence of the conductance on time and voltage is known, the time course of the membrane potentials can be studied with cable theory. In the Hodgkin and Huxley model such dependence is determined by empirical fitting of the experiments.

The capacitive term in eq.(1.1) is derived in the assumption of constant capacitance. The membrane capacitance, however, is not constant in phys-

¹An action potential is a transient voltage change across the membrane, which propagates along neuronal cells.

iological conditions [19]. Biological membranes are known to undergo melting transitions few degrees below their physiological temperature [20]. Such transitions involve severe structural changes of the membrane (like area and thickness changes [21]), which can dramatically affect the value of the capacitance. Furthermore, the temperature at which biomembranes melt can be affected by a number of variables, including voltage. In addition to this, the voltage dependence of the capacitance of lipid bilayers and biological membranes is a known phenomenon that has been widely investigated in the past [3, 22]. Nevertheless, all these considerations are neglected in the interpretation of electrophysiology experiments, where membrane currents are described by eq. (1.1). Next to this, strong electro-mechanical couplings are observed in experiments with lipid bilayers when external voltages are applied [23]. Since the membrane, in physiological conditions, is exposed to significant voltages and it's close to the melting transition where large fluctuations in the mechanical properties occur, these coupling phenomena are worth of further investigation.

1.4 Outline

The topics addressed in this thesis have been investigated both theoretically and experimentally.

In chapter 2, the theoretical background is presented. It introduces the thermodynamical and electrical features of lipid membranes highlighting their coupling with the mechanical properties, providing the reader with the basic knowledge and methods used in the theoretical part.

The materials and methods used in the experimental part of this thesis are presented in chapter 3. In particular, a new instrument for creating synthetic lipid bilayers has been used and is described.

Chapter 4 contains the theoretical investigation and the preliminary results obtained with the new instrumentation.

Finally, a summary of this work together with future perspectives is presented in the conclusions.

Chapter 2

Background Theory

Biological membranes are a very inter-disciplinary research field for their relevance in biology, their chemical composition and their physical properties. Especially for a physicist, they represent an extremely interesting topic which requires knowledge and techniques from different physics areas such as thermodynamics, electrostatics and mechanics. Their properties are often a coupling between different fields, which makes it hard to distinguish between them. In this chapter the basic physical properties of biomembranes are summarised and roughly divided in thermodynamical and electrical properties, the mechanical features being included in both. The aim of these sections is not only to give some basic knowledge but also to introduce the reader to some methods and formalism that will be used in the theoretical part of the thesis. The last section treats permeability properties of membranes, which is the topic of the experimental part of this thesis.

2.1 Thermodynamics of lipid membranes

Biomembranes are mesoscopic systems: the typical length scale is of the order of the μm , and their properties cannot be fully understood by looking at the atomic level. In experiments with artificial membranes, patches with a diameter between 1 and 100 μm are usually investigated. Considering an area per lipid of about $0.629 nm^2$ (DPPC molecules in the fluid state [21]), such patches contain approximately between 10^6 and 10^{10} lipid molecules, which is a large number of statistical significance. Their average properties can be then understood with classical thermodynamics laws, the most relevant of which are reviewed in the following¹.

¹The whole section is inspired by [4, 24]

The first law of thermodynamics is a conservation law for the internal energy:

$$dU = \delta Q + \delta W \quad (2.1)$$

Any change in the internal energy dU can be written as the sum of the heat absorbed by the system δQ and the work performed on the system δW . Note the use of δ instead of d , since both the infinitesimal heat and the work are path dependent quantities, whereas their sum dU is a perfect differential, being U a function of state². Traditionally the work in eq.(2.1) is the mechanical work done to change the volume of the system against the bulk pressure ($-pdV$). This is, of course, one contribution, but not the only one. The work in eq.(2.1) is any kind of work that can be performed on the system:

$$\delta W = -pdV - \pi dA - fdl + \Psi dq + EdP + HdM + \dots + \sum_i \mu_i dn_i \quad (2.2)$$

where

- $-\pi dA$ is the work to change the area of a quantity dA against the lateral pressure π ,
- $-fdl$ is the work to change the length l of a spring against the force f ,
- Ψdq is the work needed to increase the charge of a capacitor of dq with the electrostatic potential Ψ
- EdP is the work done by an electric field to polarize a material,
- HdM is the work done by a magnetic field to orientate magnetic dipoles,
- $\mu_i dn_i$ is the work done to increase the number of particles of species i of a quantity dn_i with the chemical potential μ_i ,
- \dots stand for any other kind of work in the form of $x dX$, where x is an intensive variable (independent of the system size) and X is the conjugated extensive variable (dependent of the size of the thermodynamical system). In general, x is called *generalised force* and X *generalised coordinate*.

²A function of state is a property of the system that depends exclusively on the actual state the system is in, no matter how it got there. Functions of state can be used to describe the thermodynamic equilibrium of a system, and they are path independent, meaning that their closed path integral is always zero

From the second law of thermodynamics we know that:

$$dS = dS_r + dS_i \geq \frac{\delta Q}{T}$$

Where in the change of the entropy dS are considered both contributions from reversible processes (dS_r) and irreversible processes ($dS_i \geq 0$). The latter include all spontaneous processes in a system which do not lead to exchange of heat with the environment or the performance of work on the environment. They induce changes in the system until no further spontaneous change happens, this state being thermodynamic equilibrium.

In the case of fully reversible processes, (such as the melting transition in membranes³), the previous expression can be written as:

$$dS_r = \frac{dQ}{T} \quad (2.3)$$

According to eq (2.2) and (2.3), the first law of thermodynamics (2.1) can be rewritten as follows:

$$dU = TdS_r - pdV - \Pi dA + \Psi dq + EdP + \dots \quad (2.4)$$

where only mechanical and electrical contributions to work are expressed explicitly because they are the ones that will be relevant throughout this thesis, but one can include all the different types of work that are performed on the system.

The internal energy $U(S, V, A, q, P, \dots)$ is a function of state, thus intensive variables can be expressed as derivatives of it with respect to the extensive conjugate:

$$T = \left(\frac{\partial U}{\partial S} \right)_{V,A,\dots}, p = - \left(\frac{\partial U}{\partial V} \right)_{S,A,\dots}, \Pi = - \left(\frac{\partial U}{\partial A} \right)_{S,V,\dots}, \\ \Psi = \left(\frac{\partial U}{\partial q} \right)_{S,V,\dots}, E = \left(\frac{\partial U}{\partial P} \right)_{S,V,\dots}$$

Eq.(2.4) can be rearranged, so that the change in entropy of the system is expressed by:

$$dS = \frac{1}{T}dU + \frac{p}{T}dV - \frac{\Pi}{T}dA + \frac{\Psi}{T}dq + \frac{E}{T}dP + \dots$$

³see section 2.1.1

from which analog relations define the the thermodynamic forces ($1/T$, p/T , π/T , Ψ/T , E/T) which drive the change in their extensive conjugated coordinates (dU , dV , dA , dq , dP):

$$\begin{aligned} \frac{1}{T} &= \left(\frac{\partial S}{\partial U} \right)_{V,A,\dots}, & \frac{p}{T} &= \left(\frac{\partial S}{\partial V} \right)_{T,V,\dots}, & \frac{\Pi}{T} &= \left(\frac{\partial S}{\partial A} \right)_{T,V,\dots} \\ \frac{\Psi}{T} &= - \left(\frac{\partial S}{\partial q} \right)_{T,V,\dots}, & \frac{E}{T} &= - \left(\frac{\partial S}{\partial P} \right)_{T,V,\dots} \end{aligned}$$

which are more intuitive if one thinks of the entropy as a potential.

Functions of state in thermodynamics are a very useful tool since important properties can be derived from them. Internal energy and entropy are function of state. Eq.(2.4), for example, can be integrated, leading to $U = TS - PV - \Pi A + \Psi q + EP + \dots$, where all the products on the right hand side are also functions of state. Thus, any combination of them is also a function of state. The most commonly used are:

$$H = U + PV \quad \text{Enthalpy} \quad (2.5)$$

$$F = U - TS \quad \text{Helmholtz Free Energy} \quad (2.6)$$

$$G = H - TS = U - PV + TS \quad \text{Gibbs Free Energy} \quad (2.7)$$

In general, for a system with internal energy $dU = TdS + \sum_i x_i dX_i$ (with $x_i dX_i$ being any of the n conjugated pair of intensive and extensive variable that contribute to the total work performed on the system) instead of the two functions U and H , one will have 2^n functions of state in the form [24]:

$$U + \sum' x_i X_i$$

Here the summation is taken over any set of the coordinates and forces.

Equivalently, instead of only the two free energy functions F and G one will have 2^n functions in the form:

$$U - TS + \sum' x_i X_i$$

The choice of a specific thermodynamic potential depends on the particular thermodynamic forces acting on the system and on the experimental conditions. In biological experiments, for example, where pressure and temperature are kept constant, the natural functions used to describe the system are the enthalpy and the Gibbs free energy. Under such conditions, for example, the minimum of the Gibbs free energy describe thermodynamic

equilibrium. Free energy functions in fact, unlike internal energy, describe the direction of spontaneous processes [4].

Considering polarization effects in membrane, the common experimental conditions are constant atmospheric pressure and fixed external electric field, where the volume and polarization are allowed to change accordingly. The appropriate thermodynamic potentials become:

$$\begin{aligned} H_{el}(S, p, \dots, E) &= H(S, p, \dots, P) - EP = (U(S, V, \dots, P) + pV) - EP \\ G_{el}(T, p, \dots, E) &= H_{el}(S, p, \dots, E) - TS = H(S, p, \dots, P) - EP - TS \end{aligned}$$

Hereafter, only explicit work contributions will be written, to ease the notation.

The transformation from one thermodynamic function to another (e.g. $U \rightarrow H$ or $H \rightarrow H_{el}$ and so on) is made by Legendre transforms, in such a way that one can change the natural coordinates of a state function. Every possible combination is allowed, as long as the the choice of coordinates reflects the physical system one is studying. The differential of the above defined *electrical thermodynamic potentials* are given by:

$$\begin{aligned} dH_{el} &= \overbrace{TdS - pdV + EdP}^{dU} + \overbrace{pdV + Vdp}^{d(pV)} - \overbrace{EdP - PdE}^{-d(EP)} = TdS + Vdp - PdE \\ dG_{el} &= \overbrace{TdS + Vdp - PdE}^{dH_{el}} - \overbrace{TdS - SdT}^{-d(TS)} = -SdT + Vdp - pdE \end{aligned}$$

In conditions of constant T (experiment performed at room temperature), constant p (atmospheric pressure), and constant electric field E , the electrical Gibbs free energy (G_{el}) is in a minimum ($dG_{el} = 0$), and can be used to define the equilibrium, as it's shown in the following.

2.1.1 Phase transition in lipid membranes

Lipid molecules undergo reversible phase transitions from a solid-ordered (*gel*) state at low temperature, to a liquid-disordered (*fluid*) state at higher temperature. This property holds both for protein-free lipid bilayers and for biological membranes. While the temperature range over which different lipids melt is very wide (from $-20^\circ C$ to up to $60^\circ C$), the phase transition of biological membranes happens slightly below (on the order of $15^\circ C$ below) physiological temperature. This happens despite the differences in the lipid and protein composition of the different membranes. Furthermore, it's known that in some organisms (such as *E.coli*), the melting temperature can change accordingly to changes in growth temperature, pH and pressure; the lipid

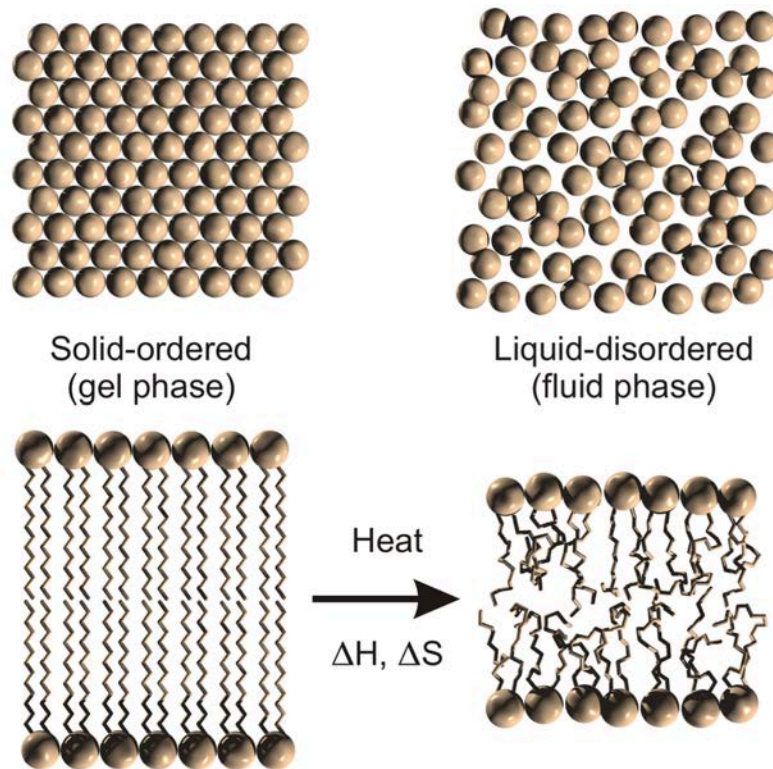


Figure 2.1: Structural changes in the transition from a solid-ordered (*left*) to a liquid-disordered state (*right*). Entropy and enthalpy increase in the transition. Adding heat to the system, the head groups break their lateral order occupying a bigger area and chains can fold decreasing the head-to-head distance. Figure taken from [8]

composition changes to adapt to the new physiological conditions so that the membrane melting is always below the body temperature [25–27].

In fig.2.1, gel and fluid phase are schematically represented. The main features of the two states can be summarised as follows:

- **Solid-ordered (gel) phase**

At low temperatures, lipids are in a solid-ordered state: *solid*, because the head groups are packed in a triangular lattice [28], *ordered* because the hydrocarbon chains are stretched in a *all trans* configuration. These configuration correspond to the lowest entropy and that is why lipids are found in this state at low temperature. As a result, the area occupied by the head group is minimum (also because of the small area occupied by the tails), whereas the thickness is maximum. A bilayer of pure DPPC in the gel phase has an area per lipid of $A_g = 0.474 \text{ nm}^2$ (

compared to $A_f = 0.629 \text{ nm}^2$ per lipid of the fluid phase) and a thickness (head-to-head distance) of $D_g = 4.79 \text{ nm}$ (which goes down to $D_f = 3.92 \text{ nm}$ in the fluid phase) [21, 29, 30].

- **Liquid-disordered (fluid) phase**

In this phase, the head groups break the lateral order and are randomly organised and free to move as in a 2-dimensional fluid. At the same time lipid chains can assume disordered chain configurations, having enough energy to access not only the *all trans* but also *gauche* isomerization of the C-C bonds in the hydrocarbon tail (see fig. 2.2). This state is characterised by a higher entropy (since the number of accessible configurations increases), which is paid off by a high energy cost; as a result lipids can be found in this state only at higher temperatures. *Gauche* conformations are achieved by a kink in the chains that then occupy more space. This and the loss in lateral order result in an area increases of about the 24% and a thickness decrease of about 16% [21, 29, 30].

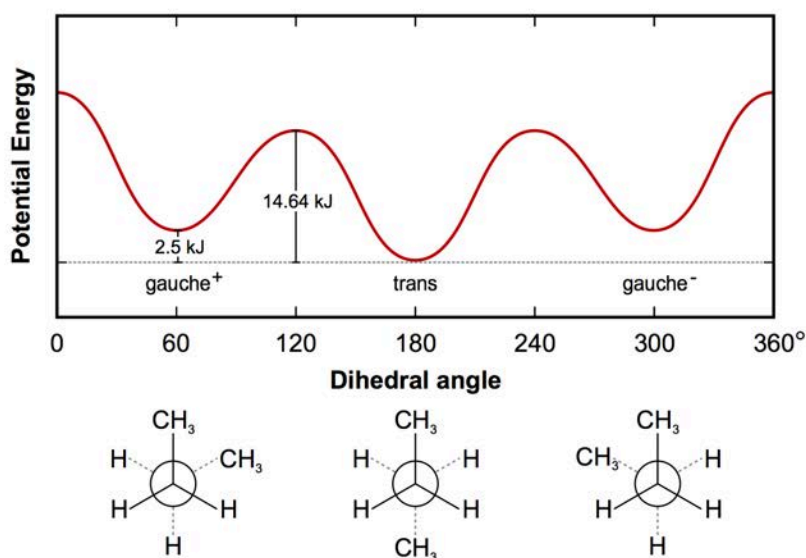


Figure 2.2: *Top*: energy of the different chain configurations. The all-trans (chains stretched, with a zig-zag pattern) is the lowest energy state. Adding heat to the system, allows for *gauche* isomers, which have higher energy and entropy. *Bottom*: rotation around the C-C bond corresponding to *gauche*⁺, *trans* and *gauche*⁻ configurations. Figure taken from [8]

This is of course an oversimplification. More than these two phases are found in lipids structures. The transition from gel→fluid requires that both head groups and chains undergo structural changes at the same temperature. In principle, mixed phases like solid-disordered or liquid-ordered should be possible. In practice, only a liquid-ordered state with order chains without any crystal organisation of the head groups has been proposed to exist for cholesterol containing membranes [4].

Furthermore, it has to be noted that pretransitions can occur a few degrees below the main transition. In fig.2.3, this is shown for DMPC, where the peaks in the curve indicate a phase transition. Between the two transition the membrane is in a ripple phase and displays periodical undulations. Nevertheless ripple phase has been observed to be easily abolished by the presence of various biomolecules and is rarely seen in biological membrane [31]. As a consequence, only the main transition between gel and fluid will be considered throughout this thesis.

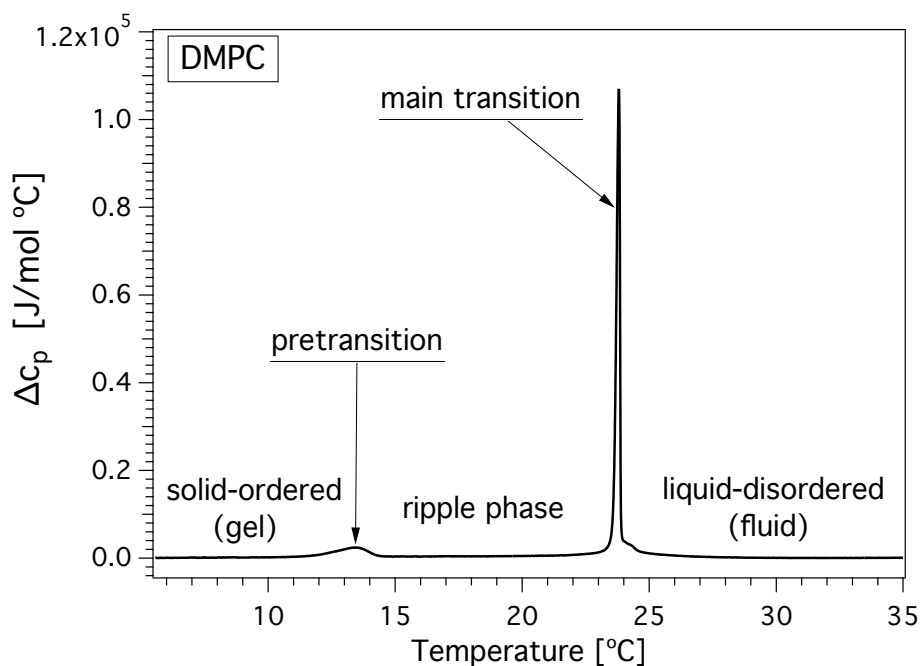


Figure 2.3: Heat capacity profile of DMPC measured with a DSC calorimeter. The curve displays two peaks. The small one with low cooperativity (wider) corresponds to the pretransition and the big narrow one (high cooperativity) corresponds to the main transition. Between the two transition the lipids are in a ripple phase. The sample was dissolved in 150mM KCl, buffered with 1mM EDTA and 1mM HEPES. Scan rate: 5°C/hour.

Considering a two state phase transitions from a solid-ordered state to a liquid-disordered, the melting point T_m is defined as the temperature at which the ground (gel) and the excited (fluid) states are found with equally likelihood:

$$\frac{P_{fluid}(T_m)}{P_{gel}(T_m)} = K(T_m) = \exp\left(-\frac{\Delta G}{RT_m}\right) = 1$$

where $K(T)$ is the equilibrium constant governed by a Van't Hoff law, $R = 8.314J/molK$ is the molar gas constant and ΔG is the difference in the Gibbs free energy of the two states, which in order to satisfy the equiprobability condition, needs to be zero at the transition:

$$\Delta G = G_{fluid} - G_{gel} = \Delta H_0 - T_m \Delta S_0 = 0 \quad (2.8)$$

Here, in the last equality, the definition of Gibbs free energy (2.7) has been used, ΔH_0 and ΔS_0 being the change in enthalpy and entropy during the melting process.

The melting temperature can be also defined as the temperature at which the Gibbs free energy of the two states is the same, or, as follows from (2.8):

$$T_m \equiv \frac{\Delta H_0}{\Delta S_0} \quad (2.9)$$

The melting temperature depends on the structure of the lipid (chain length, head group size and charge, chain saturation etc) [32]. Entropy (and thus T_m) has been found to increase linearly with the chain length. However, in biomembranes, many other factors, such as hydrostatic pressure, pH and the presence of anaesthetics (and every other quantity that influence ΔH_0 or ΔS_0) can alter the transition temperature [4, 33]. In this thesis the effect of voltage will be considered.

In addition, several physical properties of membranes are affected upon melting, such as the already mentioned increase of membrane thickness and decrease in area. The peculiar behaviour of mechanical properties, such as area and volume compressibilities or bending elasticity, show a decrease of mechanical stability. The trend of the physical susceptibilities, confirms a scenario in which the membrane in the phase transition is more susceptible: little changes in the intensive variables lead to large fluctuations of the correspondent extensive ones.

Cooperativity

Phase transitions in biomembranes are a cooperative phenomenon. This means that lipid molecules don't melt independently from each other but

rather form macroscopic domains that melt in a cooperative fashion [4]. The equilibrium constant $K(T)$ introduced above defines the probability that a mole of lipids has enough thermal energy to access a state with a higher energy, i.e. to pass from a gel state to a fluid one. Assuming that the system is characterised by only two states, namely gel and fluid, one can express the fraction of lipids that are in a particular state with the use of the equilibrium constant:

$$P_f(T) = \frac{K(T)}{1 + K(T)} \qquad P_g(T) = \frac{1}{1 + K(T)} \qquad (2.10)$$

$P_f(T)$ and $P_g(T)$ can be also interpreted as the probability that a single molecule is in the fluid or in the gel state at a given temperature.

Taking into account the cooperativity of the transition, one assumes that lipid don't melt all together but in clusters of a certain size. The size of the cluster (cooperative unit) is denoted by n . Then, the equilibrium constant can be expressed as:

$$K(T) = \exp\left(-n \frac{\Delta G}{RT}\right) = \exp\left(-n \frac{\Delta H_0 - T\Delta S_0}{RT}\right) \qquad (2.11)$$

According to (2.9), we can rewrite the previous equation as a function of the enthalpy:

$$K(T) = \exp\left(-n \frac{\Delta H_0}{R} \left(\frac{1}{T} - \frac{1}{T_m}\right)\right)$$

One can now write the mean enthalpy at temperature T :

$$\langle \Delta H(T) \rangle = \Delta H_0 \frac{K(T)}{1 + K(T)} \qquad (2.12)$$

Fig. 2.4 shows the results of the calculation for the melting enthalpy and entropy, assuming a cooperative unit size of $n = 100$.

This approach allows to study the mean properties of the system with the use of statistical averages over all the possible microstates. However, this is a simplification of the real system. More detailed models require the use of other methods, such as Monte Carlo simulations.

Susceptibilities and fluctuations

Among the different experimental methods to detect a phase transition, the most suitable to derive the thermodynamical properties of the system is calorimetry. Calorimetry measurement will be widely explained in chapter

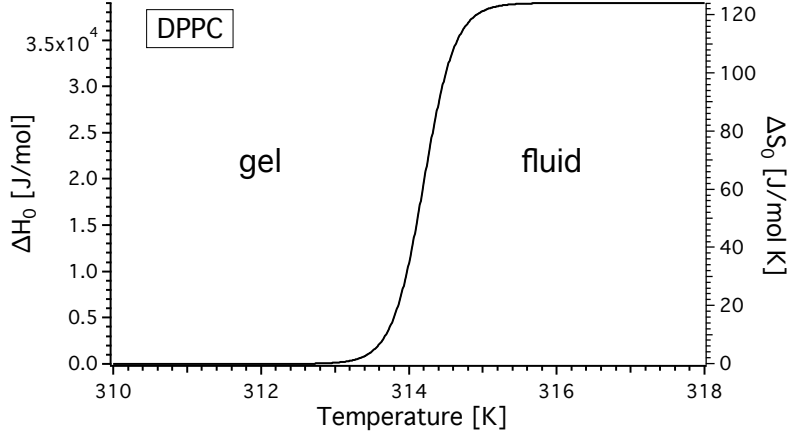


Figure 2.4: Change in enthalpy (*left axis*) and entropy (*right*) as a function of temperatures from the gel to the fluid state for DPPC using eq.(2.14). $T_m = 314.2K$, $\Delta H_0 = 39kJ/mol$, $n = 100$.

3. For the time being, it is defined as a method to measure the heat capacity of a sample as a function of temperature⁴.

Heat capacity is the amount of heat required to change the temperature of a substance of a certain amount. Note that heat capacity is an extensive quantity while in the rest of this thesis the molar heat capacity (heat capacity per unit mole) at constant pressure, with the units of $[J/K \cdot mol]$, will be used. Phase transitions are characterised by a peak in the heat capacity (the heat required to change the temperature of a substance is maximum during the transition).

Thermodynamically it is defined as:

$$c_p \equiv \left(\frac{dQ}{dT} \right)_P = \left(\frac{dH}{dT} \right)_P = T \left(\frac{dS}{dT} \right)_P \quad (2.13)$$

where $dH = dQ + Vdp = TdS + Vdp$ has been used.

From the heat capacity the change in enthalpy can be calculated:

$$\Delta H_0 = \int_{T_g}^{T_f} c_p dT \quad (2.14)$$

and the same for the change in entropy:

$$\Delta S_0 = \int_{T_g}^{T_f} \frac{c_p}{T} dT \quad (2.15)$$

⁴This is not the only type of calorimetry. Calorimetric measurements include also, for example, isothermal calorimetry or pressure jump calorimetry.

One can show that the heat capacity and the fluctuations of the enthalpy are proportional:

$$c_p = \frac{d\langle H \rangle}{dT} = \frac{\langle H^2 \rangle - \langle H \rangle^2}{RT}$$

Similar relations hold between all the other susceptibilities of the system and the magnitude of the fluctuation of the related extensive variable. In general, susceptibilities are defined as the derivatives of an extensive variable with respect to its intensive conjugated variable. In the case of the pairs pressure-volume and lateral pressure-area, the susceptibility correspond to volume and area compressibility, respectively:

$$\begin{aligned} \kappa_T^V &= -\frac{1}{\langle V \rangle} \left(\frac{d\langle V \rangle}{dp} \right)_T = \frac{\langle V^2 \rangle - \langle V \rangle^2}{\langle V \rangle RT} \\ \kappa_T^A &= -\frac{1}{\langle A \rangle} \left(\frac{d\langle A \rangle}{d\pi} \right)_T = \frac{\langle A^2 \rangle - \langle A \rangle^2}{\langle A \rangle RT} \end{aligned}$$

So, the volume and area isothermal compressibilities are proportional to the fluctuations in volume and area, respectively.

One of the striking properties of membranes is that geometrical changes in the phase transition are proportional to changes in enthalpy. This has been proven experimentally [34] for the volume change. The same relation is assumed for area changes [21, 35] :

$$\Delta V(T) = \gamma_V \Delta H(T) \qquad \Delta A(T) = \gamma_A \Delta H(T) \qquad (2.17)$$

The coefficients $\gamma_V = 7.8 \cdot 10^{-10} m^3/J$ and $\gamma_A = 0.89 m^2/J$ have been found to be independent of the lipid species or the lipid mixture [21]. A similar relation can be assumed for the membrane thickness which undergo significant changes in the transition. The behaviour of area, volume and thickness in the melting regime is shown in fig.2.5.

In a system where these kind of relations hold between extensive variable, the same relations applies to their correspondent susceptibility. Indeed, assuming that the proportionality holds for all temperatures, one finds:

$$\begin{aligned} \langle \Delta V^2 \rangle - \langle \Delta V \rangle^2 &= \gamma_V^2 (\langle \Delta H^2 \rangle - \langle \Delta H \rangle^2) \\ \langle \Delta A^2 \rangle - \langle \Delta A \rangle^2 &= \gamma_A^2 (\langle \Delta H^2 \rangle - \langle \Delta H \rangle^2) \end{aligned}$$

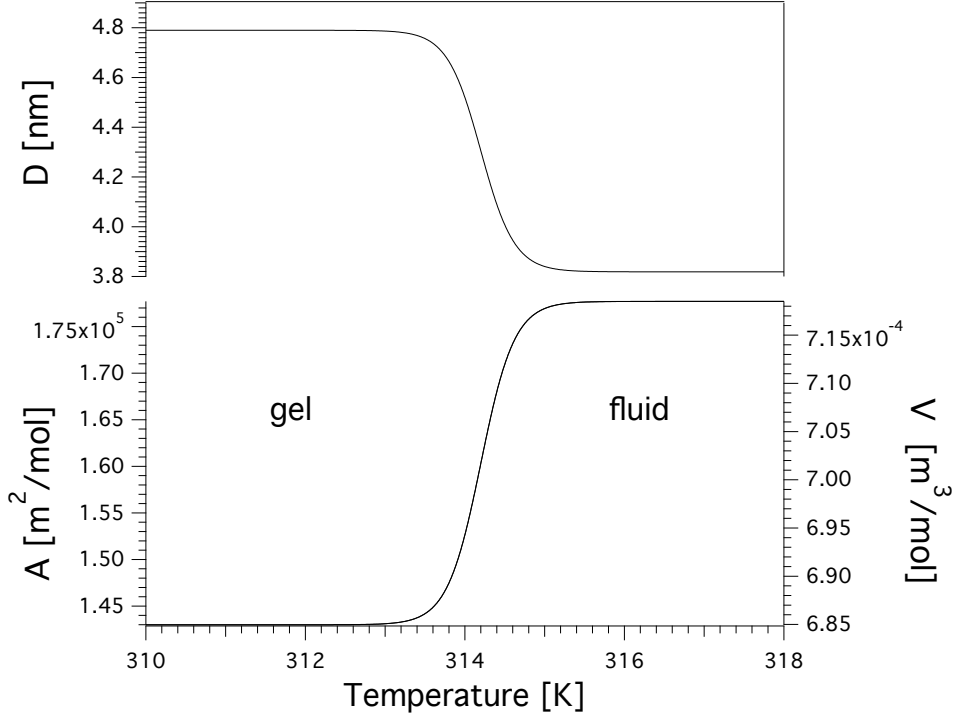


Figure 2.5: *Bottom*: changes in area and volume for a DPPC bilayer, assuming the proportionality with the melting enthalpy (compare it to fig. 2.4). *Top*: thickness is known to change during the transition. The curve is calculated assuming that a relation similar to (2.17) holds for the mean thickness D , namely $\Delta D(T) = \gamma_D \Delta H_0(T)$, with $\gamma_D = -2.49 \cdot 10^{-14} \text{m/J}$. The values of the parameter are taken from [21].

Therefore, proportionality relations hold for the compressibilities and the heat capacity as well:

$$\Delta \kappa_T^V = \frac{\gamma_V^2 T}{\langle V \rangle} \Delta c_p \quad (2.19a)$$

$$\Delta \kappa_T^A = \frac{\gamma_A^2 T}{\langle A \rangle} \Delta c_p \quad (2.19b)$$

They are shown in fig. 2.6.

Proportionality between the elastic properties of the system and the heat capacity means that also the compressibilities have a maximum in the phase transition (see fig 2.6). The membrane is more compressible and the fluctuations in area and volume are bigger in the phase transition, meaning that very small changes in the intensive variables (T, p, Π, \dots) result in large changes in the correspondent extensive variables (S, V, A, \dots).

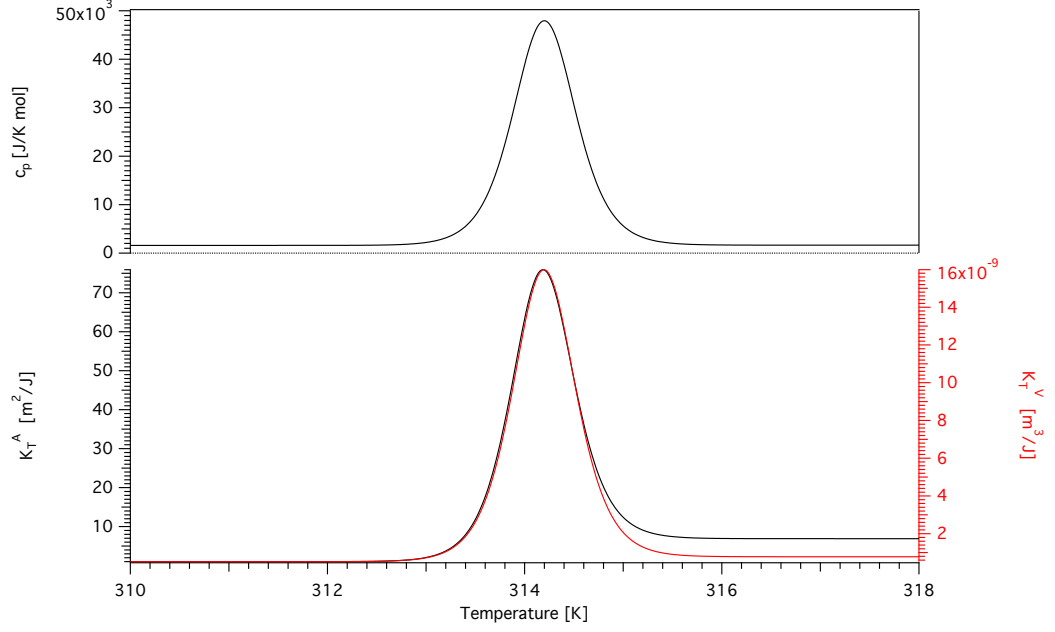


Figure 2.6: *Top*: heat capacity profile calculated from $c_p(T) = c_{p,0}(T) + \Delta c_p(T)$. The excess heat capacity Δc_p is calculated from the enthalpy (2.14), while $c_{p,0} = c_p^{gel} \cdot P_g + c_p^{fluid} \cdot P_f$. P_f, P_g have been defined in (2.10). *Bottom*: isothermal area (black) and volume (red) compressibility, calculated like the heat capacity. The three susceptibilities are super-imposable. Parameters taken from [21]: $c_p^{gel} = 1600 \text{ J/K} \cdot \text{mol}$, $c_p^{fluid} = 1650 \text{ J/K} \cdot \text{mol}$, $\kappa_{T,gel}^A = 1 \text{ m}^2/\text{J}$, $\kappa_{T,fluid}^A = 6.9 \text{ m}^2/\text{J}$, $\kappa_{T,gel}^V = 5.2 \cdot 10^{-10} \text{ m}^3/\text{J}$, $\kappa_{T,fluid}^V = 7.8 \cdot 10^{-10} \text{ m}^3/\text{J}$.

2.2 Electrical properties

One of the functions of biological membranes is to separate the different compartments of the cell (in the case of the membrane of cell organelles) or to create a barrier between the interior of the cell and the surrounding environment (in the case of plasma membranes). The latter is responsible of maintaining electrostatic potential differences across itself by keeping a non equilibrium distribution of ions between the interior of the cell and the outside. Such potential differences are believed to be responsible for many necessary processes in the cell, for example the transmission of nerve pulses along neurons. Therefore, biological membranes sustain voltages of the order of several hundreds mV in physiological conditions. It is thus of primary importance to understand what is the effect of such voltages on the membrane. These can be observed in patch-clamp experiments where a small "patch" of a cell membrane is investigated.

In this section, the membrane capacitance and polarization properties are treated. We assume that the main role in biological membrane properties comes from their major constituent: lipids. Therefore, the following considerations apply for reconstituted lipid membranes. As already mentioned, the coupling of electric properties with mechanical and thermodynamical features is stringent and will be highlighted, with a special attention to their behaviour in the phase transition, because of its relevance in biological systems.

2.2.1 Membrane capacitance

In the following, the membrane in the aqueous environment will be considered as a capacitor filled with a dielectric medium.

The capacitance of the membrane, C_m , is a measure of how much charge q is stored on the two leaflets at a certain voltage V_m :

$$q = C_m \cdot V_m \quad (2.20)$$

In the assumption of a perfectly flat bilayer, the two leaflets are parallel, and the bilayer can be modelled as a planar capacitor filled with a dielectric:

$$C_m = \epsilon_0 \epsilon \frac{A}{D} \quad (2.21)$$

where $\epsilon_0 = 8.854 \cdot 10^{-12} F/m$ is the vacuum permittivity, $\epsilon \sim 2 - 4$ is dielectric constant of the membrane, A and D are the area and thickness of the membrane. The capacitance is uniquely determined by the geometrical and dielectric properties of the system: if they remain constant, the capacitance

will also be constant. In biological membranes, the first assumption (fixed geometry) is particularly not true, especially close to the melting transition.

Changes in the voltage across the membrane result in changes of charge with time, i.e. capacitive currents:

$$\frac{dq}{dt} = \frac{d(C_m \cdot V_m)}{dt} = C_m \frac{dV_m}{dt} + V_m \frac{dC_m}{dt}$$

Traditional models, such as the Hodgkin and Huxley model for the nerve pulse propagation consider only the first term on the right side of the previous equation, considering the capacitance as a constant property of the system, thus independent of the voltage.

As above mentioned, during the melting transition the area of a lipid membrane changes of about the 24.6% and the thickness of the -16.3% [21]. According to (2.21), this would result in a relative change of the capacitance from gel to fluid of approximately the 50% [19]:

$$C_m^f = \epsilon_0 \epsilon \frac{A_g(1 + 0.246)}{D_g(1 - 0.163)} = 1.49C_m^g$$

The capacitance is a function of the state of the system. Furthermore it is also a function of any quantity that can affect the physical state of the membrane, like (as we saw in the last section) pressure, lateral pressure, pH, and also voltage. Hence, it is reasonable to consider also the voltage dependence of the membrane capacitance. In the next paragraph a brief excursus of the literature about the membrane capacitance will show that this dependence has been studied since the 1960s.

Previous studies on membrane capacitance

Membrane capacitance has been studied since the 1960's, and its dependence on voltage was observed both in artificial⁵ [36] and biological membranes [22, 37–41].

Back in 1966, Babakov and collaborators investigated the electromechanical properties of artificial phospholipid membranes, recognising their importance in the activity of the cell membrane, and finding a quadratic dependence of the capacitance on the voltage [3]. This was explained as a

⁵ Electrical measurements on artificial membranes were (and still are) most commonly performed on patches of lipid membranes reconstituted on the tip of glass pipettes (typical size $1 - 10 \mu m$) or on the aperture of Teflon films (typical aperture size is $50 - 250 \mu m$) [9]. The latter are usually referred to as BLM experiments, which stands for Black Lipid Membrane (sometimes also called planar lipid membrane), because they look dark in reflected light.

thinning of the bilayer due to an electrostrictive force (since the effect was not dependent on the direction of the applied field), but they also claimed a contribution from the optically measured area enlargement at the membrane border.

Proportionality between the capacitance and the square of the voltage has since been confirmed by different authors in both artificial [42–44] and recently also in biological membranes [45]:

$$C(V) = C_0(1 + \beta V^2) \quad (2.22)$$

Nevertheless the mechanism behind voltage dependence was not clear. While the electrostrictive thinning of the bilayer was an intuitive effect on the capacitance which could be quantified, quantifying the influence of changes in area was more controversial. This was due to the limitations in the optical methods used to detect area changes [46], and to the unclear role of solvents in artificial membrane patches [47]. The latter effect includes both the presence of the solvent at the border of the bilayer ⁶ and the presence of microlenses (smaller than $1\mu\text{m}$) of trapped solvent in the bilayer [48, 49].

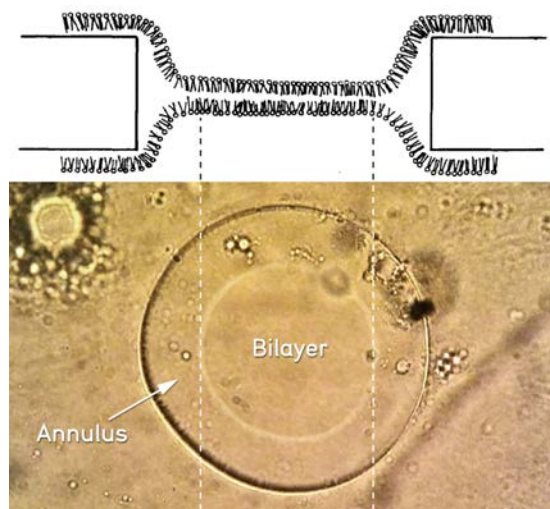


Figure 2.7: *Top*: schematisation of the BLM apparatus. Here only the section of the aperture is shown. The central part is the bi-molecular film. Close to the edge, the bilayer becomes thicker because of the presence of solvent. Picture taken from [50]. *Bottom*: picture of a BLM used in the experiments from the top, showing clearly the annulus surrounding the central bilayer.

⁶The bilayer film in BLM experiments is in equilibrium with an annulus (or torus) of solvent that surrounds it (see fig.2.7) . For further details see chapter 3

A noticeable contribution in understanding the effects of solvent on the specific capacitance in BLM measurements had been made starting from the 70's by White. He quantified the annulus contribution using variational calculus and found that its contribution is on the order of the 0.01% if the bilayer diameter is large compared to the width of the annulus, and thus can be neglected [51]. He also quantitatively investigated the effect of microlenses and, comparing it to the electron micrographs made by Henn and Thompson [49], he arrived to the conclusion that their effect can be accounted by considering a non-uniform thickness which is on average close to the bilayer thickness. In that way, one doesn't need to consider the lenses separately. Nonetheless, capacitance of solvent-free membrane do show smaller voltage dependence.

An interesting variation of the functional form (2.22) has been given by Alvarez and Latorre [52] who measured the nonlinearity of the capacitance on asymmetric membranes, finding that this is influenced by a resting potential V_0 , which is responsible of shifting the voltage dependence:

$$C(V) = (1 + \beta(V - V_0)^2)C_0$$

Their findings are shown in fig. 2.8.

In all these studies not only the nonlinearity of capacitance was a known property of lipid bilayer but also the electromechanical coupling between capacitance change and mechanical stress appears to be clear.

Recently, electromechanical aspects of the membrane capacitance have been discussed in the context of outer ear hair cells especially by Kuni Iwasa [53–55] and William E. Brownell [56–58] with findings remarkably close to those derived by Heimburg [19] for lipid membranes, as it will be shown in the next paragraph.

Nevertheless, to the best of our knowledge, most of the literature about membrane capacitance doesn't consider any temperature dependence, or, when it does [59], it does it far from the melting transition, with the only (experimental) exception of White [60] and Bagaveyev [61]. Membrane capacitance, though, is expected to be dramatically affected by changes in membrane geometry related to phase transitions [19]. The fact that biological membranes at body temperature are only few degrees above their melting point, justify the relevance of further in-depth analysis. A first step in this direction has been done recently by Heimburg [19] whose finding are briefly summarised below.

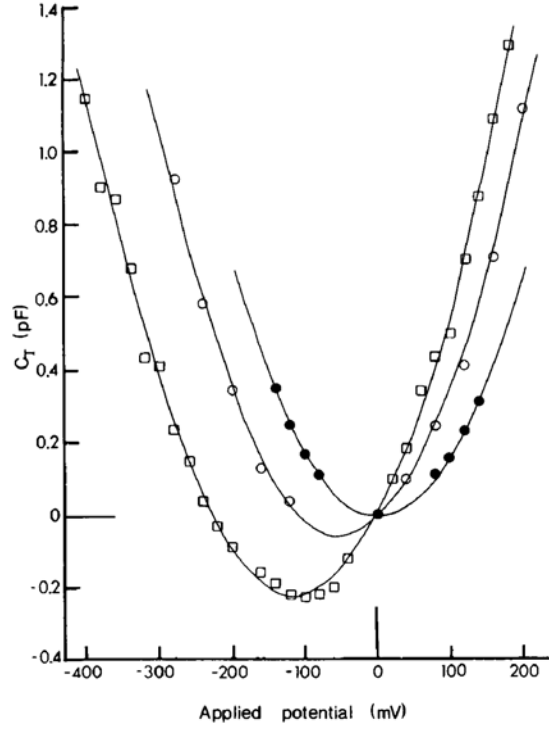


Figure 2.8: Voltage dependence of the capacitance from [52]. Synthetic lipid membranes were formed by apposition of two separate monolayers on the hole of a Teflon film separating two chambers containing the electrolyte solution (1M of KCl). *Solid circles* represent the values for a symmetric membrane made of phosphatidylethanolamine (PE) which are well fitted by a parabola with the minimum in the origin ($V_0 = 0V$). *Open circles* and *squares* are the results for an asymmetric membrane (made of one monolayer of PE and one of phosphatidylserine, PS) in electrolyte solution of different concentration. The parabola are shifted with respect to the origin, and the minimum occurs at $V_0 = -51mV$ (for a salt concentration of 1M) and -115 (for 0.1M KCl).

Capacitive susceptibility

Consider to keep constant all the intensive variables of the system, except the voltage. The equilibrium properties of such a system will then only depend on the voltage:

$$dq = \left(\frac{\partial q}{\partial V_m} \right) dV_m \equiv \hat{C}_m dV_m \quad (2.23)$$

where $\hat{C}_m = (\partial q / \partial V_m)$ is called *capacitive susceptibility*. It was already used before by Carius and called differential capacitance [62] Using eq.(2.20), then

eq.(2.23) becomes:

$$dq = \left(\frac{\partial(C_m V_m)}{\partial V_m} \right) dV_m = \left(C_m + V_m \frac{\partial C_m}{\partial V_m} \right) dV_m = C_m dV_m + V_m dC_m$$

The changes of the charge on the capacitor are not only due to the change in the voltage but also to voltage induced changes in the capacitance. Both contributions are taken into account in the capacitive susceptibility:

$$\hat{C}_m \equiv C_m + V_m \frac{\partial C_m}{\partial V_m} \quad (2.24)$$

If the capacitance doesn't depend of the voltage or if the transmembrane voltage is zero we have $\hat{C}_m \equiv C_m$, so the capacitance is a constant of the system and it coincides with the definition (2.21). The second term in (2.24) is proportional to the voltage so it is small for small voltages but can become large in the transition. It can be considered as an excess capacitance.

The capacitive susceptibility is the derivative of an extensive variable (q) with respect to its conjugated intensive one ($V_m = -\Psi$). Therefore, like the other susceptibilities already introduced, fluctuation relations hold also for it:

$$\hat{C}_m = -\frac{dq}{d\Psi} = \frac{dq}{dV_m} = \frac{\langle q^2 \rangle - \langle q \rangle^2}{RT}, \quad T, p, \pi, \dots = const$$

Thus, not only the capacitive susceptibility in the present assumptions is a positive quantity (being the fluctuation in charge a quadratic form), but also its integral has to be positive, since:

$$\Delta q = \int_{V_1}^{V_2} \hat{C}_m dV_m > 0 \quad \text{with } V_1 < V_2$$

An increase in voltage would still result in an increase of charge (as in the traditional linear capacitance), as long as the other intensive properties of the system are kept constant. Furthermore, note that the fact that the susceptibilities are positive forms holds only when they are defined in respect to a couple of conjugated variables.

Electrostriction

In a planar capacitor the two plates are oppositely charged thus attracting each other electrostatically. This attraction result in a mechanical force on the capacitor which is known as *electrostriction*: increasing the voltage in absence of other forces will increase the force that will tend to deform

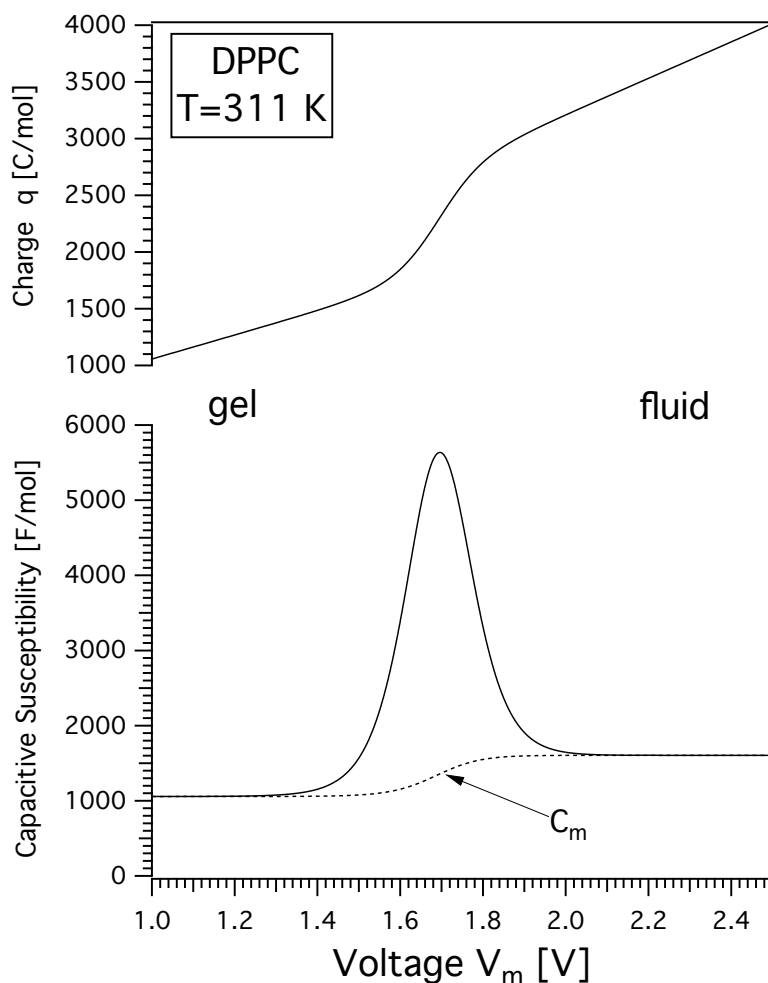


Figure 2.9: *Bottom*: voltage dependence of the capacitance susceptibility, \hat{C}_m (*solid line*) and the capacitance, C_m (*dashed line*) for DPPC at $T = 312\text{ K}$ (below the melting point). The area between the two curves is the excess charge Δq . *Top*: charge as a function of voltage. The voltage induced changes in the capacitance results in the nonlinearity of the relation between q and V_m .

the capacitor reducing the distance between the plates. In general planar capacitors, constraint forces provide enough reaction to compensate for electrostriction so that the geometry and thus the value of the capacitance of the capacitor remains constant with the voltage. This is not valid for biological membrane, where the internal constraint forces (such as steric repulsion or electrorepulsion of the lipids) are not big enough to compensate for this

effect.

Let's consider a membrane with thickness D and capacitance C_m . If the transmembrane voltage is V_m , then the field across the membrane assuming a uniform dielectric constant is $E = V_m/D$ and the charge on the two "plates" is $q = C_m V_m$. Therefore, the electrostrictive force, \mathcal{F} , acting on it is in the direction normal to the membrane and can be written as [19]:

$$\mathcal{F} = \frac{1}{2} E \cdot q = \frac{1}{2} \frac{V_m}{D} q = \frac{1}{2} \frac{C_m V_m^2}{D}$$

The effect of this force on membranes is a reduction of thickness and increase of the area, phenomena that are generally linked to the melting transition. Therefore, an increase in transmembrane voltage could in principle melt the membrane.

The work done upon the melting transition by the electric field, at fixed voltage is given by:

$$\Delta W_c = \int_{D_g}^{D_f} \mathcal{F} dD = \frac{1}{2} \epsilon_0 V_m^2 \int_{D_g}^{D_f} \epsilon \frac{A}{D^2} dD \quad (2.25)$$

where D_g and D_f are the membrane thickness in the gel and in the fluid state. The area of the membrane is also state dependent while we will keep for the time being the assumption of [19] of a constant value for the dielectric constant.

Voltage dependence of the melting temperature

The enthalpy of the system in presence of a voltage V_m , at temperature T as:

$$\Delta H(V_m, T) = \Delta H_0(T) + \Delta W_c(V_m) \quad (2.26)$$

where ΔH_0 is the change in the melting enthalpy at temperature T introduced in section (thermodynamics) in absence of any external contribution, and $\Delta W_c(V_m)$ is the electrostrictive work defined in eq. (2.25), according to which we have:

$$\Delta H(V_m, T) = \Delta H_0(T) + \frac{1}{2} \epsilon_0 \epsilon V_m^2 \int_{D_g}^{D(T)} \frac{A(T)}{D(T)^2} dD(T)$$

where $\Delta H_0(T)$ is the change in enthalpy in absence of an electric field, and the second term on the right hand side is the electrostriction work introduced before. Using the proportionality relation (2.17) for the area changes, and

assuming that a similar one holds for thickness changes, one can solve the integral and find the change in enthalpy as a function of temperature and voltage (see [19] for the details of the calculations). The main feature is that, considering a fluid phase where $T \gg T_m$, one has $\Delta H_0(T) \equiv \Delta H_0$, and the resulting voltage dependence of the enthalpy is:

$$\Delta H(V_m) = \Delta H_0 + \alpha_0 V_m^2 \quad \text{with } \alpha_0 = -141.7 \frac{J}{V^2}$$

According to the definition (2.9) the melting temperature of the membrane in absence of voltage is $T_{m,0} = \Delta H_0 / \Delta S_0$, with ΔH_0 and ΔS_0 the enthalpy and entropy change during the transition. In presence of voltage, the melting temperature can be written as :

$$T_m = \frac{\Delta H(V_m)}{\Delta S_0} = \frac{\Delta H_0 + \alpha_0 V_m^2}{\Delta S_0} = \frac{\Delta H_0}{\Delta S_0} + \frac{\alpha_0}{\Delta S_0} V_m^2 = (1 + \alpha V_m^2) T_{m,0} \quad (2.27)$$

with $\alpha = \alpha_0 / \Delta H_0 = -0.003634 [1/V^2]$. The melting temperature has a quadratic dependence of voltage. The effect of electrostriction is small at physiological voltages. For a transmembrane voltage of 500 mV the shift in the melting temperature of DPPC due to electrostriction does not exceed 0.3K. For 1V the melting temperature decreases of about 1K. Remarkably, Helfrich in 1970 predicted a similar quadratic shift of the melting temperature in the electric field for liquid crystals; furthermore he speculated on the possible role of the different values of the relative permittivity in the different state of the crystal [63]

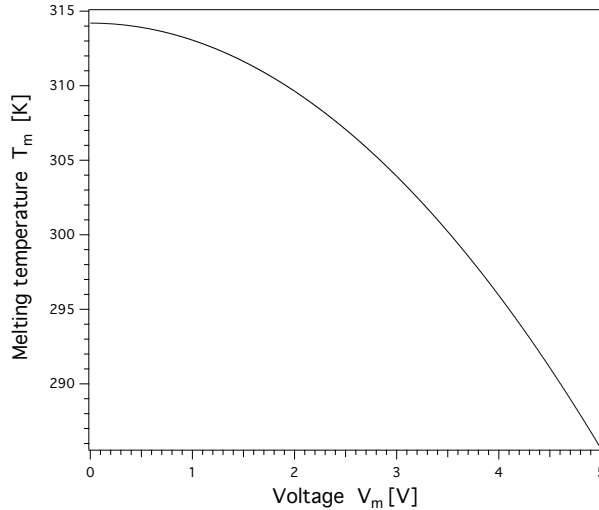


Figure 2.10: Shift in the melting temperature as a function of voltage as derived in eq.(2.27).

Further independent experiments would be essential to put some light on the topic. Nevertheless, it seems that electrostriction is one of the possible electrical effects influencing the melting transition of lipid bilayers. It has to be noted that the whole derivation is made in the assumption of a constant relative permittivity of the membrane interior, thus neglecting dielectric and polarization effects. These will be considered in the theoretical part of this thesis.

Piezoelectricity

The above mentioned effect of electrostriction can be summarised as voltage induced mechanical force acting on the capacitor-like system. In biomembranes the opposite is also true: mechanical forces or pressure can induce an electric field. This particular case of electromechanical coupling goes under the name *piezoelectricity*. Electro-mechanical properties have received much attention in the biomembrane community both theoretically and experimentally [23, 64], mainly because of the analogy between lipid membranes and liquid crystals, as it will be pointed out in the polarization section. Here the thermodynamical approach of Heimburg [19] is presented.

At fixed temperature, the change in the charge on the membrane leaflets is only a function of voltage and mechanical force \mathcal{F} acting on the membrane:

$$dq = \left(\frac{\partial q}{\partial V_m} \right)_{\mathcal{F}} dV_m + \left(\frac{\partial q}{\partial \mathcal{F}} \right)_{V_m} d\mathcal{F}$$

Here, \mathcal{F} is the mechanical force perpendicular to the membrane. Because of the coupling between area and thickness changes in membranes, a force such as \mathcal{F} is equivalent to a lateral pressure Π , so that the previous can be written as:

$$dq = \left(\frac{\partial q}{\partial V_m} \right)_{\mathcal{F}} dV_m + \left(\frac{\partial q}{\partial \pi} \right)_{V_m} \left(\frac{\partial \pi}{\partial \mathcal{F}} \right)_{V_m} d\mathcal{F} \quad (2.28)$$

Where, writing explicitly the mechanical coupling between perpendicular forces and lateral pressures, all the other quantities being constant:

$$d\pi = \left(\frac{\partial \Pi}{\partial \mathcal{F}} \right) d\mathcal{F}$$

Therefore, eq. (2.28) becomes:

$$dq = \left(\frac{\partial q}{\partial V_m} \right)_{\pi} dV_m + \left(\frac{\partial q}{\partial \Pi} \right)_{V_m} d\pi \quad (2.29)$$

At fixed lateral pressure, eq. (2.29) is equivalent to eq. (2.23) and one sees only voltage induced changes in charge. When the voltage is kept constant one can still see changes in charge produced by changes in lateral pressure.

The effect of lateral pressure is a change in the area of the membrane, phenomenon that, as we've seen in section (thermodynamics), is linked to the melting process.

In the context of membrane phase transition, in presence of piezoelectricity, the melting enthalpy (2.26) must now include also the work done by the pressure to change the area from A_g to $A(T)$:

$$\Delta H(T, V_m, \pi) = \Delta H_0(T) + \Delta W_c(V_m) + \Delta W_A(\Pi) \quad (2.30)$$

with:

$$\Delta W_A(\Pi) = \Pi \gamma_A \Delta H_0(T)$$

In the fluid phase ($T \gg T_m$), one sees that the enthalpy is quadratic in the voltage and linear in the lateral pressure:

$$\Delta H(V_m, \Pi) = \Delta H_0(1 + \alpha V_m^2 + \gamma_A \Pi)$$

which result in a shift in the melting temperature of:

$$T_m = \frac{\Delta H(V, \Pi)}{\Delta S_0} = (1 + \alpha V_m^2 + \gamma_A \Pi) T_{m,0}$$

Starting from eq. (2.29) one can find all the electromechanical coupling coefficients. The case of constant temperature and pressure has been already treated and corresponds to voltage induced changes in charge which are expressed by the capacitive susceptibility. The other cases of constant voltage or constant charge are more interesting because the electromechanical properties and the susceptibilities of the electromechanical system come out naturally from the formalism introduced:

- $T, V_m = \text{const}$

Lateral pressure induced change in charge. Starting for example from the fluid phase, the pressure will make the membrane more solid; this corresponds to a decrease in the capacitance, and thus a release of charge at constant voltage (pressure induced capacitive currents). The correspondent susceptibility is the derivative of an extensive variable with respect to a non conjugated intensive one, so it can assume negative values:

$$dq = \left(\frac{\partial q}{\partial \Pi} \right)_{T, V_m} d\Pi \quad \Longrightarrow \quad \beta_V \equiv \frac{\partial q}{\partial \Pi}$$

- $T, q = \text{const}$

Pressure induced change in the voltage, i.e. piezoelectricity. Starting from a fluid phase, with the value of q correspondent to a voltage of $1V$, the mechanical work done by the pressure to change the distance between the fixed charges would result in a change in voltage (and vice versa):

$$0 = \left(\frac{\partial q}{\partial V_m} \right)_{T, \Pi} dV_m + \left(\frac{\partial q}{\partial \Pi} \right)_{T, V_m} d\Pi$$

$$dV_m = - \left[\frac{\left(\frac{\partial q}{\partial \Pi} \right)_{V_m}}{\left(\frac{\partial q}{\partial V_m} \right)_{\Pi}} \right] d\Pi \quad \implies \quad \beta_q = \frac{\partial V_m}{\partial \Pi} = - \frac{\beta_V}{\hat{C}_m}$$

2.2.2 Polarization

Lipid membranes are considered as insulators. Electrically speaking, one can distinguish between conductors and insulators (as well as semiconductor, superconductor or more exotic materials) based on their peculiar interaction with an external electric field. Conductors are characterised by the presence of charges that are free to move through the material. In insulators, on the other hand, the electric charges (electrons or ions) are only free to move around their specific atom or molecule. Based on this definition, one can describe the interaction between electric field and the lipid membrane in analogy with the dielectric materials. While in conductors the effect of an electric field is the production of a current (flux of free charges), in insulators the effect would be the *polarization* of the material. Polarization (or, more precisely, polarization density) in a material is defined as the average dipole moment per unit volume:

$$\vec{P} = \frac{\langle \vec{\mu} \rangle}{V} \quad (2.31)$$

where the electric dipole moment $\vec{\mu}$ is a measure of the separation of positive and negative charges in a system of charges. For a system of two opposite point charges q separated by a distance d , the corresponding electric dipole is given by $\vec{\mu} = q\vec{d}$, where \vec{d} points from the negative to the positive charge.

A note on units: electric dipole has the units of $C \cdot m$, thus the polarization density has the units of C/m^2 .⁷

Microscopic polarization mechanisms There are two mechanism by which a material can be polarized depending on the nature of its constituent molecules: inducing an electric dipole, or orientating a pre-existing one.

⁷The whole section is inspired by [65]

The former mechanism is a distortion of the charge distribution through stretching. In a neutral atom under an electric field, the centre of mass of the negative and positive charges are teared apart until this is counterbalanced by their electrostatic attraction. The result is a separation of positive and negative charges, i.e. an electric dipole. For normal electric fields (small compared to the dielectric breakdown voltage ⁸), the induced dipole is approximately proportional to the electric field, $\vec{p} = \alpha \vec{E}$, where α is the atomic polarizability, and it's different for every atom. In the most general case of an asymmetrical non polar molecule, the polarizability is substituted by the polarizability tensor α_{ij} , since it may be polarized with different degree in the different directions.

In the latter mechanism, a polar molecule experiences a torque in a uniform electric field (uniform on the molecular scale), which tends to align its preexisting dipole moment in the direction of the field.

The general case is usually a combination of the two, since also polar molecules can undergo displacement polarization (even though the alignment effect is dominant). Nevertheless, the two mechanisms have the same result, that is the presence of microscopic dipoles aligned with the field. The material is then said to be polarized, its macroscopic polarization being defined as in (2.31).

Being made of a non polar hydrocarbon chain and a polar head group, lipid molecules interaction with electric fields can be described by their polarization.

Linear dielectrics In linear dielectrics the presence of an electric fields produces a polarization, by lining up the atomic or molecular dipoles. The polarization for this kind of material is considered proportional to the field itself in the following way:

$$\vec{P} = \epsilon_0 \chi \vec{E} \quad (2.32)$$

The proportionality constant χ , the *electric susceptibility*, is dimensionless and it depends on the microscopic structure of the material and on other external quantities such as temperature.

In most cases, the temperature dependence of χ means that the value of the polarization will also change with T , but the proportionality relation will hold for every temperature. In a system like lipid bilayers, this is not necessarily true. If the electric susceptibility is a function of temperature (or, of the state of the membrane), then thermoelectric (or electrocaloric) effect could arise [66], in which a change in electric field produces a change in

⁸Dielectric breakdown appears in dielectrics when the field is so high to make the medium conductive

temperature, thus resulting in a non linearity of the relation between \vec{P} and \vec{E} . This could also be caused by electromechanical effects, where mechanical strain could result in nonlinear polarization.

In these cases (2.32) is just an approximation and one would have to quantify those effects and eventually correct it.

It is also known that (2.32) holds only for small electric fields (small compared to the dielectric breakdown of the materials). For general strengths, it represents the first nonzero term in the Taylor expansion of P in powers of E , whereas for higher values of the field one would have to consider higher nonlinear terms.

By these considerations it follows that a linear polarization in the field can be considered as first order approximation of the more general theory of nonlinear dielectrics.

Electric susceptibility and permittivity The electric susceptibility (χ) is closely related to the dielectric constant (ϵ), since they are both quantities related to the microscopic structure of the dielectric and to its response to electric fields. Their relation can be explicitly written by using the definition of the electric displacement field \vec{D} in linear media:

$$\vec{D} \equiv \epsilon_0 \vec{E} + \vec{P} = \epsilon_0 \vec{E} + \epsilon_0 \chi \vec{E} = \epsilon_0 (1 + \chi) \vec{E}$$

where in the second equality eq. (2.32) has been used. The proportionality coefficient between the displacement and the electric field is the *permittivity* of the material:

$$\epsilon \equiv \epsilon_0 (1 + \chi)$$

Here ϵ is the permittivity of the material, which coincides with ϵ_0 in vacuum (from which the name *vacuum permittivity*, since there is no matter and thus χ is zero).

The permittivity has to be distinguished from the *relative permittivity*, ϵ_r , commonly referred to as *dielectric constant*. This a dimensionless quantity defined by:

$$\epsilon_r \equiv 1 + \chi = \frac{\epsilon}{\epsilon_0}$$

It's straightforward that all the considerations done for the electric susceptibility apply also for the relative permittivity, which can thus also be function of external quantities like temperature or electric fields.

A final remark on the nomenclature: it's easy to get confused by the symbols and the names for the dielectric properties, which happen to vary a lot among the literature. Throughout this thesis the following terminology and notation will be adopted:

- Vacuum permittivity: $\epsilon_0 = 8.854 \cdot 10^{-12} F/m$
- Relative permittivity: $\epsilon = 1 + \chi$ (the subscript r will be omitted). When ϵ is a constant and doesn't depend on other variables, it takes the most common name of *dielectric constant*
- Absolute permittivity: $\epsilon = \epsilon_0 \epsilon$, which, in order to avoid confusion, it won't be used in the rest of the thesis.

Flexoelectricity

Flexoelectricity is a phenomenon predicted by Meyer [67] in the context of liquid crystals and the further developed by Alexander G. Petrov [68], who studied its relevance in lipid bilayers.

Meyer started from the work of Frank [69] who demonstrated through symmetry arguments the intrinsic relationship between splay strains⁹ and electric polarization in liquid crystal. While Frank considered polar systems with preexisting spontaneous splay or polarizations, Meyer applied his consideration to non polar systems where either splay or polarization is externally induced by mechanical stress or an electric field, respectively [67]. He called this phenomenon "*a peculiar kind of piezoelectricity*"; the term *flexoelectricity* was coined later on by De Gennes [71] to distinguish the flexion origin of the phenomenon in liquid crystals from the stress origin of normal piezoelectricity in solid crystals [72]. In the end, flexoelectricity is the liquid crystal analog of piezoelectricity: while the latter involves a translational degree of freedom (such as area stretching, thickness compression as pointed out in the previous section), flexoelectric effects involve an orientational degree of freedom, namely the membrane curvature [70, 72].

The system studied by Meyer is in full analogy to lipid bilayer structure, with the difference that he studied bulk properties (so volume polarization) of a 3D liquid crystal, whereas membranes are commonly described by their surface properties. Both structures (liquid crystals and biomembranes) show long range translational disordering in contrast to a long range orientational ordering of their building units, lipids or general rod-like molecules [70]. Liquid crystals can be divided in two major families: thermotropic and lyotropic. Biological structures, and especially biomembranes, can be considered lyotropic for their amphiphilic nature and their behaviour in solvents [72] and

⁹splay is a term of liquid crystals elasticity which in the context of bilayers can be translated as a fan-like deformation in the lipid molecules orientation [68]. Splay, bend and torque are all expressed as partial derivatives of the liquid crystal director. In 2D, curvature of the membrane surface corresponds to a splay deformation [67, 70]

thermotropic since their structural properties are strongly affected by temperature.

Let's consider a symmetric flat membrane. Let's also fix a frame of reference with origin in the midplane of the bilayer and coordinate z in the direction of the normal to the membrane plane. If no electric fields are applied to it, then symmetry consideration lead us to the conclusion that the total polarization is zero.

$$P_s = \int_{-\infty}^{\infty} P(z)dz = \int_{-\infty}^0 P(z)dz + \int_0^{\infty} P(z)dz = 0 \quad (2.33)$$

where P_s is the polarization per unit area (C/m)¹⁰.

The antisymmetry of the polarization distribution $P(z)$ guarantees that surface polarization vanishes in such a system. Every mechanism able to break this antisymmetry will result in a non zero polarization. One of the possible mechanisms is the presence of curvature and this is the object of study of flexoelectricity. Another possible cause could be an asymmetric composition in the two leaflets of a membrane.

In the end, flexoelectricity is an electromechanical coupling between curvature and polarization: curvature can induce electric polarization and electric fields can induce curvature. It has to be noted that flexoelectricity is not a mere physical speculation for its own sake, but it has a great relevance in biology. Curved membranes are ubiquitous in biological system. Highly convoluted shapes are assumed by some biomembranes (the cristae of inner mitochondrial membranes, the edges of retinal rod outer segments and discs, the brush border of intestinal epithelial cells and so on [72]), with curvature radii on the nanoscale [70]. Their dynamical nature makes it possible to deform themselves adapting to external conditions [73, 74] (just think of erythrocyte cells, which can change dramatically their shape in order to pass through very narrow blood vessels), therefore the importance of understanding the resulting polarization effects in curved membranes. On the other hand, biomembranes can sustain huge curvature deformations, compared to in-plane distortions such as stretching or compression, and this is due to the

¹⁰ When studying membrane properties, definitions of material properties are commonly given in area units (averaged over membrane thickness) rather than in volume units [72]. Therefore P_s is the surface polarization (units of C/m), in contrast to the volume polarization defined in (2.31) and referred to as P (units of c/m^2). The two are related by:

$$P_s = P \cdot d$$

where d is the thickness of the bilayer. This clarification will be useful later on.

relative small value of their bending rigidity. Thus the response in curvature to external stimuli like external fields is expected to be relevant. In addition to this, membrane curvature has been studied by the physics community since the inspiring work of Helfrich ¹¹ [76] on the elastic properties of membranes and Evans [77], representing an exemplary case of applications of pure physical methods and laws to a biological system.

Eq. (2.33) is based on intuitive symmetry considerations, but what are the real sources of polarization in membranes? To answer to this question we have to analyse closely the lipid structure in order to find which parts contributes to the vertical dipole moment.

Dipole moments in lipid bilayers Lipid molecules, either charged or zwitterionic, possess large dipole moments. Most of the information concerning such electric dipole moment can be extracted from monolayer experiments. Monolayers are formed at the air-water or oil-water interface and the interfacial potentials between the two medium are measured. Dipole potentials and moments are related by the Helmholtz equation which states that the voltage difference across an array of dipoles μ of surface density $n = 1/A$ (with A are per lipid molecule, so area per dipole) is given by :

$$\Delta V = \frac{\mu}{\epsilon_0 A}$$

Experimentally, most of the lipids display similar potentials of the order of 300 to 500 mV, the air or oil being positive with respect to water [78]. Taking an area per lipid of $0.7nm^2$, one obtains a dipole moment per lipid in the range $1.9 \div 3.1 \cdot 10^{-30}C \cdot m$ directed toward the hydrophobic core [72, 79]. If one assumes that the electric dipole of a lipid molecule is entirely produced by the polar head group, this value is much smaller and in the opposite directions respect to our intuition. Furthermore, calculations made with quantum-chemical procedures for the same system in vacuum (in absence of water) produced values one order of magnitude smaller and in the intuitive direction (pointing out of the hydrophobic core) [80, 81]. The reason for this discrepancy is the effect of the hydration shell made of water molecules around the dipolar heads of lipid.

In contrast to our intuition, the electric dipole moment of lipid molecules is not exclusively concentrated in the polar head group. The electric dipole of the zwitterionic (or charged, the reasoning is the same) head group $\mu_{zwitter}$ produces a strong local field which orients the nearby water molecules. Water dipoles, μ_{H_2O} , are oriented towards the interior of the membrane, and

¹¹who, interestingly, has been also investigating on flexoelectricity [75]

compensate μ_{zwitt} . As a result, the total dipole moment of a phospholipid molecule in excess water is largely dominated by two dipolar groups which are hidden in the hydrophobic part, thus inaccessible to water, namely the polar ester linkage between fatty acid and the glycerol backbone (μ_{ester}) and the terminal CH_3 groups (μ_{end}) which carry a positive charge [79]. Both these contribution points in the right direction. Consequently, the dipole moment in the previous equation can be written as a sum of three contributions:

$$\mu = \mu_{head} + \mu_{H_2O} + \mu_{end} \quad (2.34)$$

where $\mu_{head} = \mu_{zwitt} + \mu_{ester}$ is the sum of the contributions from dipolar head group and the ester linkage.

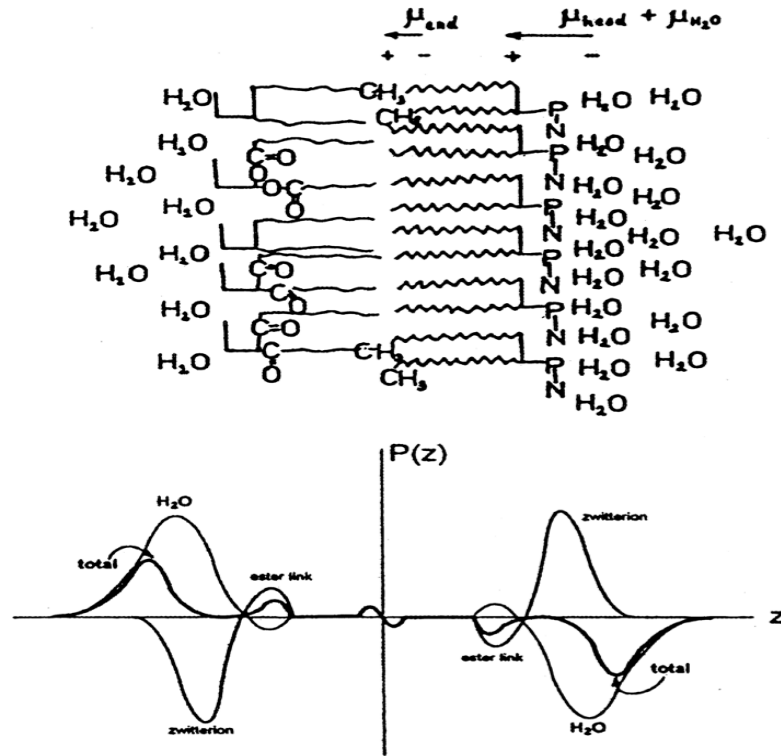


Figure 2.11: *Top*: Schematic representation of a phospholipid bilayer. The arrows show the direction of the electric dipole contributions. *Bottom*: asymmetry of the total polarization distribution with respect to the bilayer midplane. The contributions from the water, the ester links and the zwitterionic head groups are also shown. Figure taken from [82]

In fig.2.11 it is shown the correspondent profile for the polarization distribution along the bilayer thickness, and the resulting antisymmetry around

the midplane. It's even more clear now, how the total dipole moment of one leaflet is exactly counterbalanced in magnitude and direction by the one of the opposite leaflet in the case of a symmetric flat membranes.

Direct flexoelectricity Direct flexoelectricity is the name for curvature induced polarization in lipid bilayers. As already anticipated, curvature is able to break the antisymmetry of the polarization distribution along the bilayer, thus yielding a non zero surface polarization. The phenomenological expression of this phenomenon has been explicitly formulated by Petrov in 1975 [68]:

$$P_s = f \left(\frac{1}{R_1} + \frac{1}{R_2} \right) \quad (2.35)$$

where R_1 and R_2 are the principal radii of curvature in $[m]$ and f is the flexoelectric coefficient in $[C]$. As a convention, the flexocoefficient is positive if the polarization points outward the centre of curvature.

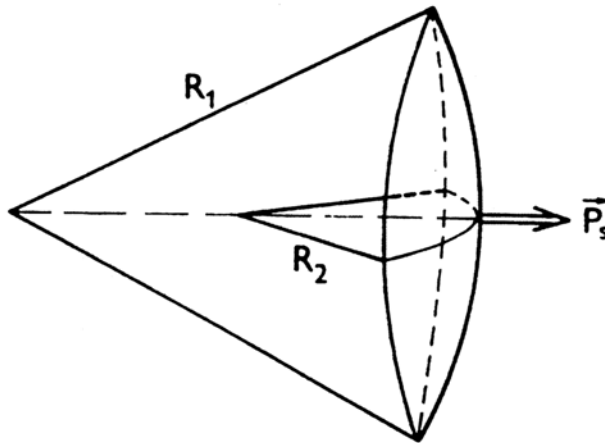


Figure 2.12: Flexoelectric polarization and sign convention about the flexocoefficient f : in this case f is positive since the polarization points outward the centre of curvature. R_1 and R_2 are the principal radii of curvature. Figure taken from [82]

Let's compare this expression with the original phenomenological one derived by Meyer for the volume polarization of a 3D liquid crystal. In presence of a splay deformation, the resulting bulk polarization is written as [67]:

$$\vec{P}_v = e\vec{S} = e\vec{n}(\vec{\nabla} \cdot \vec{n})$$

where $\vec{S} = \vec{n}(\vec{\nabla} \cdot \vec{n})$ is the polar splay vector and \vec{n} is the normal to the surface. Since in two dimensions one has:

$$\vec{\nabla} \cdot \vec{n} = \frac{\partial n_x}{\partial x} + \frac{\partial n_y}{\partial y} = c_1 + c_2 = \frac{1}{R_1} + \frac{1}{R_2}$$

and since we consider surface polarization, the analog in 2D is:

$$P_s = P_v \cdot d = e \left(\frac{1}{R_1} + \frac{1}{R_2} \right) d$$

which is the same as (2.35), provided the splay and the flexoelectric coefficients are related by:

$$f = e \cdot d$$

This will turn out to be useful in the context of membrane phase transition, where the thickness cannot be considered constant anymore.

In the theory of Petrov two dipolar mechanisms are considered, which can break the symmetry of the system with a curved membrane: blocked lateral diffusion and blocked *flip-flop*, and free lateral diffusion and free *flip-flop*. Flip-flop as already mentioned in the introduction, is the transverse redistribution of lipids between the two leaflets of the membrane.

- **Blocked lateral diffusion and blocked flip-flop**

This mechanism corresponds to the pure bending of a connected bilayer. Suppose the membrane is made of two coupled layers, corresponding to the two leaflets. Then, pure bending constraints imply that one layer is stretched and the opposite is compressed of the same quantity, the midplane remaining unchanged.

Let's call the number of lipids per unit area of the midplane $n_0 = 1/A_0$, and μ_0 the electric dipole per lipid in the flat state. As a result of the stretching-compression, lipid molecules will change conformation, these area changes being maximal in the head group region [79]. Consequently the dipole moment per lipid will be different in the two monolayers. Because of the lateral and transverse redistribution constraint, the density of dipole in the two layers will remain constant (see fig.2.13a).

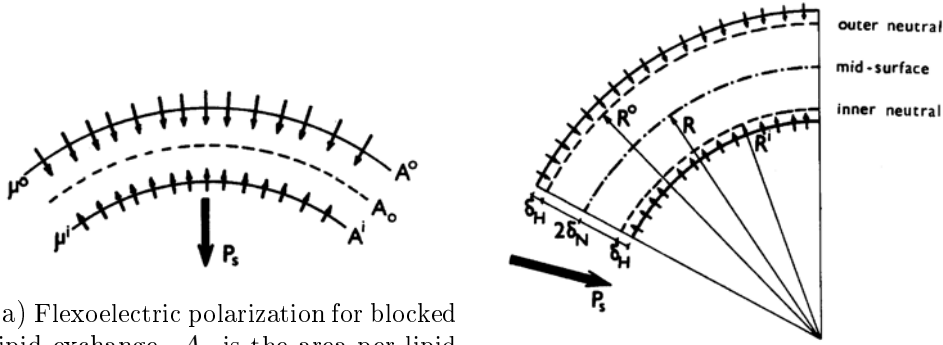
Finally, as a result of the bending, the bilayer displays a dipole unbalance between the two leaflets, thus having a nonzero total dipole moment. The curved membrane is thus polarized:

$$P_s = P_s^i - P_s^o = n_0(\mu^i - \mu^o)$$

Assuming the the changes in the dipole moment are only due to the mechanical stress, one finds for the flexocoefficient:

$$f^B = - \left(\frac{d\mu}{dA} \right)_{A_0} \cdot d$$

The values for the change in μ with the area are given either by Monte Carlo simulations or by experimental curves of the surface potential as a function of the area per lipid.



(a) Flexoelectric polarization for blocked lipid exchange. A_0 is the area per lipid with respect to the midsurface. A^o and A^i are the area per lipid of the outer (expanded) and inner (compressed) membrane surface. μ^o and μ^i are the dipole moment per lipid of the outer and inner surface, respectively. The number of lipids per unit area of the midsurface is the same in the two monolayers.

(b) Flexoelectric polarization of a bent membrane for free lipid exchange. δ_N is the distance between the neutral surface and the midsurface, δ_H is the distance between the neutral surface and the headgroup surface. The dipole moment per lipid is the same in the two monolayers.

Figure 2.13: Flexoelectric polarization for blocked and free lipid exchange. The pictures are taken from [83].

- **Free lateral diffusion and free flip-flop**

This mechanism correspond to the bending of two uncoupled monolayers (or of an unconnected beam). In this case dipoles can redistribute in both directions, thus the dipole density can be different in the two leaflet. As a result of the bending, flip-flop and lateral diffusion can occur to relax the differences in density and mechanical stress.

The dipole moments are assumed to stay constant, so the two leaflets differ in their area (now they have their own neutral surface which doesn't coincide to the midplane) and in the dipole density (see fig.2.13b). The curved membrane is again polarized, the surface polarization being:

$$P_s = P_s^o - P_s^i = (n^o - n^i)\mu_0$$

The flexocoefficient is now expressed by:

$$f^F = \frac{\mu_0}{A_0} 2\delta_N$$

δ_N being the distance between the midplane and the neutral surfaces of the two layers.

Flip-flop in bilayers are known to be slow and energetically expensive processes. Furthermore they are likely to play a role when the stress induced by the curvature is so large, that it may be convenient for the membrane to redistribute its lipids rather than sustain the stress.

For this reason, the flexoelectric considerations at the melting transition made in this thesis, will consider mainly the blocked case.

Direct flexoelectricity has been experimentally proven in the 70's. No matter how it is generated, if a membrane has a non vanishing polarization, the Helmholtz equation quantifies the voltage difference across it. The flexoelectric part of it is:

$$\Delta V = \frac{P_s}{\epsilon_0} = \frac{f}{\epsilon_0} (c_1 + c_2) \quad (2.36)$$

Such a voltage difference can be measured across curved membranes. The simultaneous measurement of the membrane curvature, makes it possible to estimate the flexoelectric coefficient.

Converse Flexoelectricity As for piezoelectricity in solids, also flexoelectricity display a direct and a converse effect. The latter corresponds to electric field induced curvature. The first observation of the converse flexoelectric effect arrived almost 20 years after the first measurements of the flexocoefficient [84] and its phenomenological expression is given by:

$$c_1 + c_2 = \left(\frac{f}{K} \right) E \quad (2.37)$$

Applying a transmembrane electric field E to a membrane of curvature elastic modulus K and flexocoefficient f , produces a curvature $c_+ = c_1 + c_2$. This is a result of the interaction of the electric field with the membrane dipoles. Due to the antisymmetric electric properties of the membrane, an external electric field perpendicular to the plane of the membrane, would orient the dipoles differently in the two leaflets, thus inducing a conformational change which result in a nonzero curvature.

All these consideration are made for lipid membranes far from the transition, and no temperature effects are considered (not even far from the melting). Sometimes it is not even clear in which lipid phase the measurements are performed. Since biomembranes at body temperature are very close to their melting transition, and since in the transition quantities as membrane thickness, area or elastic moduli have peculiar behaviours, it's interesting to see study the flexoelectric effects in the membrane phase transition. This will be done in section 4.1.2.

2.3 Permeability

Cells are not closed systems with respect to their environment (and neither the different compartments inside the cells). As higher organisms, they constantly need nutrient elements from the outside (sugars, amino acids, oxygen, etc.) to stay alive, and at the same time they need to get rid of waste substances. Besides this transport functions, the cell membrane has to provide signaling and communication. For these reasons biological membranes must have permeability properties. This function is achieved through channels which can regulate the permeability and select which ions can flow. Such electrical currents through the membrane are used to explain several cell activities: from nerve pulse propagation in excitable cells, to cell-to-cell signaling or transport in cells and organelles.

Permeability measurements on pure lipid membranes are the main content of the experimental part of this thesis. In this section a theoretical framework is provided, which will be useful to understand the relevance of permeability investigation on lipid membranes.

Ion channels are mainly believed to be pore-containing transmembrane proteins. However, pure lipid bilayers show the same properties in the absence of proteins, suggesting the existence of lipid channel. Both are briefly reviewed in the following.

2.3.1 Protein ion channels

Protein channels are believed to be selective doors for ions (especially sodium and potassium), imbedded in a apparently inert and impermeable membrane. They can exist in a closed (non conductive) and an open (conductive) state¹². The closed channels can open as a consequence of voltage, binding of ligands,

¹²Structure and functioning of protein channels won't be described in details, because it is beyond the purposes of this thesis. Furthermore, only protein-free lipid bilayers will be considered hereafter

temperature, pH or mechanical changes. Such a property is called *gating* (note that the same variables can affect the thermodynamical state of the membrane). When a channel opens, ions can diffuse inside and outside the cell following their concentration gradients (such a property is called *permeation*). This flow of ions is the origin of electrical currents that can change the potential difference across the membrane.

Experimental studies about protein channels involve mainly their structure and their function.

- **Structure**

Information about the atomic structure of ion channels can be obtained with X-ray crystallography. Potassium channel was the first channel to be crystallised in 1998 by MacKinnon [85]. The problem of structural studies is that they are necessarily static. They give no information about the functioning of the protein.

- **Functioning**

Information about the functional role of protein channel is obtained by measuring the electrical current flowing through them when they are in their open state. Single channel recording in biological membranes were first performed by Neher and Sakmann in 1976 [86, 87]. They introduced the patch-clamp technique, for which they won the Nobel Prize in 1991. The technique consists in placing a small pipette on a cell surface applying little suction. This allows to investigate patches with size of the order of few μm , thus containing few channels. The electrical properties of the patch of membrane are measured through two electrodes: one in the body of the cell and the other inside the pipette. With the introduction of the patch-clamp technique, systematic measurements of channel currents through biological membranes have been performed ever since. Such currents present common features. Current recordings show quantised step from a closed state (zero current) to open state with characteristic amplitudes. Typical time scales of such opening-events are in general between 1 and 100 ms and their typical amplitude for voltages of 100 mV is about 1 – 50 pA (corresponding to a characteristic conductance of 10 – 500 pS) [9].

The ionic current flowing across the membrane is the result of the diffusion of ions along their concentration gradient and the drift current of ions along the potential difference across the membrane¹³. For an ion species i of

¹³Voltages across the membrane can be originated by unbalanced charged particles (ions) concentrations, or (for example in electrophysiology experiments) by holding the membrane at a certain voltage through electrodes.

valence z , with different concentrations inside, $[C_i]_i$, and outside, $[C_i]_o$, such a balance is described by the Nernst equation:

$$E_{0,i} = \frac{RT}{z_i F} \ln \frac{[C_i]_o}{[C_i]_i} \quad (2.38)$$

where R is the gas constant, T is temperature, F is the Faraday constant ($F = e \cdot N_A$, with e electron charge and N_A the Avogadro number). E_0 is called the Nernst potential (or reversal potential) and it is the value of the membrane voltage at which there is no net flow of ion of a species i through the membrane. This corresponds to the equilibrium, where diffusion and drift flow cancel out.

For voltages different from $E_{0,i}$, one sees a current of ions of specie i through their channel which is given by:

$$I_i = g_i(V_m - E_{0,i}) \quad (2.39)$$

where g_i is the conductance of the channel, and $(V_m - E_{0,i})$ is the driving force for the current of ions i . It is the difference between the actual membrane voltage and the equilibrium voltage, for which no flow of ions i is observed.

If more channels (permeable for different ions) are present in the membrane, then the membrane ionic current, I_m , is the sum of all the contributions from the different channels. The equilibrium potential, in this case, must be redefined since it has to take into account the concentration gradients of all the ions species the membrane is permeable to. In the case of sodium (Na^+), potassium (K^+) and chlorine (Cl^-), it is given by:

$$E_R = \frac{RT}{zF} \cdot \ln \frac{P_{Na}[Na^+]_o + P_K[K^+]_o + P_{Cl}[Cl^-]_i}{P_{Na}[Na^+]_i + P_K[K^+]_i + P_{Cl}[Cl^-]_o}$$

where P_{Na} , P_K , P_{Cl} are the permeabilities of the different ions.

Finally, the membrane conductance G_m (the sum of all the conductances g_i), can be written as:

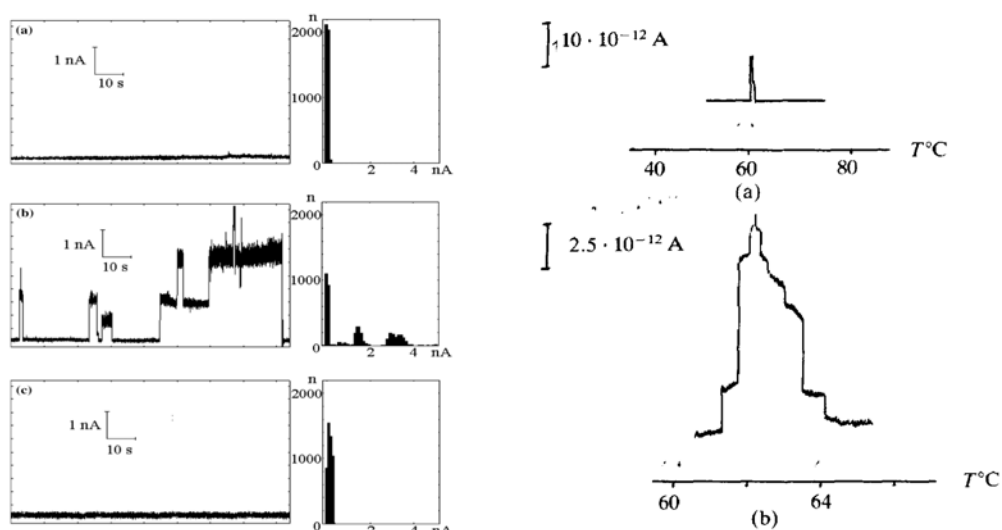
$$G_m = \frac{I_I}{V_m - E_R}$$

where $I_I = \sum_i I_i$ is the total ionic current. G_m is a function of any quantity which can gate the opening of channels (e.g voltage in the Hodgkin-Huxley model).

2.3.2 Lipid ion channels

Parallel to the development of proteins channel research field, permeability studies on pure lipid membranes advanced starting from the 1970's.

Experimental evidence Increase in permeation rates of ions at the lipid melting transition was already known back in 1973 [88]. The year after Yafuso et al. recorded channel events on oxidised cholesterol membranes [89]. This happened two years before the same events were recorded on biological membranes. Since then, several studies reported channel-like conduction events on lipid films [50,90–95]. The striking feature of such lipid channels is the resemblance to the behaviour of protein ones. Conductance, amplitudes, mean lifetime, are all of the same order of magnitude.



(a) Antonov measurements on the increase of channel-like activity of a pure lipid bilayer of DPPC in the phase transition [94]. *Left panel*: current fluctuations for different temperatures. *Right panel*: current histograms of the correspondent current traces. From the top: (a). Fluid phase. $T = 50^\circ\text{C}$. (b). Melting transition. $T = 43^\circ\text{C}$. (c). Gel phase. $T = 35^\circ\text{C}$.

(b) Measurements of phase transition temperature in a DPPA (phosphatidic acid) bilayer by conductance jump, performed by Antonov [96]. The applied voltage is 10 mV . The melting temperature measured by differential scanning calorimetry for DPPA is $T_m = 67^\circ\text{C}$, [97], thus in agreement with the jump in conductance measured by Antonov. Picture taken from [96].

Figure 2.14: Increase in permeability and channel-like activity at the phase transition of lipid bilayers.

The techniques to investigate permeability on lipid membranes will be explained in chapter 3. It has to be noted that, while it is possible to measure channel activity of lipid bilayers in the absence of proteins, the opposite is not possible. Therefore, the appearance of channel-like events in biological

membranes cannot be taken as unique proof for the protein channel behaviour without accurate controls on the lipid matrix. Two current traces showing channel events in lipid and biological membranes are shown in fig. 2.15.

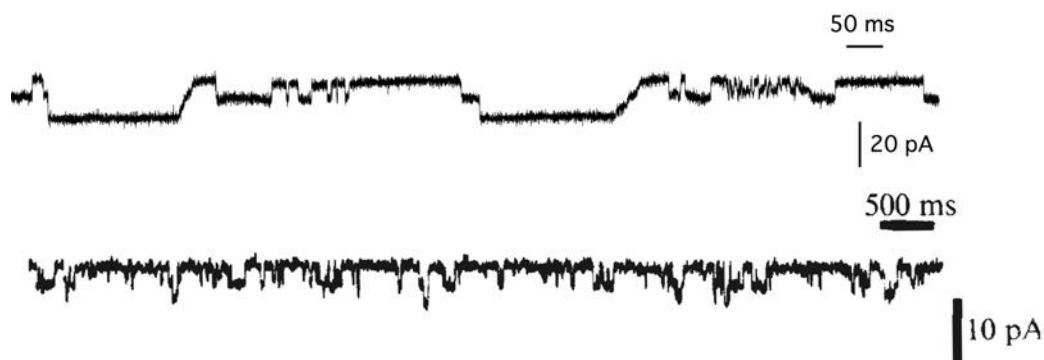


Figure 2.15: *Top*: channel events in a DMPC bilayer, measured as described in chapter 3. *Bottom*: patch-clamp recordings from a biological membrane. [86]

Lipid pores The lipid pore model is one mechanism that has been proposed to explain the increase in permeability and in the channel-like activity of lipid membranes in their melting transition. It assumes that ions can cross the bilayer through transient hydrophilic pores that result from thermal fluctuations [9, 95, 98, 99]. In such a way, ions don't need to overpass the hydrophobic barrier, but can easily permeate through the pores.

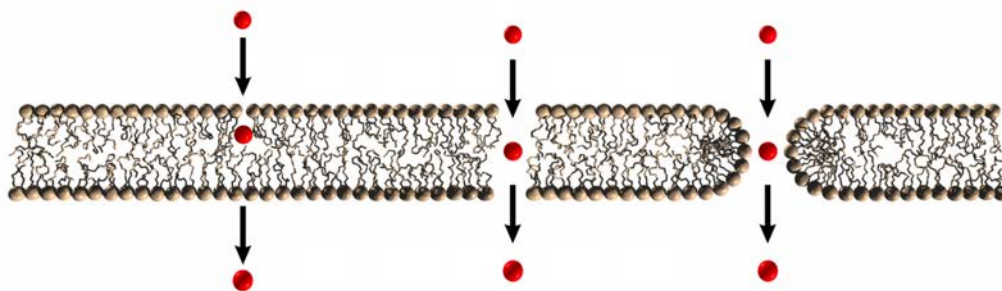


Figure 2.16: Models for lipid channels. *Left*: the solubility-diffusion model. Particles permeate through small defects in the bilayer crossing the hydrophobic core. *Center*: hydrophobic pore. *Right*: hydrophilic pore. Picture taken from [8]

Pores have been estimated to have a size of the order of the nm [100, 101]. Both their opening likelihood and open lifetimes are related to fluctuation

amplitudes and lifetimes, thus they reach a maximum value in the melting transition (see section 2.1.1). The relative conductivity of lipid membranes has been shown to be correlated to the heat capacity profile in the melting transition [102]¹⁴(see fig.2.17). Furthermore, all the quantities which are known to gate the opening of protein channels (voltage, temperature, pH, mechanical stress and so on), have been proved to influence the melting behaviour of lipid bilayers, and thus the appearance of pores [92,96]. Therefore, if the basic properties characterising an ion channel are permeation and gating, lipid pores seem to have both of them.

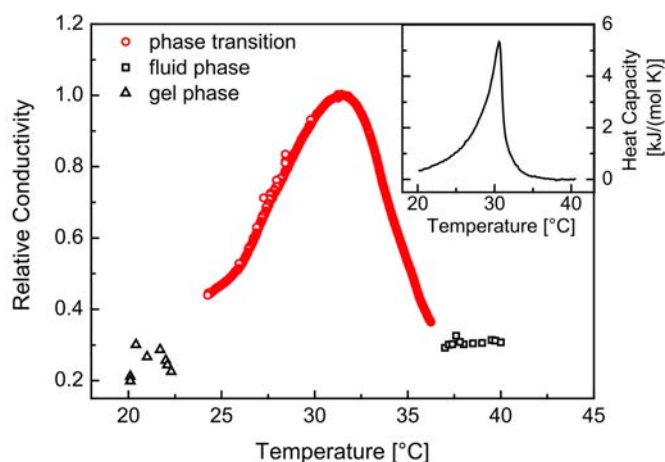


Figure 2.17: Correlation between the heat capacity (*black curve*) and the relative conductance of a lipid bilayer made of D15PC:DOPC=95:5 (*red curve*). Both the curves show a pronounced peak in the melting regime (between 25°C and 35°C). Figure taken from [102]

It has been proposed [99] that the free energy for pore formation in presence of voltage is given by:

$$\Delta G = \Delta G_0 + \alpha(V_m - V_0)^2 \quad (2.40)$$

Here ΔG_0 is the free energy difference between an open and a closed pore in absence of voltage (thus depending mainly on composition, temperature and pressure), α is a coefficient that is constant when temperature and pressure are constants, V_m the applied voltage, V_0 is an offset voltage reflecting the asymmetry of the system. A possible explanation for the offset voltage will

¹⁴This, in principle if not in practice, would lead to use the increase in conductivity as a sign to detect phase transition in lipid bilayers. Note that this approach has already been used by Antonov and collaborators [96].

be given in section 4.1.2. Eq.(2.40) is derived assuming that voltage induced pores are originated by the electrostrictive forces induced by charging the membrane capacitor.

The equilibrium constant between an open and a closed state for a lipid pore, $K(V_m)$, is defined in analogy to eq.(2.11), with ΔG given by (2.40). One can then calculate the likelihood of the opening of a pore as in (2.10):

$$P_{open} = \frac{K(V_m)}{1 + K(V_m)}$$

In permeability experiments where electrical currents are measured for different fixed potential, the current-voltage relation can be interpreted in the framework of the pore model in the following way:

$$I_m = \gamma_p \cdot P_{open} \cdot (V_m - E_0) \quad (2.41)$$

where E_0 is the Nernst potential defined in (2.38)¹⁵, γ_p is the conductance of a single pore and P_{open} is the probability that a pore is open.

One can see that eq.(2.41) is similar to eq.(2.39). In such analogy the term $\gamma_p P_{open}$ would correspond to the membrane conductance. The likelihood P_{open} is a function of every variable which can influence the transition. Therefore, P_{open} contains the gating mechanism of lipid pore channels.

Fore the sake of completeness, it has to be mentioned that the pore model which assumes the formation of transient hydrophilic pores in the membrane is not the only model proposed to explain permeability in lipid bilayers. Other models are represented in fig.2.16. Nevertheless only the hydrophilic pore model will be considered in this thesis.

¹⁵For lipid membranes in aqueous solution with the same ions concentration on both sides, the Nernst potential is zero.

Chapter 3

Materials and Methods

3.1 Materials

1,2-Dimyristoyl-*sn*-Glycero-3-Phosphocholine (DMPC) and 1,2-Dilauroyl-*sn*-Glycero-3-Phosphocholine (DLPC) were purchased from Avanti Polar Lipids (Birmingham/AL, USA), stored in a freezer at -18°C and used without further purification. Purity was higher than 99%.

Potassium chloride (KCl) were provided by from Fluka Chemie AG (Deisenhofen, Germany). EDTA (*ethylenediaminetetraacetate acid*) and HEPES (4-(2-hydroxyethyl)-1-piperazineethanesulfonic acid) were obtained from Sigma Aldrich (St. Louis/MO, USA). Chloroform, methanol, *n*-decane were purchased from Merck (Hohenbrunn, Germany).

MilliQ water with a resistivity higher than $18\text{M}\Omega\cdot\text{cm}$ has been used throughout all the experiments. Purification was performed by a desktop EASY pure RF water purification system from Barnstead/Thermolyne (Dubuque/IA, USA). Measurements of pH were done using a "pH 538" pH-meter (WTW GmbH). For dissolving the lipids, an ultrasonic cleaner Sonorex (Bandelin electronic GmbH, Berlin, Germany) and a magnetic stirring hotplate Heidolph 3001 (Sigma Aldrich) were used.

Calorimetric measurements were performed using a differential scanning calorimeter (DSC) of type VP-DSC produced by Microcal (Northhampton/MA, USA). Permeability experiments were mostly made using a Ionovation Bilayer Explorer purchased from Ionovation GmbH (Osnabrück, Germany), employing an EPC10 amplifier (HEKA, Lambrecht/Pfalz, Germany).

An automatic chlorider ACI-01 (npi electronic GmbH, Germany) was used to chlorinate the electrodes in the permeability experiments. Optical monitoring of the bilayer was performed through an inverted microscope Olympus (Tokyo, Japan) IX70 in optical mode. The objective used was an Olympus

UPlan APO 60x, water immersion. Numerical aperture, N.A.=1.20. Working distance, W.D= ∞ /0.13 – 0.21 mm.

3.1.1 Sample preparation

In order to mimic the physiological environment of the lipid membranes, for both calorimetry and permeability studies, a saline solution with concentration 150mM of KCl has been used. The electrolyte solution consisted also of 1 mM EDTA and 1mM HEPES. The former helps avoiding bacteria contamination by binding to calcium (among the other) which is a nutrient for bacteria. The latter is a buffer compound which is used to keep the pH constant. Keeping the pH constant is essential, since the phase transition of phospholipid has been proved to depend strongly on the pH [4, 113]. Throughout the experiments, the pH of the electrolyte has been adjusted to a final value between 7.3 and 7.4. The solution was gently heated and stirred with a magnetic bar for approximately 20 minutes until all the components were uniformly dissolved.

The preparation of the lipid samples may introduce errors due to differences in the lipid amounts (mainly linked to the precision of mass and volume measurements). This could result in melting temperatures and behaviour which is different than the ones reported in the literature. To reduce the error, syringes and scale with the highest precisions have been used. However, the residual error can be neglected, since for all the samples used in permeability experiments, heat capacity profiles have been determined with the calorimeter and taken as reference for the transition behaviour.

Lipid sample preparation

The lipids were taken out of the freezer and warmed at room temperature before opening of the container to avoid the absorption of water molecules from the environment and the consequent change in their molecular weight.

Stock solutions of each lipid species were prepared by dissolving the lipid in chloroform to a final concentration of 10 mM. Lipid mixtures were obtained by mixing the stock solutions at the desired ratio. The sample was dried under a gentle flow of nitrogen and then placed under vacuum overnight, to remove residual solvent. This has been done throughout all the experiments concerning lipids. Dissolving lipids in chloroform (or other organic solvents like dichloromethane), is essential for having an homogeneous mixing of the single lipid components.

Calorimetric measurements For calorimetric measurements, the dried sample was resuspended in the buffer solution to a final concentration of 10 mM. The sample was then shaken in a ultrasonic cleaner until the solution was uniformly milky, which indicates that it consisted of mostly multilamellar vesicles dispersion. Before filling the calorimeter, both the lipid sample and the reference solution were degassed for 10 minutes in order to remove air micro-bubbles.

Permeability experiments For permeability experiments with Ionovation Bilayer Explorer (IBE), the dried lipid sample was dissolved in *n*-decane to a final concentration of 10 mg/mL. Finding a proper solvent for the lipid samples investigated in this thesis turned out to be a problematic task. Not only the solvent has to properly dissolve the lipids but it also has to be suited for the setup used. IBE is a slight modification of a BLM setup (as it will be explained in section 3.2). Having been recently introduced in the market, it lacks of literature one can refer to. Most of the literature refers to bilayers made of mixtures of lipids (mainly POPC and POPE) which have different solubility properties and different transition temperatures respect to the ones employed in this thesis (mainly DMPC and DLPC) [114]. In a first attempt, decane:chloroform:methanol=7:2:1 (by volume) has been tried, being the solvent used by Antonov in his 30 years of experiments with BLMs [115]. Nevertheless, the bilayer formation and stability turned out to be problematic. Other different solvents and concentration had been tried, with poor results in terms of membrane formation. Finally, the best compromise was to use decane. The problem with decane is that the lipid mixtures used are not soluble in it at room temperature. Therefore, the lipid solutions were heated to a final temperature above the sample phase transition, until it looked perfectly transparent, and then used immediately after.

3.2 Methods

The experimental techniques used in this thesis concerned calorimetric measurements and permeability experiments. The latter has been mainly investigated through a new instrument which has similar features to the BLMs setup. For a short period, (preceding the purchase of the IBE), a patch clamp setup has been used. Therefore, not only the method used for most of the experiments will be described, but, for sake of completeness, also the Montal-Mueller and patch clamp technique will be briefly reviewed.

3.2.1 Calorimetry

Calorimetric measurements were made on every sample used in this thesis to determine the transition of the lipid mixtures.

Differential Scanning Calorimetry (DSC) is a very powerful and sensitive experimental technique by which the melting properties and structural transitions of a sample can be investigated. For the purposes of this thesis calorimetry has been used to determine the heat capacity of a sample as a function of temperature.

The DSC consists of two cells which are contained in an adiabatic box to avoid uncontrolled heat exchange with the environment. A schematic representation of the apparatus is shown in fig. 3.1. One cell contains the sample (in our case the lipid in the buffer solution) and the other one contains a reference solution (in this case the buffer). The temperature of the cells is changed at a fixed rate (set by the experimenter) by two Peltier heaters, one for each cell. At the same time, the temperature difference between the two cells is kept to zero. The power of the two heaters is adjusted in order to fulfil these two requirements (constant scan rate and zero temperature difference). The DSC records the power difference between the two cells as a function of temperature. In an endothermic process, such as the melting of lipids, the sample requires more heating power than the reference in order to increase its temperature, therefore melting processes are characterised by a peak in the power difference between the cells.

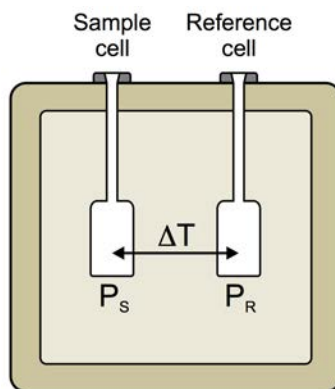


Figure 3.1: Scheme showing the cells inside the calorimeter.

The excess heat, ΔQ , of such a process can be obtained by integrating the excess power, ΔP with respect to time:

$$\Delta Q = \int_t^{t+\Delta t} \Delta P(t') dt' \simeq \Delta P \cdot \Delta t$$

According to eq.(2.13), the excess molar heat capacity at constant pressure can be calculated:

$$\Delta c_p = \left(\frac{dQ}{dT} \right)_P \simeq \left(\frac{\Delta Q}{\Delta T} \right)_P = \frac{\Delta P}{\Delta T / \Delta t}$$

where $\Delta T / \Delta t$ is the scan rate. Knowing the heat capacity profile, one can calculate the melting enthalpy and melting entropy by simple integration, as it's been shown in eqs.(2.14-2.15).

3.2.2 Summary of permeability experimental technique

Artificial lipid membranes can be formed and studied by means of different techniques. During this thesis a modified version of the Montal-Mueller method has been mostly used for permeability experiments. However, few preliminary measurements have been performed using the droplet method, which is a modified version of the patch-clamp technique. This method will be also briefly described and compared to the one used.

The droplet method

This technique has been developed by Hanke [116] and consists of the formation of a planar lipid bilayer at the tip of a glass patch-clamp pipette. The glass pipette is prepared according to the patch-clamp procedure [86], and the whole setup resembles the one used in patch-clamp experiments. A scheme of the protocol for membrane formation is shown in figure 3.2.

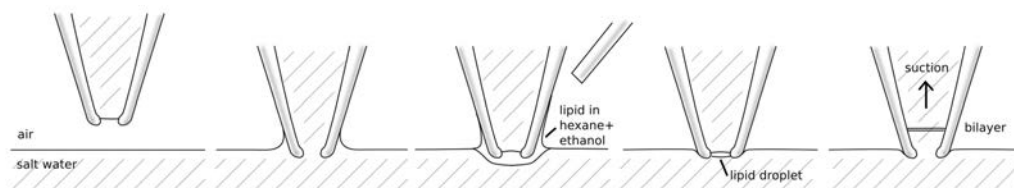


Figure 3.2: Sequence of pictures schematically showing the formation of a lipid bilayer with the droplet method. Picture taken from [117].

The pipette and a beaker are filled with an electrolyte solution and placed closely on top of each other (with the tip of the pipette a few mm over the surface of the salt solution of the beaker). Fine movements of the pipette are allowed by a micromanipulator holding the pipette. Lipids are dissolved in a highly volatile solvent (i.e. hexane in the original paper of Hanke) and a drop of lipid solution ($10 - 20 mm^3$) is allowed to run down the pipette's

outer surface. The lipid spreads out and spontaneously forms a bilayer, thus sealing the tip. The solvent diffuses in the aqueous solution of the beaker and later evaporates. This leaves the tip of the pipette closed by a solvent-free bilayer. The pipette is then lowered 4–5 mm below the bath surface to avoid the mechanical stress at the bath surface. Gentle suction can be applied so that the lipid droplet thins out into a bilayer.

Electrical measurements are performed through two electrodes connected to a headstage that works as pre-amplifier. One electrode is inside the pipette, and the second one (connected to the ground of the headstage) is placed inside the beaker. One has to be careful that the ground electrode doesn't touch the pipette. The beaker is placed on top of a brass block (heater jacket in fig. 3.3), whose temperature can be controlled through a thermostatic bath.

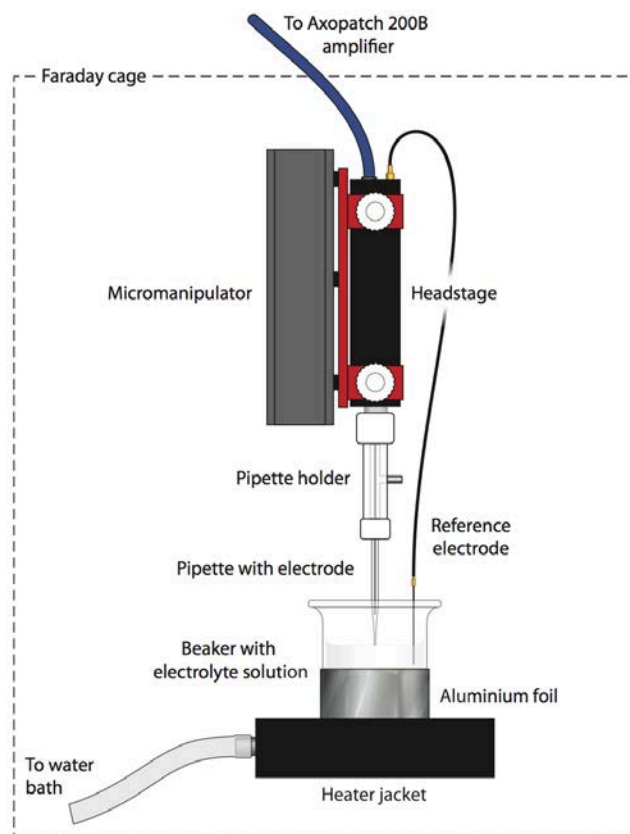


Figure 3.3: Schematic representation of the setup described in the text. The picture is taken from [8]

The signal coming from the headstage is then further amplified by a patch

clamp amplifier. The formation of a bilayer is monitored through capacitance measurements. A scheme of the setup is shown in fig. 3.3.

A variation of the droplet method is the so called *tip-dipping* technique [116]. It uses the same setup described above, with the difference that the formation of the bilayer is enhanced by slowly dipping the pipette tip into a monolayer a couple of times. The advantages of the method are that the bilayer is guaranteed to be solvent-free and asymmetrical membranes can be created by dipping the tip in different monolayers. The former advantage, however, is payed off by a decrease of mechanical stability respect to the bilayers formed with the droplet method.

The Montal-Mueller method

The Montal-Mueller method is the standard technique when dealing with BLM. It consists of the formation of a planar lipid bilayer on the aperture of a Teflon film by the apposition of two monolayers spread at the water/air interface. Most of the literature about electrical measurements on artificial membranes cited in this thesis, refers to planar bilayer formed using the method developed by Montal and Mueller in 1972 [118].

The setup consists of two compartments containing an electrolyte solution, which are separated by a hydrophobic film (most commonly made of Teflon). The principle of the technique is showed in fig.3.4

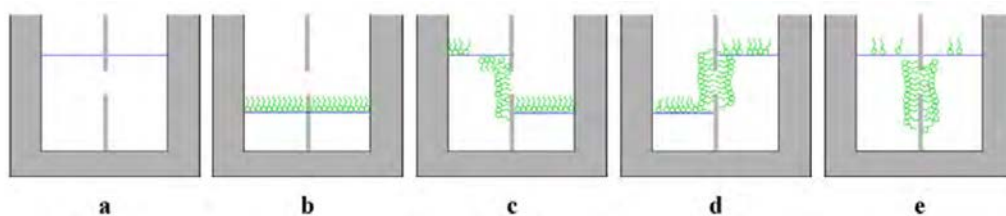


Figure 3.4: Schematic representation of the BLM formation, as explained in the text. The picture is taken from [119]

Initially, the hydrophobic septum is preprinted with a non volatile solvent (such as hexadecane) which helps to reduce the mechanical stress at the edges of the aperture. Afterwards, the two compartments are partially filled with an electrolyte solution (to a level below the aperture on the septum), and the lipid solution is spread on the bath surface in both the compartments. The lipids will then self-assemble in the form of a monolayer at the air/bath surface. The solvent is allowed to evaporate for 10-15 minutes, after which the bath level in the two compartments is raised and lowered until the bilayer is formed. One Ag/AgCl electrode is placed in each compartment. As for

the droplet method, formation of a bilayer is monitored through resistance and capacitance methods.

3.2.3 Ionovation Bilayer Explorer

For the purposes of this thesis, planar lipid bilayers were studied using a Ionovation Bilayer Explorer purchased from Ionovation GmbH (Osnabrück, Germany).

The instrument allows to combine semi-automated horizontal bilayer formation to high resolution microscopy and single molecule spectroscopy. The principle of the method resembles the Montal-Mueller technique. The main differences are two. On one hand the bilayer is formed horizontally in the so called *detection unit*, which can fit any inverted microscope, allowing optical monitoring of the membrane at any step of the experiment. On the other hand, the buffer exchange in the micro-chambers and thus the bilayer formation is achieved through the *control unit* of the instrument, which allows for precise liquid handling.



(a) Detection Unit



(b) Workstation of the detection unit

Figure 3.5: Pictures of the detection unit containing the bilayer. The pictures are taken from the website of the company, [120]

Description of the setup

The detection unit is placed on the work stage of an inverted microscope (see fig 3.5b). It is connected to the control unit through 4 silicone microtubes, and to an EPC10 amplifier through the headstage. The control unit and the amplifier are also connected. The amplifier is connected to a personal computer where the Patchmaster software allows complete control of the whole setup.

Detection unit The detection unit of the instrument is shown in fig. 3.5a. It consists of:

- A shielding lid which acts as a Faraday cage. It has an aperture on the top to allow inverted microscopy, which, if needed, can be perfectly closed ensuring electrical shielding of the unit.
- A headstage (coloured in blue in fig. 3.5a) which provides preamplification of the signal. It has a BNC-port a ground port in which two electrodes can be plugged in. The signal collected by the headstage is preamplified and sent to a HEKA EPC 10 patch-clamp amplifier.
- A mobile carriage. It carries the microfluidics of the system. They consist of four silicon microtubes with an inner diameter of 1.6 mm . They provide automatic perfusion of the buffer solution in the two chambers and they are connected to the control unit.
- The stage unit, where the bilayer slide is placed. It has a triangular cut on the bottom to allow optical measurements.

Bilayer Slide The two compartments of the Montal-Mueller setup are substituted by a compact disposable bilayer slide containing two microchambers (*cis* and *trans*) with a volume of approximately $150\ \mu\text{L}$ each. A detailed representation of the slide is given in figure 3.6. The upper (*trans*) and lower (*cis*) compartments contain a laser-edged channel structure each, which are filled with the saline buffer. The only connection between the two channels is the small aperture in the $25\ \mu\text{m}$ Teflon film. The aperture of the slide has a diameter between 80 and $100\ \mu\text{m}$, it is laser-edged but can vary between different slides. The cover slide is transparent and the distance between it and the planar bilayer is $100\ \mu\text{m}$, thus within the working distance of high-numerical-aperture objectives. Finally, the top slide contains four openings for perfusion (two for each chamber), two ports for the electrodes and an opening for the lipid injection. Once the bilayer slide is placed on the stage unit, the carriage fits the four perfusion microtubes in the corresponding apertures in the bilayer slide. A section of the bilayer slides with a scheme of the electrical circuit is shown in figure 3.7.

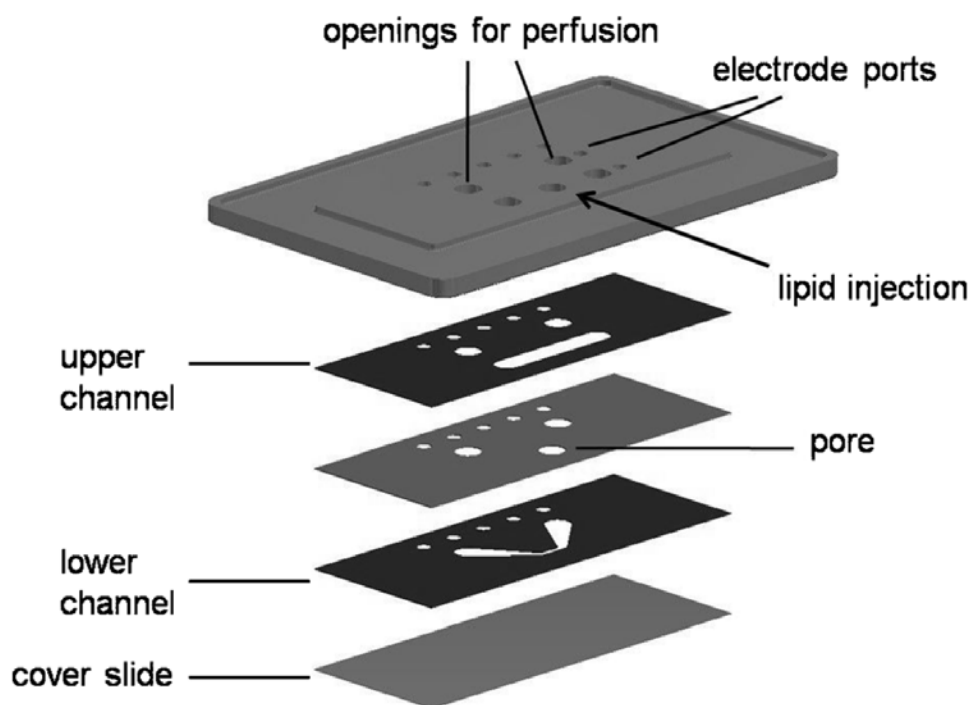


Figure 3.6: Structure of the bilayer slide. A PTFE (polytetrafluoroethylene, *Teflon*) foil contains the aperture (pore) for the bilayer formation and it is sandwiched between the *cis* and *trans* chamber, as explained in details in the text. The figure is taken from [114].

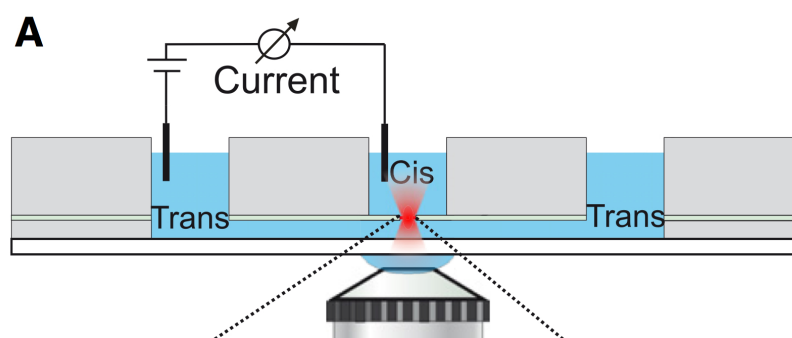


Figure 3.7: Schematic section of the bilayer slide, showing the two compartments and the inverted microscope on the bottom. No distinction between the electrodes port and the perfusion apertures is shown in the picture. Picture adapted from [121]

Control unit The control unit (see fig. 3.8) consists of an automated liquid handling and perfusing system. Buffer solution is contained in two 10 mL syringes with "Luer lock" flange. Perfusion of buffer solution in the chambers is provided by two syringe motors, which allow the content of the syringes to flow in the microtubes and then in the two chambers independently. In this way, one is able to set an asymmetric aqueous environment for the bilayers, for example by varying the ionic strength of the solution in one of the two chambers. The excess buffer perfused in the bilayer slide is aspirated by a peristaltic pump which pumps it into a waste container. Both the syringe motors and the peristaltic pump can be controlled manually on the control unit through a control panel. However, complete control of the unit's functions can be achieved through the software.



Figure 3.8: Control unit. The picture is taken from the website of the company, [120]

Electrodes Two Ag/AgCl electrodes are plugged in the BNC-port and into the ground port of the headstage. They are connected to the two chamber through two L-shaped glass tubes. The bended tip of the glass tube is dipped into a flask with melted agarose (in our case 1% agarose in a 2M KCl buffered solution), so that the agarose fills only the bended part. The rest of the tube is filled with the high concentrated salt solution. The electrodes are placed in the glass tubes and are in contact with the buffer but not with the agarose. The bended tip of the glass tube is immersed in the electrode ports of the bilayer slides. Attention must be paid in filling the glass microtubes in order to avoid microbubbles. The agar bridge helps to reduce the

noise by allowing only the flow of ions through it and towards the electrodes. Electrodes functioning can be checked by inserting them in a beaker with measuring buffer while plugged to the headstage. This should correspond to a short circuit, and the eventual electrode offset potential can be cancelled through the software. The electrodes were chlorinated every time the offset potential exceeded 10 mV . In practice, this was required approximately once every two or three days of experiments. Chlorination was performed through an automatic chlorider, which contains an electronic control unit that automatically chlorides silver wires by electrolysis. The electrodes are connected to the electronic control unit and immersed in a beaker with a 2 M KCl solution. By inverting the polarity of the internal battery, both the electrodes are coated with chloride.

Bilayer formation

Before starting the experiments, the bilayer slide needs to be filled with the measuring buffer. This simple operation must be done with attention, since, due to the small dimensions of the channels, microbubbles of air can hinder the free flow of the solution. Once the bilayer slide is properly mounted in the detection unit and connected to the headstage, a voltage pulse test is performed to assure the presence of a short circuit.



Figure 3.9: Optical monitoring of the bilayer formation.

After this preliminary test, a volume of about $0.2\ \mu\text{L}$ of lipid solution is added on the aperture of the Teflon foil through the bilayer access port with a microliter syringe. Lipid painting on the aperture and the subsequent membrane formation through thinning of the bilayer is performed automatically by pumping cycles controlled by the software. The software monitors the bilayer formation via capacitance measurements and repeats the procedure until a stable bilayer is in place. The threshold value of the capacitance

above which a bilayer is considered formed can be set by the experimenter. Assuming a bilayer diameter of $100\ \mu\text{m}$ and a typical membrane capacitance value of $0.5 - 1\ \mu\text{F}/\text{cm}^2$ [122–124], the absolute capacitance value should lie approximately in the range $35 - 75\ \text{pF}$. A value of $40\ \text{pF}$ was set as a threshold. The formation was then checked by optical observation of the aperture. An example of optically well behaving membrane is given in fig.3.9.

Temperature Control The rate of success of IBE in forming stable bilayers can be increased by controlling the temperature, since bilayers are more likely to form when the lipids are in their fluid phase. The Ionovation Bilayer Explorer in our lab has been recently equipped with a temperature control unit (*Thermomaster*, Ionovation GmbH). The unit is connected to a water bath and regulates the temperature by adjusting the volume of water circulating in the new designed bilayer slides through an internal pump. However, at the time of the experiments of this thesis, the Thermomaster was not on the market yet. When dealing with electrical properties of membranes at their melting transition, being able to change the temperature of the system is an essential task. Therefore, alternative home made methods have been adopted to achieve the purpose. First of all, only lipid mixture with their melting transition close to room temperature (which varied between 23 and 26°C) were used. The system was cooled by the apposition of ice close to the bilayer, and heated exploiting the irradiation heat of an office lamp. These procedures resulted in the following problems:

- The range of temperatures that could be covered was limited, usually never more than 5° below or above the room temperature. Therefore, only lipid mixtures with a relatively narrow transition could be used, in order to investigate their properties in both the gel and the fluid phase.
- The heating and cooling rate could not be regulated and it was generally very fast, on the order of $1^\circ\text{C}/\text{minute}$. Therefore, lipid mixtures with too narrow transition couldn't be used.
- As it will be shown in the results (chapter 4), the scan rate of heating or cooling can influence the behaviour of the phase transition. This is mainly due to the fact that the typical relaxation time scales of membranes are larger in the transition. Therefore not being able to regulate the scan rate may affect the reproducibility of the results.

The temperature was monitored with 0.1°C accuracy, through a sensor immersed in the upper channel.

Electrical measurements

The electrical measurements were done in a voltage-clamp whole cell mode of the EPC10 amplifier, controlled through the Patchmaster software. The signals were digitalised with a sampling frequency of 10 kHz ¹. The current traces were filtered by a 2 kHz low-pass filter. The output gain was set to 10 mV/pA .

Extreme care has to be taken in connecting everything to ground, in order to decrease the electrical noise. Even though the detection unit is shielded by its grounded metal lid, the whole workstation of the detection unit was placed inside a Faraday cage.

The company provides several protocols for electrical measurements. They are based on different voltage pulse sequences, which can be slightly modified and tailored by the experimenter. However, the design of a complete measurement protocol from scratch can be very much time-consuming.

The Patchmaster software allows to perform online data analysis simultaneous to the data acquisition. This is a very powerful tool, since it permits to change the parameters in order to optimise the recording.

Comparison between the techniques

Despite the automatic procedure employed by the IBE to form bilayer, the number of attempts per membrane formation is way bigger than 1. Furthermore, this rate seems to be almost independent on the experimenter skills, because of the little number of variables that can be changed in the procedure. Therefore, after working with this setup one realises that planar lipid membranes are an intrinsically tricky system to work with and very instable mechanically. The automatic procedure, however, makes the technique much less time consuming.

Another big difference is in the size of the membrane patches. Pipette tips in the droplet method have diameters which can change between 1 and $5\text{ }\mu\text{m}$, the regularity of their shape depending on the experimenter skills. This corresponds to a difference in areas between different tips that are comparable or even bigger than the typical tip size. The apertures on the bilayer slide, however, are made with a laser (thus regular in shape) and can vary between 80 and $100\text{ }\mu\text{m}$, thus inducing a smaller variability between different experiments.

A part from reproducibility problems, the droplet method has another intrinsic defect. The size of the tip is comparable with the size of lipid do-

¹which corresponds to a time resolution of $100\text{ }\mu\text{s}$, thus small enough to catch channel-like events, whose lifetime is on the order of the ms .

mains [125]. This could mean that in a sample made of a lipid mixture, the membrane on the tip is only made of one lipid species or that during the transition only macro-domains of one state are observed. Having a bigger aperture, the IBE allows to have a statistically more significative view of the system, which however, is payed off by a smaller stability and a higher background noise from the leaky currents, thus resulting in problems in optimising the signal to noise ratio.

Finally, the optical monitoring of the bilayer turned out to be a very powerful tool. Some membranes, in fact, have to be discarded despite their capacitance value is above the threshold. It is very easy to detect optically whether a membrane is well formed or it is the result of massive intrusion of solvent. A pure capacitance monitoring is not able to discern it. Control experiments have been performed adding only the solvent on the aperture. These resulted in small values of the capacitance (smaller than the threshold) and in optically recognizable patterns. The droplet method is free of such problem because it is assumed to be solvent-free [116]. However, in a Montal-Mueller setup this could induce considerable errors in the measurement.

Chapter 4

Results and Discussion

From the background theory of the electrical properties of membranes, two questions arise which up to now haven't been answered:

1. How would the electrical properties (especially related to capacitive and electrostrictive effects) change, if one considers a change in the relative permittivity of the medium with its physical state instead of assuming it constant and unaffected by quantities, such as temperature or electric field? Is it possible to extend the findings of the last chapter to this case?
2. How can one extend the flexoelectric theory to include explicitly thermodynamical changes of the system close the phase transition? How relevant are the flexoelectric effects for the thermodynamics of the system?

The aim of the theoretical part of this thesis (and the content of the first part of this chapter) is to answer to these two questions. The concepts introduced in the theoretical background, not only helped to formulate such questions, but provided the knowledge and the methods to find the answers, or eventually, to address new questions.

In the experimental part of the thesis, the theoretical predictions were investigated using the methods explained in chapter 3. Due to the absence of a temperature control at the time of the experiments, only preliminary results have been obtained. They are shown and discussed in the second part of the chapter, together with suggestions on how to perform and improve the measurements in order to test the theoretical predictions.

4.1 Theory

Assumptions In order to catch the main features of the problem, the following assumptions have been made:

- The bilayer in the aqueous medium is assumed to behave as a planar capacitor filled with dielectric, with the peculiar property of changing its macroscopic geometry (and thus its capacitance) in response to external stimuli like voltage or temperature.
- The dielectric inside the capacitor is now also allowed to change its molecular structure (and thus, its relative permittivity) as a consequence of the structural changes in the phase transition.
- The membrane interior is considered a linear material with respect to dielectric properties. This assumption differs from [19], where the capacitive susceptibility introduces nonlinearity of the electric charge with the voltage.
- In absence of any reliable data on the change in ϵ with the state of the membrane, it will be assumed that like other geometrical properties of the system, also the relative permittivity is proportional to the melting enthalpy. This assumption will be discussed in detail later.
- Changes in the orientation of the polar heads due to an external electric field will be neglected. The molecular effect of the field, at this stage, is studied only through its effect on the dielectric constant.
- The relative permittivity is assumed to be uniform in space. The bilayer is considered as a slab of uniform dielectric material. Its value is considered the same in the hydrophilic and hydrophobic parts, which are known to have very different dielectric properties. This is a frequent assumption, especially in investigations on the macroscopic properties of this kind of systems¹. From this assumption it follows that a voltage V_m across the membrane results in an electric field $E = V_m/D$, where D is the thickness of the membrane. However, the membrane thickness is not a constant of the system. It's been already showed that it's value changes of about the 16% during the melting transition, and it is also affected by voltage. As a result, at fixed voltage, the electric field inside

¹One could avoid this assumption by modelling the membrane as a series of three capacitors having different dielectric constants.

the membrane is also function of its physical state:

$$E(T) = \frac{V_m}{D(T)}$$

4.1.1 Dielectric effects

Being related to the molecular structure of the material, the dielectric constant of lipid membranes is very likely to change between the fluid and gel state. This is suggested for example by the fact that paraffin oil has a higher dielectric constant (2.2-4.7) than the paraffin wax (2.1-2.5) [19], this accounting for a change in the bulk properties of the membrane (paraffin has a similar structure to the hydrocarbon interior of the membrane). The same can be expected for the head groups, which undergo changes in their orientation in the gel→fluid transition [103], as shown in fig. 4.1.

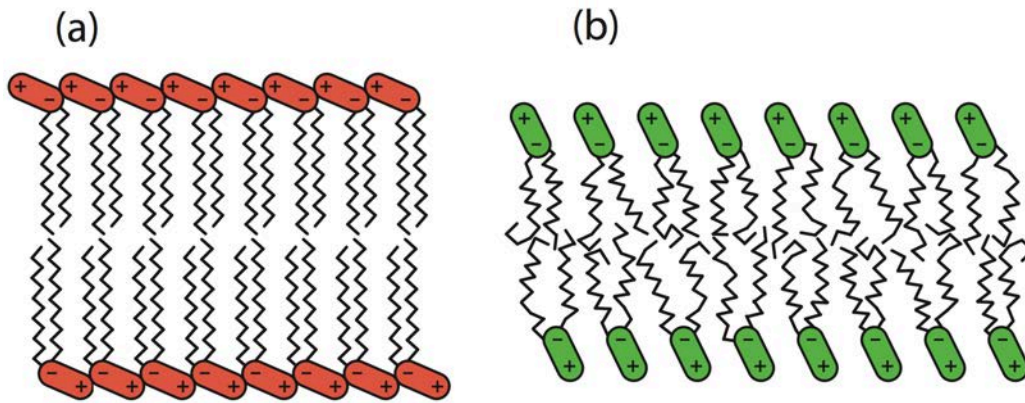


Figure 4.1: Schematic configuration of a lipid bilayer in the gel (a) and in the fluid phase (b). Note the different orientation of the polar heads in the two states. Picture taken from [8].

Most of the literature on the electrical properties of membranes uses the assumption adopted by Heimburg [19] of a constant relative permittivity. Some authors do consider the space-dependence and anisotropy of the dielectric constant using complicated tensor models, disregarding other kind of dependence, especially temperature dependence [104, 105]. One remarkable exception is represented by Helfrich, who as early as 1970, speculated on the effect of voltage on the mesomorphic-isotropic transition of liquid crystals. He found similar results to [19], but in his model he also considered the contribution from the different values of ϵ in the different states of the lipids [63]; his quantitative results though, are strongly dependent on the

system studied and thus not so relevant for our purpose. In the context of the voltage dependence of the membrane capacitance, while everyone was pointing the attention on electrostrictive effects and thus on changes in area and thickness, White speculated on the possible role played by the change in the relative permittivity with applied voltage, unfortunately without proceeding and further investigating his initial intuition, [59].

At fixed voltage V_m , the properties of the system can be described by the capacitance of the membrane (which gives information about the charge stored on the capacitor plates at that voltage, $q = C_m \cdot V_m$), and by the electric susceptibility, which relates the total polarization of the membrane to the electric field that is created inside:

$$P = \epsilon_0 \chi E = \epsilon_0 (\epsilon - 1) E \quad (4.1)$$

The previous equation, together with the one relating charge and voltage (2.20), is valid in general for linear dielectrics, for which both the capacitance and the relative permittivity are constants of the system. In lipid membranes this is not generally true: both the capacitance and the susceptibility depend on the geometrical and molecular (respectively) structure of the lipid membrane, which are known to undergo significant changes during the melting transition. This has been shown for the capacitance but it is true in principle also for the relative permittivity (and thus the electric susceptibility), whose dependence on the molecular structure is more complicated, making it difficult to estimate its change in the different phases.

In general, considering the temperature dependence of the different variables (keeping the voltage fixed), one would have:

$$q(T) = C_m(T) \cdot V_m = \epsilon_0 (\epsilon_g + \Delta\epsilon(T)) \frac{A_g + \Delta A(T)}{D_g + \Delta D(T)} V_m \quad (4.2a)$$

$$P(T) = \epsilon_0 (\chi_g + \Delta\chi(T)) E(T) = \epsilon_0 (\epsilon_g + \Delta\epsilon(T) - 1) E(T) \quad (4.2b)$$

In the first equation, the definition of the capacitance as a function of the geometrical properties of the system has been used. This (plus the proportionality between those properties and the melting enthalpy) allowed us to study the electrical properties in a thermodynamical framework. Unfortunately, there is no such an explicit expression for the relative permittivity which takes into account the elementary structural properties of the membrane. Therefore, for the time being, it's sufficient to know that $\epsilon = \epsilon(T)$, and the explicit dependence will be expressed later on.

Being a function of the physical state of the membrane, the capacitance and the relative permittivity are also function of every quantity that can influence the position of the melting transition, such as hydrostatic and lateral

pressure, pH and thus, also voltage . The latter has been considered in [19], where voltage induced changes of the capacitance introduce nonlinearity in the properties of the system (namely, in the relation between the charge and voltage). However, dealing with the dielectric structure and polarization of the system, we will consider the membrane interior as a linear media. The temperature dependence of the relative permittivity will be considered (especially in the transition) but no higher order effects will be treated (such as electric field induced changes in ϵ). This is a first order approximation. Linearity of the medium with respect to polarization means that in eq.(4.2b), P, ϵ and E will all change with temperature, but for each temperature the relation between polarization and electric field will remain linear. Releasing this assumption would result in the introduction of a differential electric susceptibility fully analogue to the capacitive susceptibility.

Effect of the dielectric properties on the voltage dependence of the melting temperature

In order to find the voltage dependence of T_m , one has to identify the processes that take place in presence of a voltage, which contribute to change the enthalpy difference between the fluid and the gel state. Up to now electrostriction has been analysed, whose effect is to decrease the melting enthalpy (thus the energy required for a lipid to undergo a transition gel→fluid) with the final effect of decreasing the melting temperature. Nevertheless, such a derivation has been done without considering the change in the relative permittivity between the two states. In addition, the work done by the electric field to polarize the material could in principle affect the melting enthalpy. One of the consequences of assuming a state dependent electric susceptibility is that also the polarization will change passing from a gel to a fluid state. However, the electric field doesn't perform any work related to the polarization of the material. This is a consequence of the assumption of linearity. If one considers also electric field induced changes in the relative permittivity, than the work done by the electric field in polarizing the material upon melting should be considered.

Therefore, at this step, only the work done by electric field going from the gel to the fluid is calculated. The enthalpy change $\Delta H(T)$, at constant voltage V_m of the membrane at temperature T is given by:

$$\Delta H(V_m, T) = \Delta H_0(T) + \Delta W_C(V_m)$$

Here, $\Delta H_0(T)$ is the enthalpy of the system at temperature T in the absence of voltage (for DPPC, it is plotted in fig.2.4) and ΔW_C is the work

contribution from electrostriction. Its explicit expression is calculated in the following.

Electrostriction In the context of electrostrictive effects, all the considerations made in section (2.2.1) still apply, with the only difference that since now the dielectric constant of the membrane can change, this could have consequences in the calculation of the work done by the electric field upon melting. One has to include the state dependence of the relative permittivity in eq.(2.25).

Up to now, it's only been assumed that ϵ is some function of the temperature but no explicit dependence has been stated. In the following we will assume a proportionality between the relative permittivity and the melting enthalpy, in the same way as for the area and thickness of the membrane:

$$\Delta\epsilon(T) = \gamma_\epsilon \cdot \Delta H_0(T) \quad (4.3)$$

Taking $\epsilon_g = 2$ in the gel phase and $\epsilon_f = 4$ in the fluid phase [19], one can estimate the proportionality coefficient, γ_ϵ . In the case of DPPC we have:

$$\gamma_\epsilon = \frac{\epsilon_f - \epsilon_g}{\Delta H_0} = \frac{2}{39 \text{ kJ/mol}} = 5 \cdot 10^{-5} \frac{\text{mol}}{\text{J}}$$

Using this assumption, the electrostrictive work (2.25) can be recalculated:

$$\Delta W_C(V_m, T) = \frac{1}{2} \epsilon_0 V_m^2 \int_{D_g}^{D(T)} \epsilon(T) \frac{A(T)}{D(T)^2} dD(T)$$

Using the proportionality relations one can express everything as a function of the enthalpy. The enthalpy change $\Delta H_0(T)$ at constant voltage due to electrostriction can be written as:

$$\begin{aligned} \Delta H_0(V_m, T) &= \Delta H_0(T) + \\ &+ \frac{1}{2} \epsilon_0 \gamma_D V_m^2 \int_0^{\Delta H(T)} (\epsilon_g + \gamma_\epsilon \Delta H_0(T)) \frac{(A_g + \gamma_A \Delta H_0(T))}{(D_g + \gamma_D \Delta H_0(T))^2} d\Delta H_0(T) \end{aligned}$$

For small x (in this case $x = \gamma_D \Delta H_0 / D_g$), one can use $(1 + x)^{-2} \simeq 1 - 2x$. The expression in the integral becomes a polynomial and can be easily solved. Taking only up to second order terms in x , it is given by:

$$\begin{aligned} \Delta H_0(V_m, T) &= \Delta H_0(T) + \\ &+ \frac{1}{2} \epsilon_0 \gamma_D \frac{A_g \epsilon_g}{D_g^2} \left[1 + \frac{1}{2} \left(\frac{\gamma_A}{A_g} + \frac{\gamma_\epsilon}{\epsilon_g} - 2 \frac{\gamma_D}{D_g} \right) \Delta H_0(T) \right] \Delta H_0(T) V_m^2 \end{aligned}$$

If we consider $T \gg T_m$, then $\Delta H_0(T) = \Delta H_0$ is constant and is the change in the enthalpy between the gel and the fluid state in absence of voltage. The previous expression is then a quadratic function of the voltage:

$$\Delta H(V_m) = \Delta H_0 + \bar{\alpha}_0 V_m^2 \quad \text{with} \quad \bar{\alpha}_0 = -97.1 \frac{J}{V^2 \cdot mol}$$

It is the excess heat of melting due to electrostriction. The transition temperature in presence of voltage becomes:

$$T_m = (1 + \bar{\alpha} V_m^2) T_{m,0} \quad \text{with} \quad \bar{\alpha} = \frac{\bar{\alpha}_0}{\Delta H_0} = -0.025 \frac{1}{V^2 \cdot mol} \quad (4.4)$$

The shift in the transition temperature considering the temperature dependence of the permittivity is even smaller than the one previously calculated. For a transmembrane voltage of $V_m = 100mV$ one obtains a shift of less than $8mK$ towards lower temperature, against the value of $11.4mK$ for the same voltage, derived in [19] in the assumption of constant ϵ .

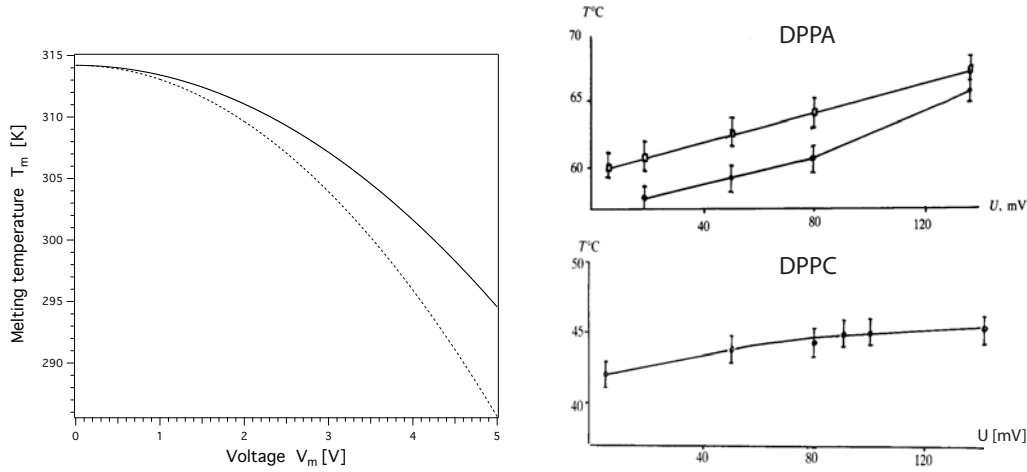


Figure 4.2: *Left*: Shift in the melting temperature as a function of voltage as derived in eq.(4.4) (*solid line*). It is compared to findings of [19] (*dashed line*), where no change in ϵ is considered (see eq.(2.27) and fig.2.10). *Right*: Linear dependence of the melting temperature on voltage, measured by Antonov [96] for phosphatidic acid (DPPA, *top*) and DPPC (*bottom*). Picture adapted from [96]. Note the different scale of the voltage between the left and the right panel.

The effect of electrostriction on the melting temperature so far estimated is evidently small but in the same direction predicted theoretically by Sugar

in [106]. The only experimental investigation in this regard, has been performed by Antonov 23 years ago [96] and is shown in the right panel of fig. 4.2. He found that the melting temperature increases linearly with the transmembrane voltage, the effect being relevant even for very small voltages ($< 100mV$). His findings are in agreement with the theoretical prediction of Bhaumik et al. [107] who discussed it in the context of excitable membranes, and Cotterill [108], who predicted a linear increase of the melting temperature due to the orientation of the polar head groups with the field (he predicted an increase of $2K$ for an applied voltage of about $50mV$). The explanation given by Cotterill does not consider electrostrictive effects and does not apply better to monolayers rather than to bilayers.

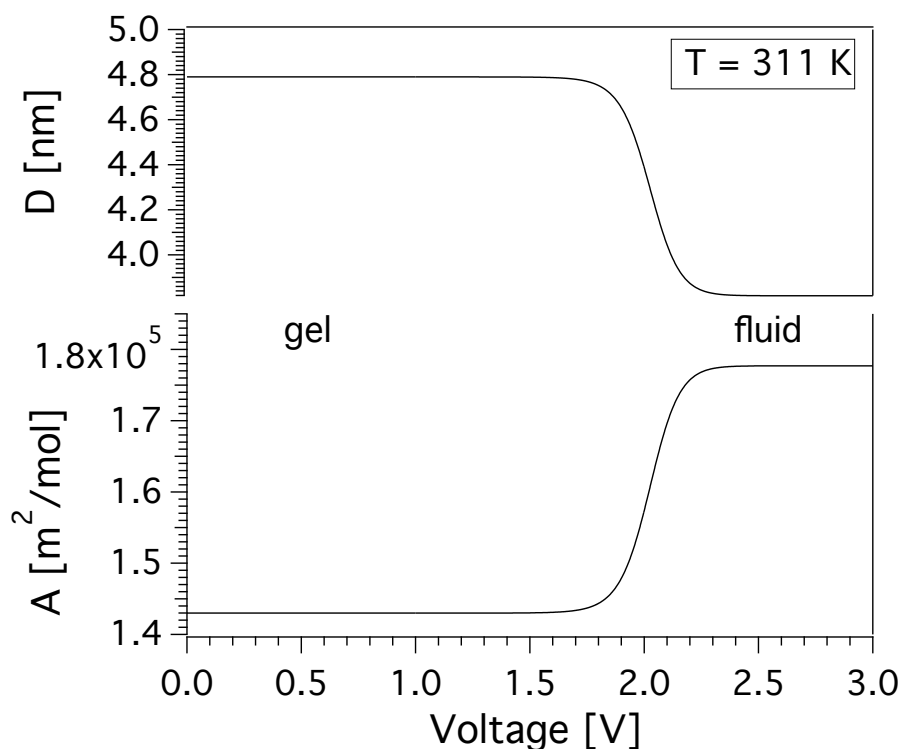


Figure 4.3: Changes in area (*bottom*) and thickness (*top*) as a function of voltage for a fixed temperature $T = 311K$. At such temperature, DPPC is in the gel state. For a threshold value of the voltage, a phase transition is induced by electrostriction.

As a consequence, a lipid membrane in the gel state close to the transition can become fluid in the presence of an external voltage of appropriate magnitude. This is shown in fig. 4.3, where, at constant temperature (below

the melting point), thickness and area undergo a voltage induced transition. The effect is qualitatively similar to the one predicted by Heimburg [19], but its magnitude is smaller, therefore the voltage required to induce a transition is bigger (about 400 mV bigger at $T = 312\text{ K}$).

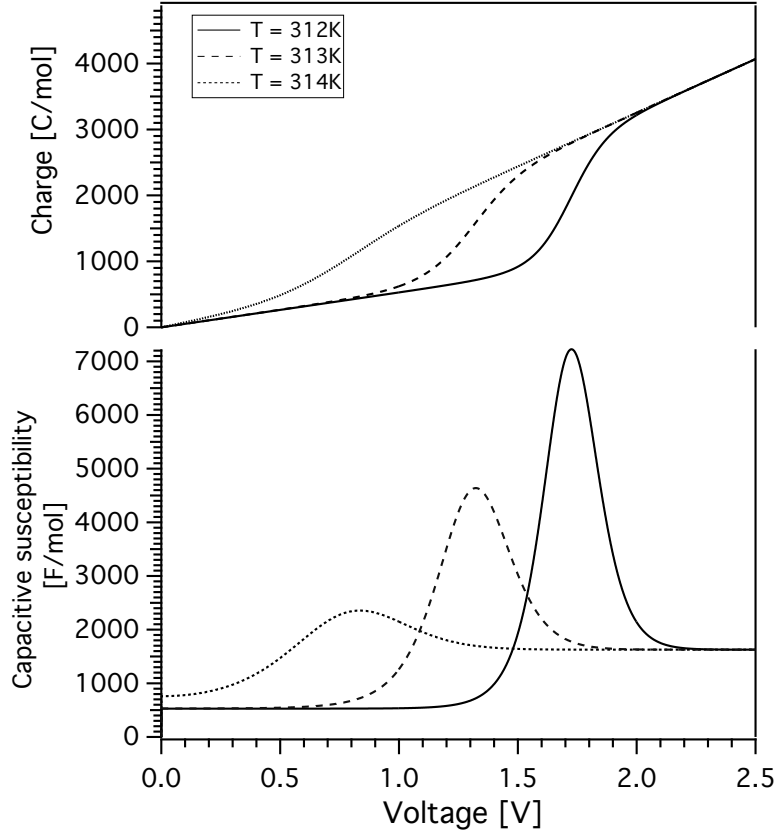


Figure 4.4: *Bottom*: capacitive susceptibility as a function of voltage for different values of temperature. As the temperature approaches the melting point of DPPC ($T_m = 314.2$ in the absence of voltage), the threshold voltage that induces the transition is smaller. *Top*: charge as a function of voltage for different temperatures. Considering a voltage dependent capacitance results in a nonlinear charge-voltage relation. The derivative of the charge as a function of voltage for each temperature, is given by the capacitive susceptibility shown in the bottom.

Finally, the nonlinearity in the charge-voltage relationship is shown in fig. 4.4 together with the capacitive susceptibilities, for different temperatures. As the voltage increases (at fixed temperature), the charge increases linearly, up to a point where the voltage induces the transition. As a result, the

capacitance of the system increases going from gel to fluid, inducing a large uptake in the charge on the plate of the capacitor.

4.1.2 Flexoelectric effects

In this section the assumption of fixed dipole orientation in the context of polarization will be removed. Lipid head groups² behave like electric dipoles, thus in an electric field they tend to align with the field. The orientation is antisymmetric with respect to the field, so that if the field is in the direction of the membrane normal, in one leaflet they will be more aligned while in the other they will tilt in the plane of the membrane. This asymmetry results in the bending of the bilayer.

Thus, releasing the assumption of fixed dipolar orientation, one allows the membrane to curve, and flexoelectric effects to take place. In the following, we will focus on patches of membrane, like the ones investigated with patch pipette or BLM techniques. The geometrical considerations made, refer to a membrane that is free to bend. In closed surfaces such as plasma membranes, one has to consider topological constraints that are not taken into account here.

Suppose to have a flat and symmetric bilayer. Its initial polarization is zero (see eq.(2.33)), and so is its curvature. The effect of an electric field in the direction of the bilayer's normal is dual: on the one hand it will produce a polarization P , which at fixed temperature T is given by (4.2b) and is linear in the field. On the other hand, for the converse flexoelectric effect the membrane bends and at the equilibrium its curvature is given by eq. (2.37). Such a curvature breaks the symmetry of the system, and for the direct flexoelectric effect its surface polarization, P_s , is not zero anymore but it is given by eq. (2.35). Combining the direct and converse effect, the resulting surface polarization can be written as a function of the applied electric field:

$$P_s = \frac{f^2}{K} E = f^2 \kappa_b E$$

where $\kappa_b = K^{-1}$ is the bending elasticity of the membrane (for DMPC bilayers one typically has $\kappa_b \simeq 10^{19} J^{-1}$, [109]) .

²As already pointed out, the total electric dipole μ in a lipid molecule is not uniquely determined by the head group, and a big role is played by ester bond in the backbone (see (2.34)). In the following, with head group we will refer to dipolar part of the lipid molecule in general.

The total bulk polarization (remember that $P_v = P_s/D$), is given by:

$$P_{tot} = \epsilon_0 \chi E + \frac{f^2 \kappa_b}{D} E = \epsilon_0 \left(\chi + \frac{f^2 \kappa_b}{\epsilon_0 D} \right) E$$

This linear relation describes the total polarization, which takes into account also flexoelectric effects. Let's call flexoelectric susceptibility, χ_{flex} , the quantity:

$$\chi_{flex} = \frac{f^2 \kappa_b}{\epsilon_0 D}$$

The total polarization can be written as:

$$P_{tot} = \epsilon_0 (\chi + \chi_{flex}) E = \epsilon_0 \chi_{eff} E$$

where $\chi_{eff} = \chi + \chi_{flex}$ contains all the physics of the system. At fixed temperature, it is a constant yielding a linear polarization. However, because of its dependence on geometrical and mechanical quantities such as membrane thickness and bending elasticity, χ_{flex} is expected to change close to transition.

At temperature T , the flexoelectric part of polarization is given by:

$$P_{flex}(T) = \frac{f^2 \kappa_b(T)}{D(T)} E(T) \quad (4.5)$$

Where the temperature dependence of the membrane thickness and thus of the electric field (assuming a fixed voltage), are known. In the following, the the bending elasticity is considered in a thermodynamical framework.

Bending elasticity The bending elasticity just introduced is a susceptibility similar to the area and volume compressibilities. It can be defined as derivative of the curvature (extensive quantity) with respect to the conjugated bending moment. One can show that it is proportional to the fluctuations in curvature (see [4] for the full derivation).

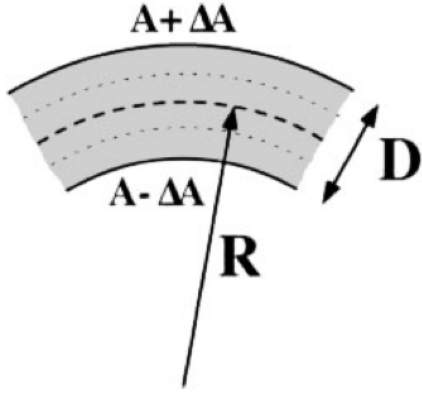


Figure 4.5: Pure bending of a connected bilayer, in the assumption of two perfectly coupled monolayers. D is the membrane thickness and A is the area of the neutral surface. Bending the membrane to a final radius R , corresponds to stretch the outer monolayer of a quantity ΔA and compress the inner one of the same quantity. Picture taken from [4]

In the case of the pure bending of a connected bilayer, bending is obtained by stretching one layer and compressing the opposite one. Using the notation of fig. 4.5, geometrical considerations allow to relate the radius of curvature of a curved membrane, to the area changes in both the monolayers [4]:

$$c = \frac{1}{R} = \frac{4\Delta A}{A \cdot D}$$

Curvature changes can thus be expressed in terms of area changes. Furthermore, the bending free energy corresponds to that of one monolayer expanded by ΔA and the other compressed by ΔA . As a result, one can relate the bending elasticity to the area compressibility [77] (see [4] for the full derivation):

$$\kappa_b = \kappa_T^A \cdot \frac{16}{D^2} \quad (4.6)$$

Being proportional to the area compressibility, the bending elasticity is also proportional to the heat capacity, and thus it is expected to have a peak in the melting transition. This has been indeed proved to be true [74, 110, 111], and for the excess bending elasticity, $\Delta\kappa_b$, in the melting transition is described by [111]:

$$\Delta\kappa_b = \frac{16}{D^2} \frac{\gamma_A^2 T}{A} \Delta c_p$$

The behaviour of of the bending elasticity as a function of temperature is plotted in fig.4.6.

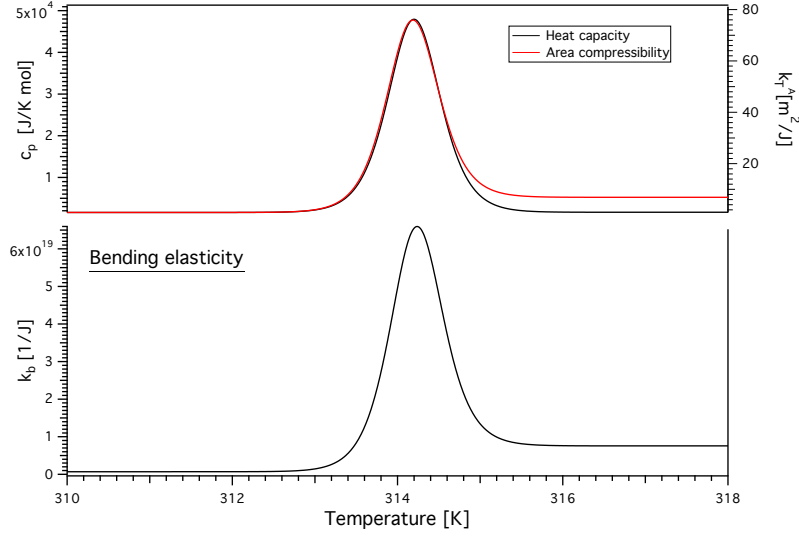


Figure 4.6: *Bottom*: bending elasticity according to eq.(4.6). *Top*: heat capacity and isothermal area compressibility. The three curves are proportional to each other

Temperature dependence of flexoelectric polarization

Using eq. (4.6) in the expression for the flexoelectric susceptibility, one can rewrite it as a function of the area compressibility. At temperature T it's given by:

$$\chi_{flex}(T) = \frac{16f^2\kappa_T^A(T)}{\epsilon_0 D^3(T)}$$

Using proportionality relations it can be expressed only in terms of enthalpy and heat capacity:

$$\chi_{flex}(T) = \frac{16f^2\gamma_A T}{\epsilon_0(A_g + \gamma_A\Delta H_0(T))(D_g + \gamma_D\Delta H_0(T))^3} c_p(T)$$

Its behaviour in the melting regime resemble the one of the bending elasticity and it is shown in fig. 4.7. As other susceptibilities of the system, it also shows a peak in the transition. Finally, in fig.4.8 the flexoelectric polarization is plotted around the melting regime for different values of the transmembrane voltage.

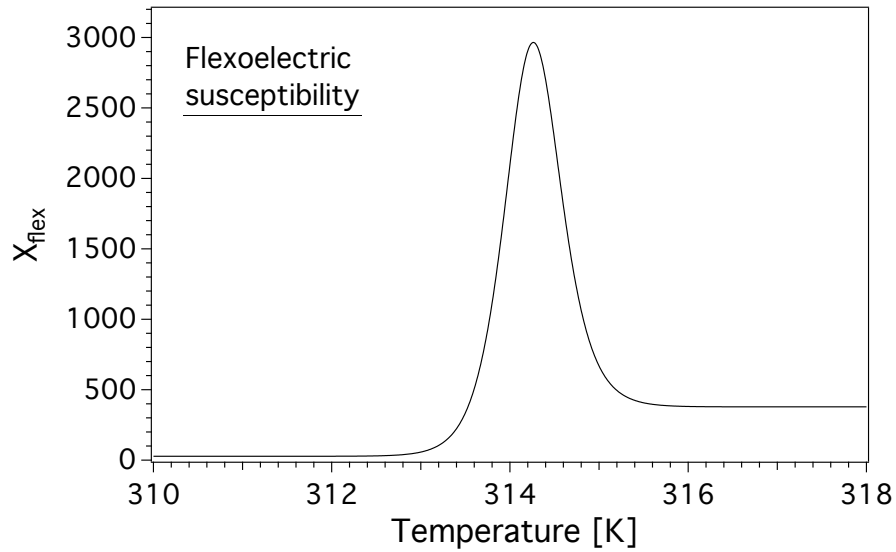


Figure 4.7: Flexoelectric susceptibility as a function of temperature. Its peak at the transition is due to the increase in the membrane compressibility and elasticity.

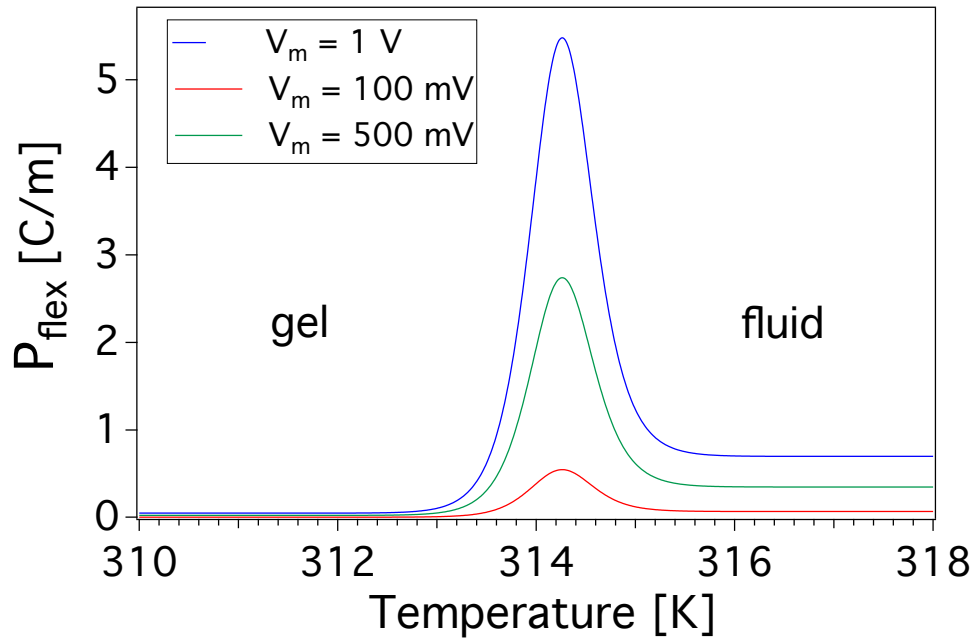


Figure 4.8: Temperature dependence of the flexoelectric polarization for different values of the voltage across the bilayer.

Effect of flexoelectricity on the voltage dependence of the melting temperature

Releasing the assumption of fixed dipole orientation, the effect of the electric field is to align the lipid dipoles according to their polarity, according to the converse flexoelectric effect. This creates an asymmetry that induces a curvature, and thus polarization. The effect of the field on the head groups resembles the structural orientation change of lipids from gel to fluid, represented in fig. 4.1. The big difference is that melting changes the orientation in a common fashion for both the leaflets. The electric field, on the other hand, is expected to change it asymmetrically in the two monolayers, due to the symmetric polarity of the dipoles. Nevertheless, one expects the electric field to affect the melting enthalpy and thus the transition properties. In addition, in the absence of external voltage, if a membrane patch is curved, a transmembrane voltage builds up, which can affect the voltage dependence of the transition temperature.

In the following these two mechanisms will be treated separately.

Effect of curvature Suppose to have a patch of membrane which is spherically curved, with curvature c . There are several mechanisms that can induce a curvature in membrane patches. For instance, an uneven distribution of lipids on the two leaflets, would result in different surface areas, and thus curvature. This can be originated by having the two leaflets in different physical state (one in the gel phase and the other in the fluid phase). Another reason can be an asymmetric composition of the two monolayers, like the membrane patches investigated by Alvarez and La Torre (see fig. 2.8), which were made by the apposition of monolayers of different lipid species. Another way to generate curved membranes is by applying pressure. In experiments where bilayers are formed on the tip of a glass pipette, suction is often applied to thin the membrane. Such suction can potentially curve the membrane.

For the direct flexoelectric effect, such a curvature results in a surface polarization P_s , which is linear in the curvature (see section 2.2.2). The Helmholtz equation quantifies the voltage across the bilayer due to the polarization. In the case of a membrane formed at the tip of a glass pipette (having a diameter of the order of $1 \mu m$), a pressure induced curvature with radius of about $3 \mu m$ can be expected. According to equation (2.36), this would correspond to an offset potential of about $100 mV$:

$$V_0 = \frac{2f}{\epsilon_0 R} = \frac{2 \cdot 13 \cdot 10^{-19} C}{8.854 \cdot 10^{-12} \frac{F}{m} 3 \cdot 10^{-6} m} \simeq 100 mV \quad (4.7)$$

This means that in absence of an external voltage, the membrane has a

significant offset voltage due to its curvature. One has to consider the offset voltage when applying external perturbations to the system. In the case of electrostriction, for example, a pre-curved membrane would change the voltage dependence of the melting temperature by shifting it on the voltage axis. Namely, eq.(4.4) takes now the form:

$$T_m = (1 + \bar{\alpha}(V_m - V_0)^2) T_{m,0} \quad (4.8)$$

The melting temperature is still quadratic in the voltage, but the peak of the parabola is shifted of a quantity equal to V_0 . This is shown in fig. 4.9, for a radius of curvature of $3 \mu m$.

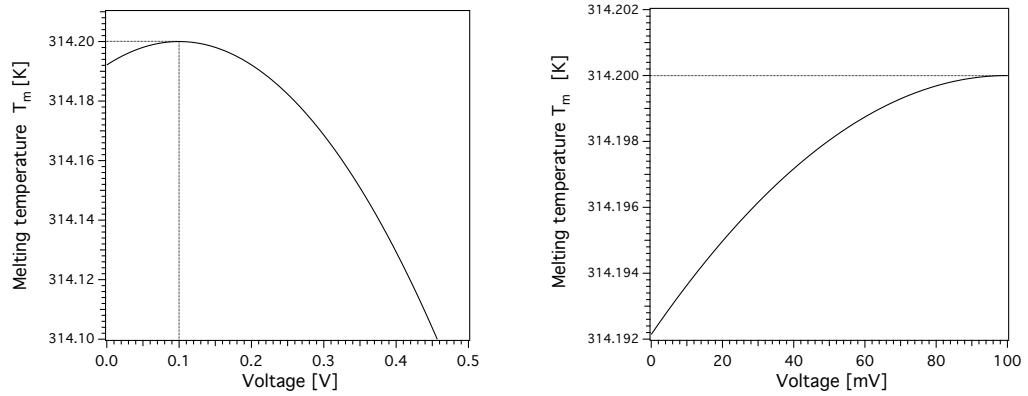


Figure 4.9: Melting temperature as a function of voltage calculated from eq.(4.8). *Left*: the dashed line indicates the offset voltage. *Right*: between 0 and 100 mV the melting temperature increases.

As a result of the curvature, the melting temperature increases for external voltages on the order of $V_0 = 100 mV$, and decreases for larger voltages as a consequence of electrostriction. Even though the magnitude of the effect is very small, it goes in the direction observed by Antonov [96]. As already mentioned, the curvature is a manifestation of the asymmetry of the system. In asymmetric membranes, like the ones of Alvarez and La Torre, an offset potential across the bilayer has been experimentally observed [52]. It could be that the membranes investigated by Antonov [96] were also asymmetric, as pointed out by Heimburg [19]. Remarkably, the results of Antonov lie in a limited voltage range of the order of the voltage offset, and give no information about effects at higher voltages. Furthermore, an offset voltage of the same order of the one here calculated, has been recently proposed in [99] to explain the asymmetric current voltage relationship observed in bilayers formed at the tip of glass pipettes.

Further experimental investigations in this regard are essential to have a complete understanding of the problem.

Effect of voltage According to the converse flexoelectric effect, an electric field E across the membrane, produces a nonzero curvature, and thereby a flexoelectric polarization. As introduced before, a pure bending corresponds to stretching and compression of the two opposite leaflets in a coupled bilayer. Therefore, the effect of an electric field is an opposite change in the area of the two monolayers (through the different alignment of the dipoles in the field). Changes in area and in the head group orientation are known to happen in the melting transition (see fig. 4.1). However, due to the symmetry of the system, one leaflet would become more fluid and the opposite more gel. Therefore, the effect of the field is a broadening of the transition rather than a shift like the one produced by electrostriction.

To estimate the effect, one has to include in the melting enthalpy, the work done by the field in *flexo-polarizing* the membrane:

$$\Delta H(E, T) = \Delta H_0(T) \pm \Delta W_{pol}(E)$$

Such work will increase the melting enthalpy in one leaflet and decrease it in the opposite one (thus the different sign).

At constant field E , it can be written as:

$$\Delta W_{pol}(E) = \int_{P_g}^{P_f} E dP = E \Delta P \quad (4.9)$$

where P_g and P_f are the values of the polarization in the gel and fluid state at constant electric field, due to the different value of the electric dipoles in the two states. An estimation of ΔP can be made based on experiments on monolayers. From the values of the surface potential as a function of the lipid area, one can determine the value of the electric dipole in the gel and fluid state, using the Helmholtz equation:

$$\mu = \epsilon_0 A \Delta V$$

Taking the values of Morgan et al. [112], one obtains a value of $\Delta P \simeq 10^{-7} C \cdot m / mol$ for DPPC. Note that the simple expression derived in eq.(4.9), assumed that the electric field is constant. For the time being we'll keep this assumption, having in mind that the error introduced is of the order of the 16% (equivalent to the relative change of the membrane thickness in the transition).

In these approximations, considering a system in the fluid phase ($T \gg T_m$), the melting enthalpy can be expressed as a function of voltage V_m . For a fixed voltage, it is given by:

$$\Delta H(V_m) = \Delta H_0 \pm \beta \cdot V_m \quad (4.10)$$

where $\beta = \Delta P/D$. In fig.4.10, the excess heat capacity calculated from (4.10) is plotted as a function of temperature for different applied voltages.

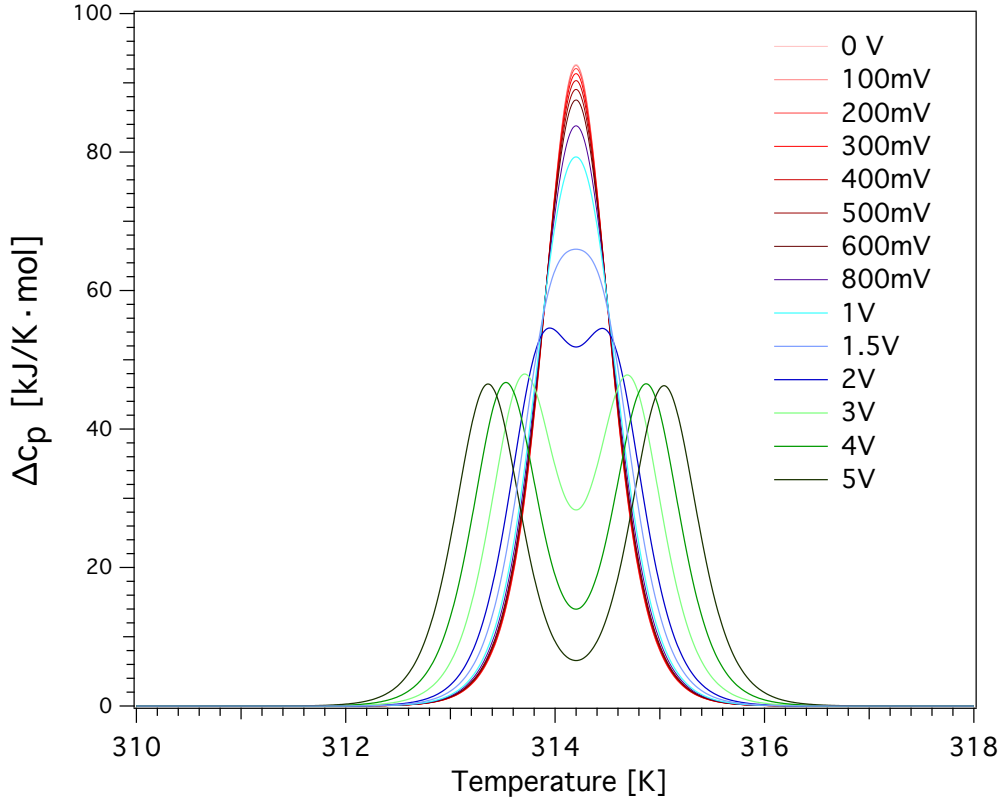


Figure 4.10: Excess heat capacity of DPPC as a function of temperature for different applied voltages. The parameters used are taken from [21, 112]. The cooperativity size is $n = 100$.

The effect is small for voltages below 1 V. For higher voltages, the excess heat capacity becomes wider. The ultimate effect for large voltages is a split of the curve in two peaks, corresponding to the melting of the two opposite layers. The magnitude of the effect may be affected by the approximations used, nevertheless fig.4.10 gives an intuition of the phenomenon.

In conclusion, the effect of an electric field, according to the converse flexoelectric effect, is to curve the membrane through its antisymmetric in-

teraction with the lipid dipoles. This lowers the melting temperature of one leaflet and rises it in the opposite leaflet, resulting in a broader heat capacity profile. For very large fields, one would observe a phase separation in the leaflets (one being in the gel state and the other in the fluid state) corresponding to the complete split of the heat capacity curve.

4.2 Experiments

In the following, the results and discussion of the experimental part of the thesis are presented.

As pointed out in the theoretical part, the assumption of proportionality between the relative permittivity of lipid bilayers and the melting enthalpy lied in the lack of reliable data in literature. During the work of this thesis, a simple experiment for measuring the temperature dependence of the relative permittivity has been designed. Unfortunately, it was not possible to complete the measurement during this thesis. However, the method is presented here as a future perspective in order to have a better insight in the dielectric properties of lipid membranes.

In addition, in order to experimentally investigate the effect of voltage on the lipid melting, experiments have been performed using a Ionovation Bilayer Explorer, as explained in chapter 3. Such experiments had also the aim of testing and quantifying the theoretical predictions regarding the flexoelectric properties of the system, with a focus on the offset potential expected for curved membranes.

4.2.1 State dependence of the relative permittivity

A better understanding of the dielectric properties of lipid bilayers could be achieved by knowing the state dependence of their relative permittivity. As pointed out in chapter 4.1, this can account for tuning the magnitude of the effect of electrostriction on the thermodynamical properties of the system. In order to do this, a simple experiment has been designed and the method is here presented.

Historically, the relative permittivity was first introduced by Michael Faraday to quantify the increase in the capacitance of a capacitor when the vacuum between the plates is replaced by a material [128], namely:

$$\epsilon = \frac{C}{C_0} \quad (4.11)$$

where C_0 is the capacitance in vacuum and C is the capacitance in the presence of a dielectric material. He called it *specific inductive capacity* [128]. The effect of the dielectric is an increase of the electric field inside the capacitor at constant voltage. This is due to the polarization of the material, in which the induced electric dipoles increase the charge stored on the plate of the capacitor. Larger charge storage at fixed voltage means larger capacitance.

The value of the capacitance for a planar capacitor filled with a dielectric material is thus expressed by the familiar expression:

$$C = \epsilon_0 \epsilon \frac{A}{d} \quad (4.12)$$

where ϵ is the dielectric constant of the material and A and d are the area of the plates and the distance between them.

Thereby, one can measure the dielectric constant of a material by means of capacitance measurements. By filling a planar capacitor with a material resembling the dielectric properties of the hydrophobic interior of membranes, one can measure the capacitance at different temperatures and then compare it with the values of the capacitance in the absence of the dielectric or in the presence of a material with a known curve of the dielectric constant as a function of temperature, using eq.(4.11). Alternatively, knowing the geometry of the capacitor, the dielectric constant can be determined using eq.(4.12).

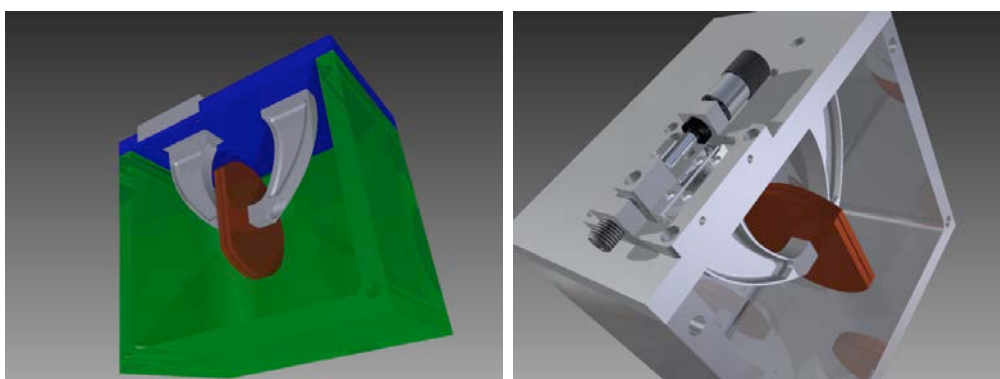


Figure 4.11: 3d image showing a section of the capacitor design. The capacitor plates are attached to the lid of the box and their distance can be regulated with a micrometer screw. The walls of the box contain channels for water circulation. The technical drawing and the realisation of the capacitor have been made by Dennis W. Wistisen.

To this purpose, an aluminium box containing a planar capacitor has been built. The box allows for water circulation and thus temperature control through a water bath. It is thermally and electrically insulated by a black anodised surface treatment. The capacitor plates are attached to the lid of the box and have an adjustable distance. A scheme of the setup is shown in fig. 4.11. Therefore, once the box is filled with the dielectric materials, the lid is closed and capacitance can be measured through the electrodes

attached to the conductor plates. The filling material has to resemble to dielectric properties of the membrane interior, which is made of hydrocarbon chain. In order to relate the results of this method to the effective dielectric properties of the membranes, one can fill the box with the fatty acid of the lipid species one wants to investigate. This could be for example palmitic acid (the fatty acid contained in DPPC) or myristic acid (the one contained in DMPC). Both these fatty acids have melting temperatures that can be investigated by means of a common water bath.

The geometry of the capacitor is designed in order to have significant readings of the capacitance, for dielectric constants of about 2-4. This puts constraints on the ratio between the area the thickness. Furthermore, in order to limit the fringing effects of the electric field at the edges of the plates, the distance between the plates needs to be much smaller than the area. Therefore round plates with a diameter of 6.5 cm were designed, with an adjustable distance between the plates between 0 and to 2 mm . The main problem with this geometry is that, due to big area of the plates, very small changes in the plates alignment can affect the behaviour of the capacitor, and the capacitance cannot be described by eq. (4.12) anymore. To avoid that, control and recalibration of the plates alignment needs to be periodically performed.

Finally, figure 4.12 shows the calibration curve.

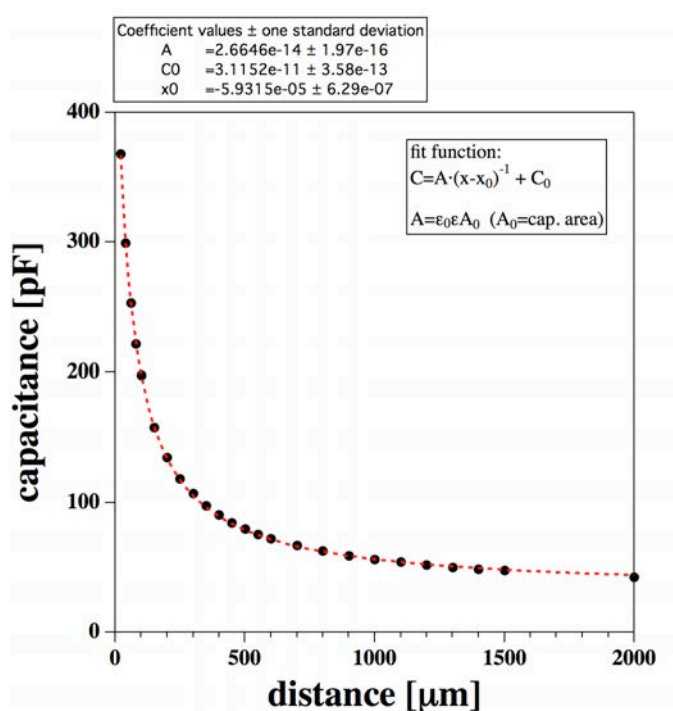


Figure 4.12: Fit of the function (4.13) to the calibration curve. The fitting parameters are expressed in SI units, thus:
 $C_0 = [F]$,
 $x_0 = [m]$,
 $A = [F \cdot m]$.

It has been obtained by measuring the capacitance of the empty capacitor as a function of the distance between the plates. It is well fitted by the function:

$$C = C_0 + \frac{A}{x - x_0} \quad (4.13)$$

Here $A = \epsilon_0 \epsilon A_0$, where A_0 is the plate area, C_0 is the capacitance of the measuring instrument at rest³, and x_0 is the zero position of the capacitor plates.

4.2.2 Calorimetry

Calorimetric measurements have been performed on each lipid sample to investigate the transition behaviour. Different lipid mixtures have been tested, in order to find a sample that matched the constraint of having a neither too narrow nor too wide transition close to room temperature. In the end, a lipid mixture of DMPC:DLPC=10:1 (mol:mol), was chosen. However, few permeability experiments were performed on a pure lipid sample of DMPC, despite the narrowness of its transition. Therefore, the calorimetric measurements for pure DMPC are also shown.

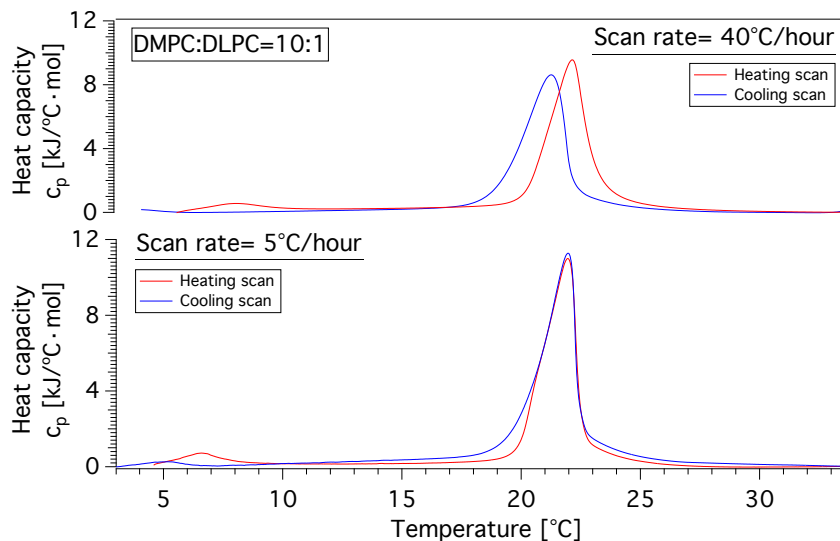


Figure 4.13: Excess heat capacity for multi-lamellar lipid vesicles of DMPC:DLPC=10:1 (mol:mol) in 150 mM KCl, 1 mM EDTA and 1 mM HEPES. The pH is 7.3. *Red curves*: heating scans (endothermic process). *Blue curves*: cooling scans (exothermic process). *Top*: scan rate of 40°C/hour. *Bottom*: scan rate of 5°C/hour. The big peak at 20-23°C is the main transition, the small peaks around 6°C are the pre-transitions.

³during the calibration an LCR meter has been used

DMPC:DLPC=10:1 Heat capacity profiles of a lipid mixture made of DMPC:DLPC=10:1 (mol:mol) of 10 mM concentration in a saline solution of 150 mM KCl, buffered at a pH of 7.3, have been measured for different scan rates and are shown in fig. 4.13.

One can see that for a scan rate of 5°C/hour (fig. 4.13, bottom), the heating and cooling curves are almost overlapping in the main transition. The main difference between the two is in the pre-transition at low temperature. When the scan rate is increased to 40°C/hour (fig. 4.13, top), one observes a mismatch of the heating and cooling scans showing hysteresis of the system. If the scan rate is too large, the system doesn't have time to reach the equilibrium for a fixed temperature, therefore its behaviour is dependent on the scanning conditions. In both cases, the pretransition exhibits hysteresis.

A detail of the main transition is shown in fig. 4.14. The purpose of the calorimetric measurements is to measure the temperature range in which the sample undergoes a transition, in order to investigate the melting of the sample in permeability experiments. The results clearly show that if the sample is heated or cooled too fast, then it doesn't have time to equilibrate, and its melting properties can change during the same experiment.

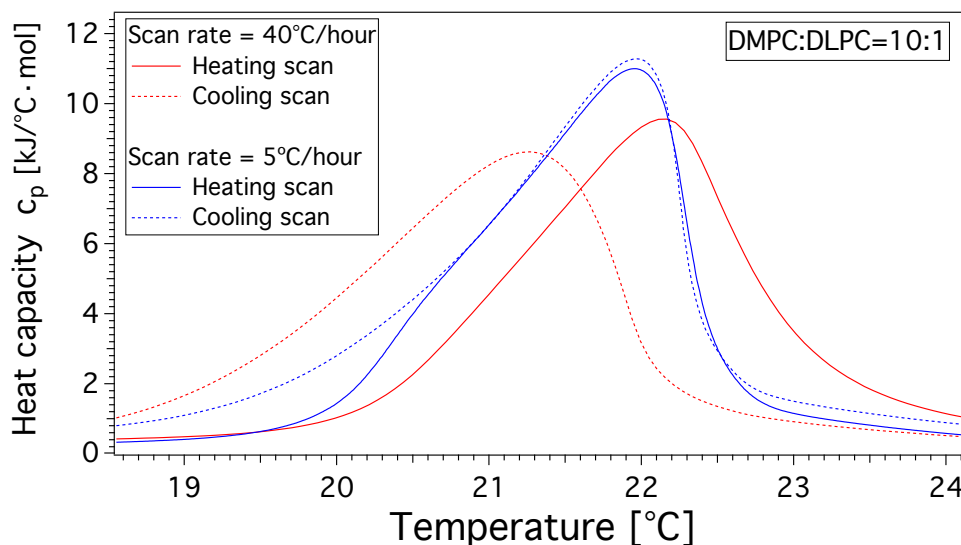


Figure 4.14: Detail of the main transition. *Blue curves*: profiles obtained at a scan rate of 5°C/hour. They are almost super-imposable. *Red curves*: heat capacities for a fast scan. Heating and cooling scan clearly show significant hysteresis. The melting temperature difference between the two is about 1°C.

Even though the effect of the hysteresis is small (the melting temperature difference between the endothermic and the exothermic process is of about

1°C), it is of the same order of the width of the transition, and approximately 10 times larger than the accuracy of the temperature sensor used in permeability experiments.

DMPC In order to investigate the permeability properties of a symmetric bilayer, a lipid sample of pure DMPC has been used. Pure DMPC has a very narrow transition around 23.7°C, thus hysteresis is significant even at a scan rate of 20°C/hour. In fig. 4.15, the heat capacity profile of DMPC is shown for different scan rates. At a scan rate of 5°C/hour, the difference in the melting transition obtained by heating and cooling is about 0.1°C, thus within the accuracy of the temperature sensor in permeability experiments. However, for higher scan rates, the difference increases up to about half a degree, which is comparable to the width of the transition. That is the reason why samples of pure lipid species are in general unsuited for permeability studies at the phase transition. However, one could obtain information about the relaxation behaviour of the lipids, as it will be pointed out in the discussions. The choice of this sample will be justified in the next section.

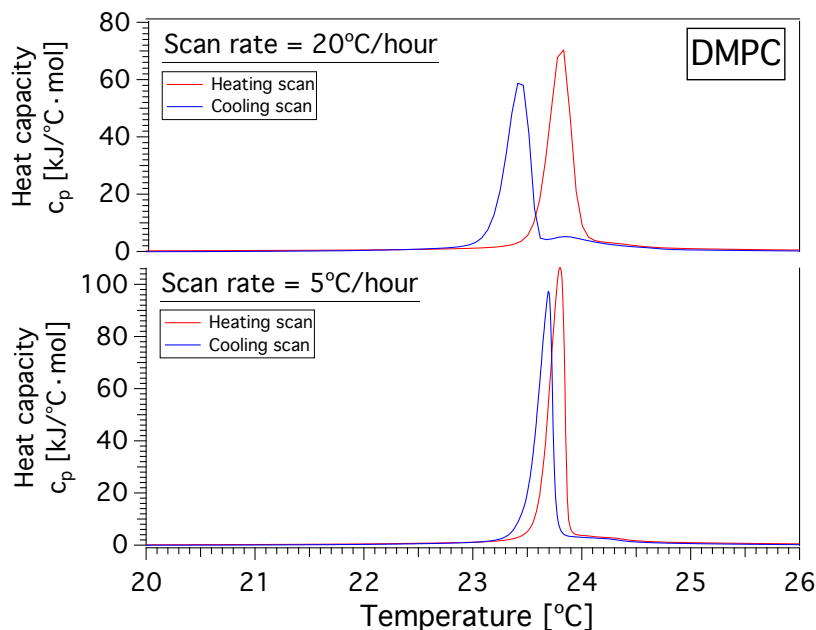


Figure 4.15: Excess heat capacity profile of 10 mM DMPC in 150 mM KCl, 1mM HEPES, 1mM EDTA at a pH of 7.3. *Bottom*: Scan rate of 5°C/hour. Due to the narrowness of the transition, a small shift in the heating *red* and cooling *blue* scans can be observed. *Top*: the effect of hysteresis increases when the scan rate is set to 20°C/hour.

4.2.3 Permeability

Temperature dependence

Current recordings were performed on patches of membrane made of pure DMPC. Fig. 4.16 shows a snapshot of the software during a typical experiment. The waveform of the output voltage is shown together with a current recording. The recordings are organised in sweeps. In the case showed here, each sweep had a duration of 4 seconds, where the voltage was changed from 0 to $+50\text{ mV}$ and after 2 seconds from $+50$ to -50 mV in a stepwise fashion.

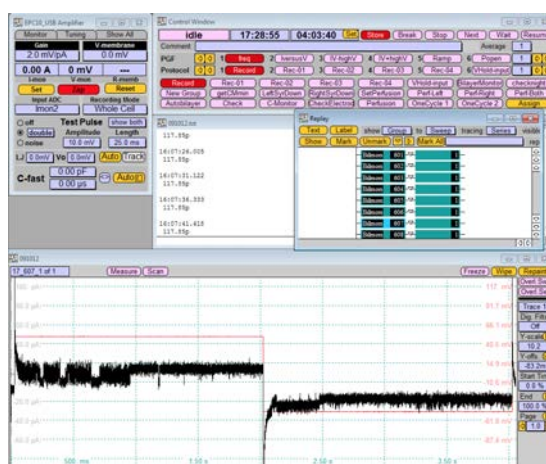


Figure 4.16: Snapshot of the software showing a sweep in a typical recording. The *red line* is the output voltage, the *black* signal is the current response. The value of temperature is measured for each sweep.

In order to relate the conductance behaviour to the melting transition, the temperature has been changed around the transition during the experiments. Lipid bilayers were formed either in the fluid or in the gel phase and then heated or cooled with the method described in chapter 3. The heating (or cooling) rate changed during the same experiment and was in general very large (on the order of $40^\circ\text{C}/\text{hour}$). The temperature was recorded once every sweep. This puts a limitation in the length of a sweep, that was set to 4 seconds. In such a way the temperature during each sweep can be assumed to be constant and for every temperature the current response to both positive and negative voltage could be measured. Nevertheless, 2 seconds of currents don't allow for a detailed and accurate statistical analysis of the trace.

Figures 4.17 and 4.18 show representative traces from a continuous recording in a temperature range between 20 and 28°C . For temperatures below the transition, no activity was present. At the transition temperature a jump

in the conductance together with an increase in the current fluctuations can be observed.

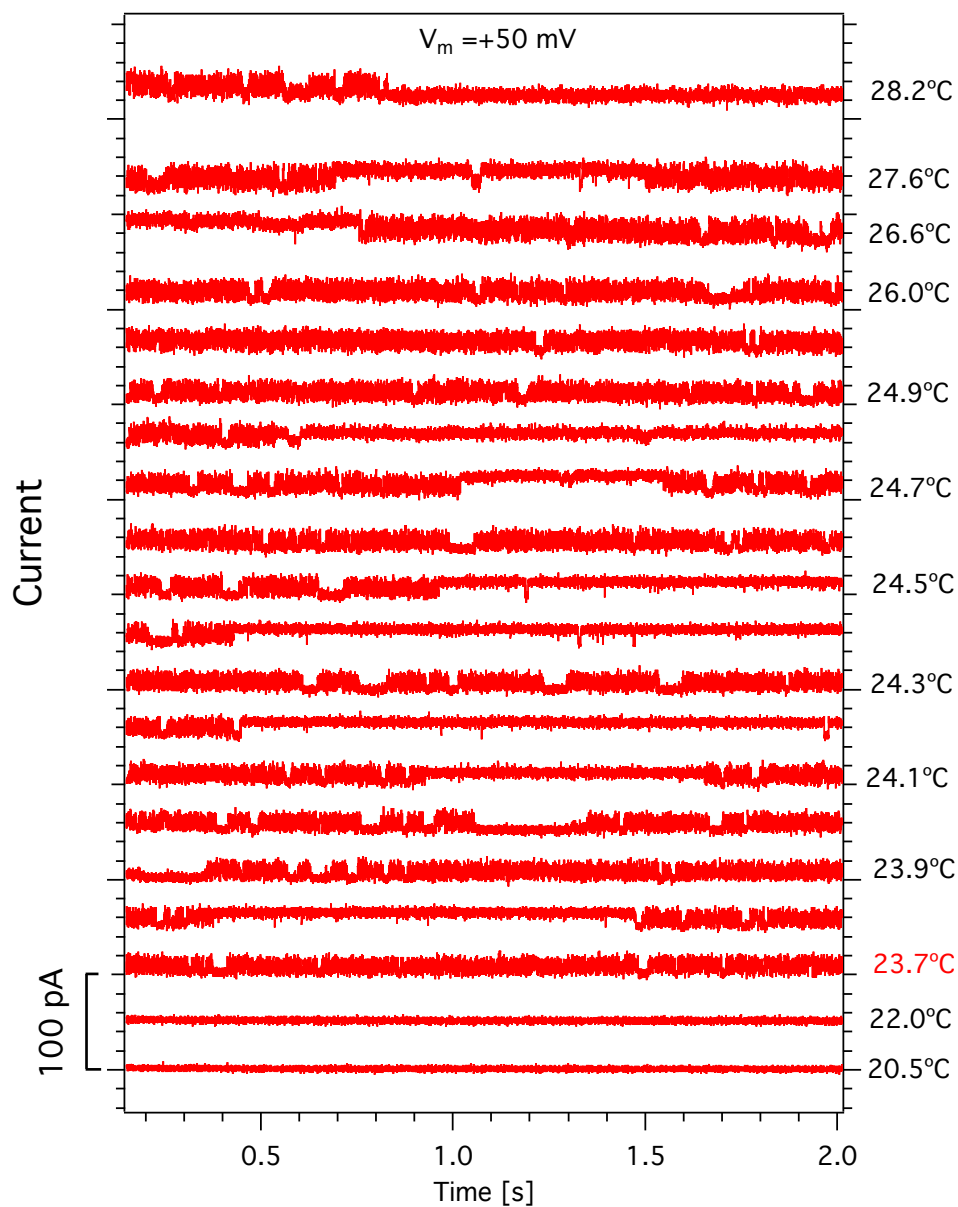


Figure 4.17: Representative current traces for different temperatures with an applied voltage of $+50$ mV. The lipid sample is pure DMPC in decane. Current traces have been shifted on the current axis. Unless otherwise specified, the temperature difference between subsequent traces is 0.1°C .

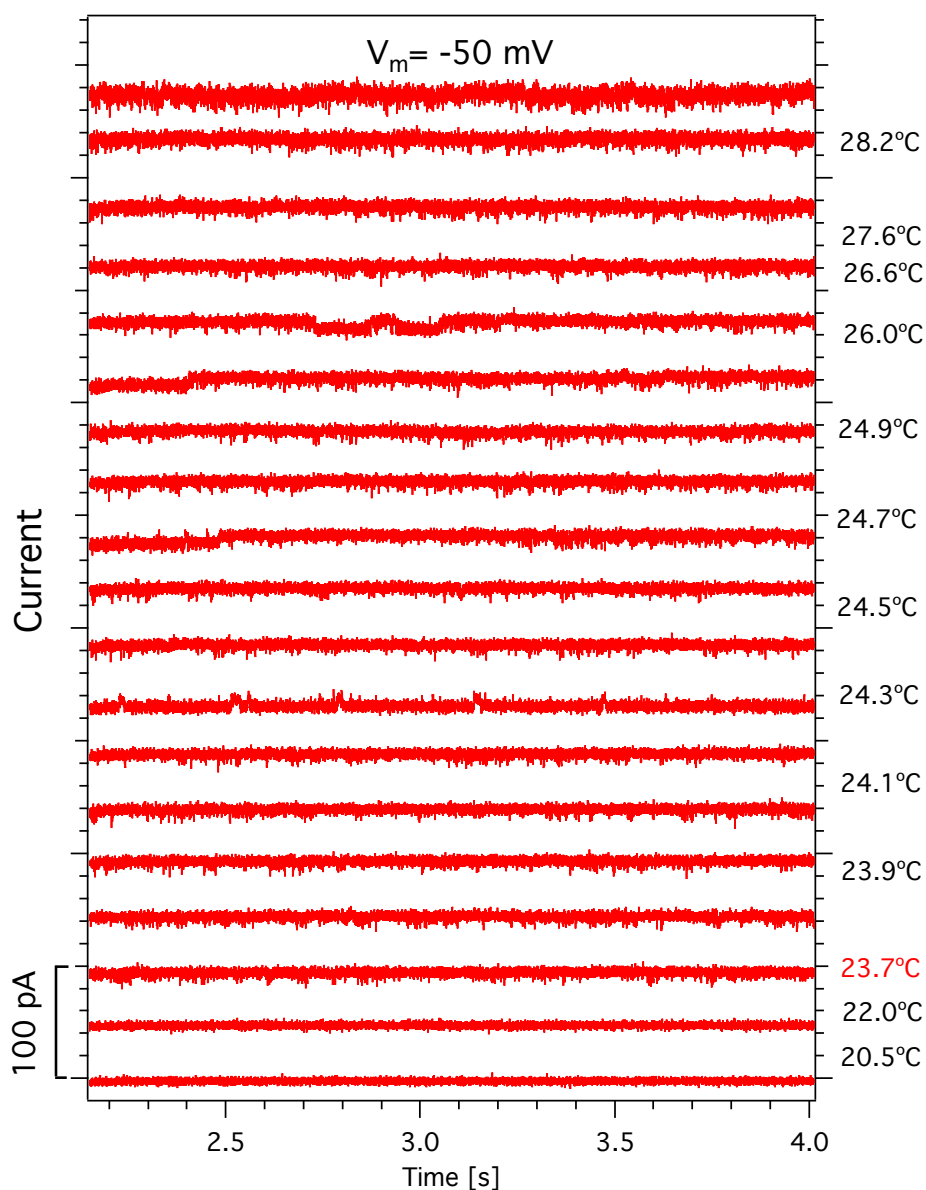


Figure 4.18: Representative current traces for different temperatures with an applied voltage of -50 mV. The lipid sample is pure DMPC in decane. Current traces have been shifted on the current axis. Unless otherwise specified, the temperature difference between subsequent traces is 0.1°C .

Current activity in the form of current fluctuations and short channel-like events were continuously observed also at temperatures above the transition. Apart from the channel-like activity, the bilayer showed a pronounced increase in the conductance during the recordings, due both to a drift in the

baseline and to quantised jumps of the conductance.

In most of the cases, what at first glance appears as current fluctuations or electrical background noise, resulted to be very fast quantised events. An example is given in fig 4.19, where the same current trace is shown at different time resolutions. What looks like a spike in the left panel, happens to be a well defined stepwise current change with lifetime of about 6 ms and amplitude of approximately 10 pA . Stepwise changes in the current of this kind were attributed to channel events (or, in the pore model terminology, in opening and closing of a lipid pore). The small amplitude of the channel events in the trace resulted in low signal to noise ratio which made it hard to perform a single-channel analysis.

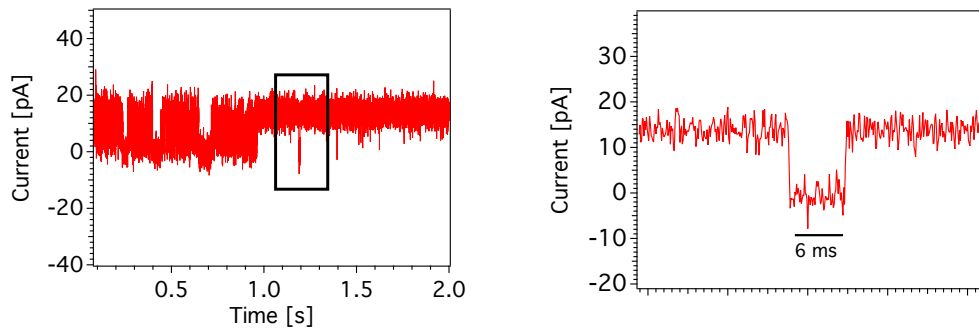


Figure 4.19: The same current trace at different time resolutions. The right figure shows a zoom of the trace in the rectangle on the left.

A noticeable property of the set of recordings shown in figures 4.17 and 4.18 and common to all the experiments performed, is a marked asymmetry in the conductance for positive and negative voltages. This can be observed for three values of temperature inside and outside the transition in fig.4.20, where the histograms of the current are shown. The peaks in the histogram represent the closed and the open states. The mean current of a pore conductance is given by the distance in the peaks of the histogram (fig. 4.20, *centre* and *bottom*). Below the transition temperature the membrane is in a closed state (fig. 4.20, *top*). For higher temperatures, the baseline and the amplitude of the channels conductance increase asymmetrically for positive and negative voltages. Such asymmetry could change magnitude and direction but it was always present. The observation is remarkable since the bilayer is made of pure DMPC and thus is expected to be symmetric. Furthermore, the geometry of the setup is also supposed to be symmetric. In the traces showed here, negative voltages resulted in a lower likelihood of channel events and with lower amplitude.

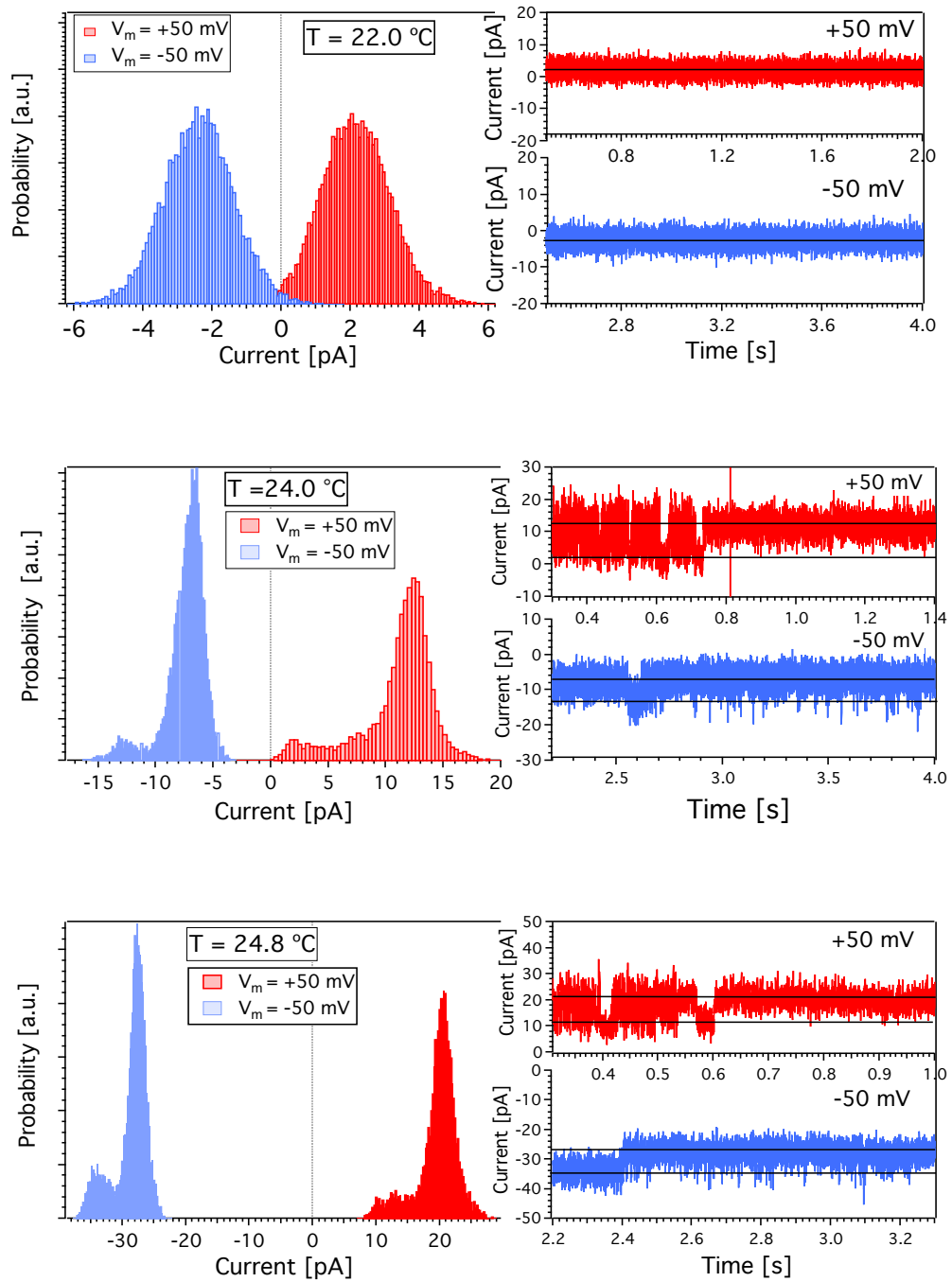


Figure 4.20: *Left panel:* normalised histograms for current traces at 22°C (below the transition, *top*), 24°C (in the transition, *centre*) and 24.8°C (above the transition, *bottom*). *Right panel:* representative sections of the analysed traces. Note the drift and asymmetry of the baseline and of the amplitude of the quantised steps.

Finally, in fig. 4.21, the overall conductance (calculated as the mean current divided by the voltage) is plotted as a function of temperature, showing a jump at the phase transition.

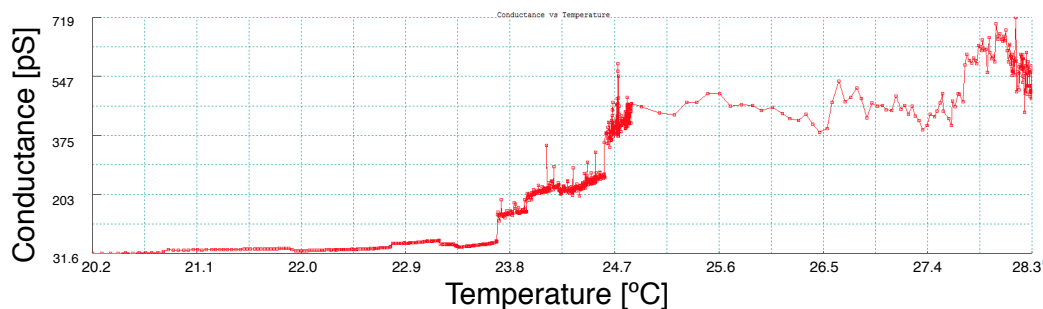


Figure 4.21: Snapshot of the software online analysis, showing the sudden change in the membrane conductance at the melting temperature from about 30 pS to a final value of about 700 pS . No jump back to a low conductance value was observed in the range of temperature explored.

Voltage dependence

In order to further investigate the asymmetric behaviour emerged in the current recordings just showed, the value of current for different voltages, either positive and negative, has been measured to determine the current-voltage relationship of the membrane patch. Like protein channels in biological membranes, lipid ion channels have been showed to be voltage gated [99]. This means that one expects to see an increase in the likelihood and in the amplitude of channel events for increasing holding potentials.

Therefore, lipid membranes made of DMPC:DLPC=10:1 (mol:mol) were investigated at different voltages. Such a measurement requires the temperature to remain constant within the experimental error. This was not always possible. During the experiments often happened that the temperature changed significantly or that the membrane ruptured as a consequence of the applied voltage.

Fig. 4.22 shows representative traces of a continuous recording where the temperature was fixed at $T = 28^\circ\text{C}$, thus above the lipid melting. The range of voltages applied is between -50 mV and $+50\text{ mV}$. Higher voltages resulted in the rupture of the membrane. One can see voltage induced current fluctuations already for a holding potential of 20 mV . Increasing the voltage in the positive direction results in a higher likelihood of well defined quantised steps. The amplitude of the current fluctuations and the current baseline all increase with increasing voltage. For negative voltages the trend is the

same but much less pronounced, showing current fluctuations which could not always be interpreted as channel-like events, lacking the characteristic quantised shape.

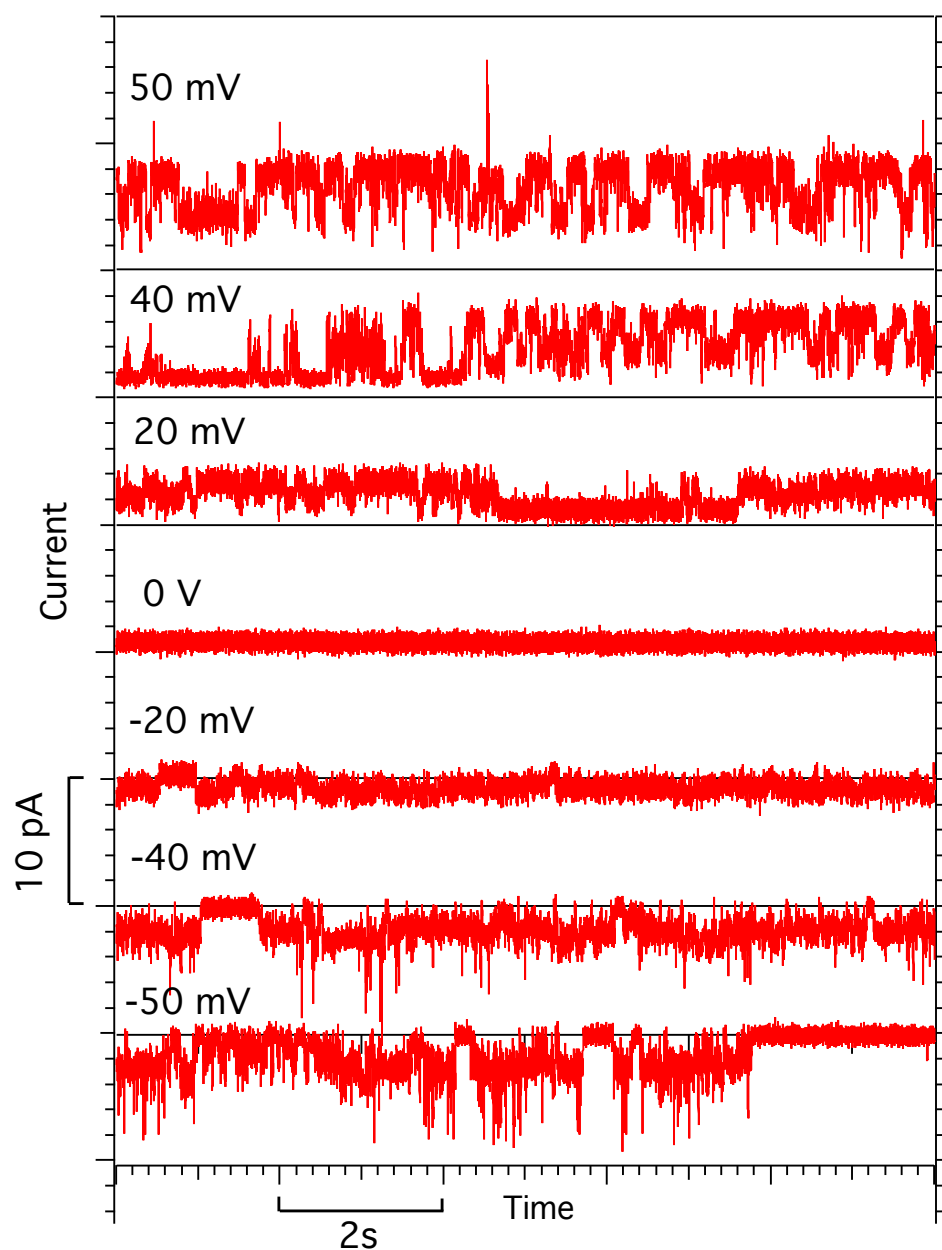


Figure 4.22: Representative current traces of a membrane of DMPC:DLPC=10:1 at $T = 28^\circ\text{C}$ for different voltages. The black lines indicate the zero value of the current for each trace.

According to the pore model and the considerations made in chapter 2 [99], information about the mean conductance and the open likelihood of lipid pores, could be extracted by fitting the current-voltage relationship with to the function:

$$I_m = \gamma_p \cdot P_{open} \cdot (V_m - E_0)$$

where I_m is the current, γ_p is the conductance of a pore, P_{open} is the likelihood of finding an open pore and V_m and E_0 are the applied voltage and the resting potential, respectively. This approach can help to determine the features of the system even when individual channels cannot be visually resolved [99].

To this end, the current-voltage relationship has been determined and it's shown in fig. 4.23. The plot is done by showing the total membrane current as a function of the voltage. This includes the baseline and the spikes due to the capacitive currents when changing the voltage. Unfortunately, the large fluctuations in current and the limited range of voltage investigated limits the information that one can extract from the plot. Furthermore, the asymmetry is less apparent respect to the raw traces of fig. 4.22.

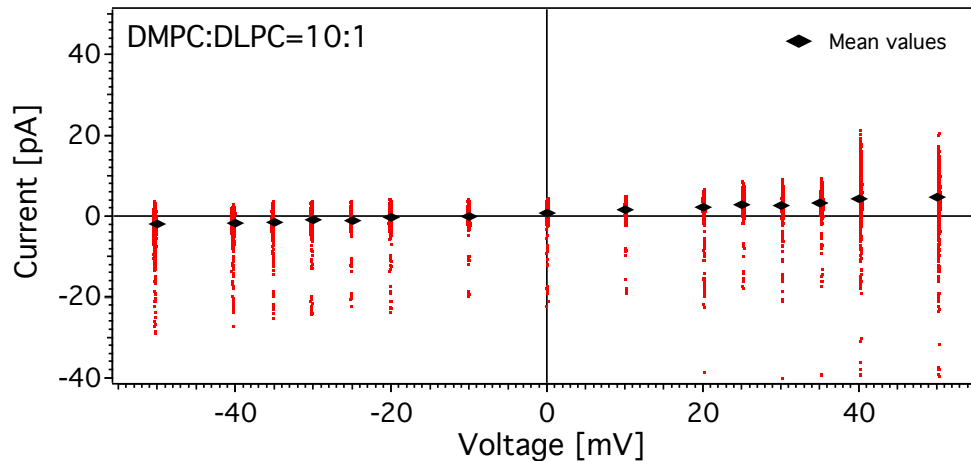


Figure 4.23: Current voltage relationship for the set of data showed in fig. 4.22. The sample is DMPC:DLPC=10:1 (mol:mol) at $T = 28^\circ C$. *Red dots*: current value from the raw data. *Black markers*: average values of the current.

In fig.4.24, the mean values of the current are plotted for each applied voltage. The dotted line is a linear fit which gives a value for the mean membrane conductance of about $1 nS$. One can clearly see an offset potential of $-10 mV$. This is of the same order of the offset potential produced by the flexoelectric polarization that is expected for membranes of diameters of about $100 mV$. However, since an offset cancellation is performed by the

software during every measurement, it is more likely to be caused by a not perfect calibration of the instrument. Anyway, further and more accurate experiments are likely to give a better understanding.

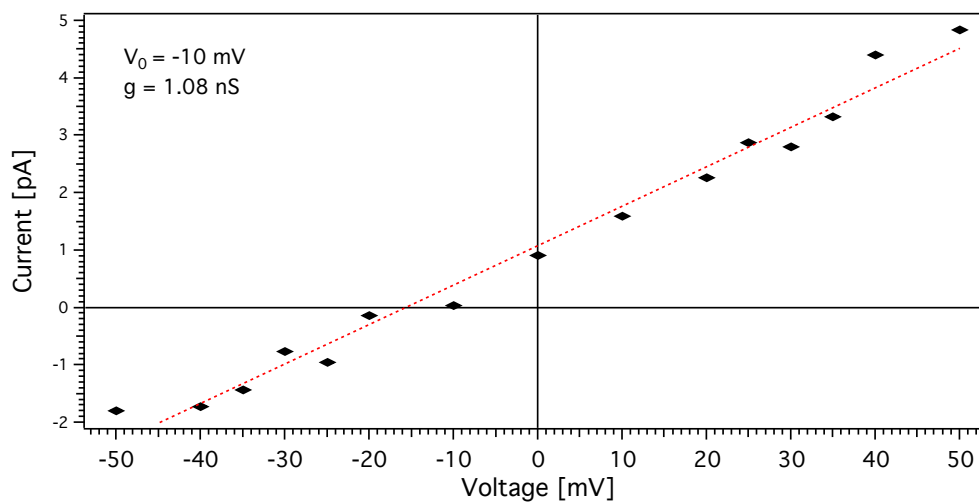


Figure 4.24: Mean values of the current as a function of the applied voltage. The sample is DMPC:DLPC=10:1 (mol:mol) at $T = 28^\circ\text{C}$. *Red line*: fit to a linear function.

4.2.4 Discussion

The preliminary results presented in the previous section show that the Ionovation Bilayer Explorer is an instrument that, in the appropriate conditions, is well suited for permeability investigations on pure lipid membranes. The absence of a temperature control at the time of the experiments severely affected the reproducibility of the measurements and limited the accuracy of the results. Nevertheless, it was possible to catch some common features about the symmetric properties of membranes, that have received little attention up to now, and seem worth of further investigation. This especially in the light of the theoretical predictions about the electro-mechanical properties of membranes at the the phase transition made in the theoretical part of this thesis.

Temperature dependence of the membrane permeability

The main purpose of the current measurements at different temperatures was to reproduce the findings of Antonov [96] and measure the voltage dependence of the melting transition. In the paper, Antonov uses the jump in the membrane current as a way to detect the phase transition of the planar bilayer. Other authors have used the same approach finding strict correlations between the conductance of the membrane and the heat capacity profile at the transition [102].

This was not possible with the membranes investigated in this thesis. In particular, it was not possible to uniquely relate the current fluctuations and the changes in conductance to the narrow temperature range expected for the transition from the calorimetric measurements. Appearance of channel-like events, increase in the current fluctuation (sometimes interpreted as an increase in the background noise) and jump in the conductance are all phenomena that have been commonly observed in the experiments. In a number of cases they happened in the melting regime. However, the same observations were made outside of the transition, and in some cases membranes didn't show any activity at all. In addition, it was very rare to observe for the same membrane an increase in the overall conductance followed by a decrease back to the non conducting state (i.e. without the membrane rupture interrupting the recording), as observed by Wunderlich et al. [102].

It has to be noted that this kind of experiment rely on the presence of external voltages, sometimes of significant magnitude (in [102], the applied voltage is $V_m = 400\text{ mV}$). From the theoretical considerations made in the first part of this thesis, one expects to see changes in the melting behaviour due to an external voltage. Such changes could be a shift in the melting

temperature or a broadening of the transition. The former would explain the absence of activity at the melting temperature determined with the calorimeter (thus, in absence of voltage), or the appearance of channel like events far from the transition. The latter could account for the "long-lasting" activity (where long is referred to the wide temperature range) observed in many membranes. In both cases, one would need to perform experiments in a wider temperature range than the one selected on the basis of calorimetric measurements.

However, if the variables that are known to affect the melting transition of the system are kept constant, one should observe similar behaviours for membranes of the same lipid species (especially in the case of membranes made of one lipid species). This can be done with regard to the voltage or the pH of the aqueous environment, but one variable that can change between different experiments and cannot be controlled is the hydrostatic pressure of the aqueous environment on the lipid bilayer. The formation of a planar bilayer with the Ionovation Bilayer Explorer requires the perfusion of buffer in the microchannels of the bilayer slide. The amount of liquid perfused is controlled by the control unit, thus it should be the same throughout the experiments. However, due to the small volume of the channels, the relative change in the liquid perfused can become significant even for small deviations. A gradient in the hydrostatic pressure can, in principle, produce a curvature in the membrane. Membrane curvature, on the other hand, has been showed to result in an offset potential across the membrane which can change the melting properties of the system. Even though the effect for patches of the size of $100\ \mu\text{m}$ is expected to be small, it is a variable that can change in different experiments. Assuming a radius of curvature of $50\ \mu\text{m}$, the offset voltage according to eq. (4.7) would be of the order $5\ \text{mV}$, thus small respect to the applied voltages. Estimations of the change in the curvature between different experiments and during the same experiment can be done by means of fluorescence microscopy using the Ionovation Bilayer Explorer (see [126] for the principle of the method).

As pointed out in the section about calorimetry results, DMPC has an extremely narrow transition which can be sensitive to scanning rates of the order of $20^\circ\text{C}/\text{hours}$, thus smaller than the heating rate used in the permeability experiments. This can affect the melting properties of the sample investigated. In particular, relaxation times in lipid membranes are known to be larger in the transition, where they reach a maximum value (it can be proven that they are proportional to the heat capacity) [33, 127]. Attention has to be made in order to let the system equilibrate. This was not possible neither with respect to the heating rate, neither for the output voltage, whose time pattern was limited by the heating rate. Therefore, further experiments

with the new temperature control, are likely to give more accurate results.

Finally, during the experiments of this thesis, the potentials of the instrument in terms of microscopy investigations has not fully implemented. This tool would allow to monitor the mechanical (like area or curvature) and the thermodynamical properties (like phase separation) of bilayers, simultaneously to the electric recording. With the optical microscope, it was possible to observe expansion and contraction of the membrane area, which were correlated to change of polarity of the applied voltage. The directionality of the change, indicates that the effect is not linked to electrostriction. Since a change in area of the order of 24% is linked to melting transition of lipid bilayers, further quantitative investigation would help in shedding light on the topic.

Current voltage relationship

As already pointed out, the determination of the current voltage relationship can give important information about the system studied. In particular, it allows the determination of the offset potential which has been predicted in the theoretical part of this thesis.

For the set of data presented here, the fluctuations in current didn't allow such investigation. The current-voltage relationship shown in fig. 4.23, in fact, appears to be linear and symmetric within the fluctuations of the current. This could indicate that the membrane studied was indeed symmetric, and that the geometry of the system results in a very small voltage offset which cannot be esteemed within the sensitivity of the method. However, it could also just indicate that the voltage range investigated is too small to determine the properties of the system. In the experiments of Blicher [99], the applied voltage span more than 100 *mV*, with the nonlinearity of the current clearly appearing for voltages above 50 *mV*.

The same experiments with different lipid mixtures on a Montal-Mueller setup showed symmetric current voltage relationships [98]. Further experiments with different lipid samples could determine whether the symmetry of the system is determined by the geometrical properties of the setup which allow for a more or less pronounced curvature, and thus offset voltages of different magnitude.

Conclusions

Summary

The electrical and mechanical properties of lipid membranes are known to be strongly affected by the melting transition [19, 21]. On the other hand, electro-mechanical coupling in membranes have been widely observed in the past [23, 70].

The theory of flexoelectricity, introduced by Petrov in the 70s to explain the coupling between the membrane curvature and the electric polarization [68], has been here extended to include the thermodynamical properties of the system, with a focus on the melting transition of lipids. The strong increase in the elastic properties of the membrane in the lipid melting, results in an electric polarization that is state dependent and has a peak in the transition. The melting behaviour of the membrane, however, seems to be mainly unaffected by the work done by the electric field to flexo-polarize the membrane.

However, according to the flexoelectric theory, curved membranes display offset transmembrane potentials in the absence of an external voltage, whose magnitude depends on the geometry of the system. The offset potential has been shown to change the voltage dependence of the melting temperature predicted on the basis of electrostrictive effects in [19]. Furthermore, it can in principle be responsible for the asymmetric current-voltage relationship observed in membranes formed at the tip of glass pipettes [99]. It is therefore suggested, that the interpretation of current measurement should take this effect into account.

Asymmetric behaviour in the electrical properties of membranes made of only DMPC (thus assumed to be symmetric) has been observed in the experimental part of the thesis. By using a new instrument for the formation of lipid bilayers, the voltage dependence of the membrane current has been investigated. No marked asymmetry can be detected by the results obtained up to now. Nevertheless further experiments are needed, in the light of the theoretical considerations.

Finally, a simple method for measuring the temperature dependence of the relative permittivity of lipid membranes, is here proposed. It would allow to quantify the change of the relative permittivity with the state of the membrane, that is expected by theoretical considerations. A state dependence of the relative permittivity is shown to affect the magnitude of the electrostrictive effects on the melting behaviour of membranes. Measuring the change of ϵ in the melting transition, would allow to quantify the effect.

Outlook

Measuring the influence of voltage on the phase state of lipid membranes is an essential task that still needs to be done. In this thesis, the approach of Antonov [96] has been followed. It is believed, that with an appropriate temperature control and increasing the temperature range investigated, it should be possible to detect the state of a membrane measuring its conductance. This would allow to measure eventual changes in the phase transition with different applied voltages. Nevertheless other methods can be used to detect the state of a lipid membrane. Significant changes in the capacitive susceptibility have been predicted in the lipid melting [19]. The capacitive susceptibility is defined as the derivative of the charge with respect to the transmembrane voltage. Thus, it can be measured by recording the current response to changes in the voltage. The main problem with capacitance measurements is that the total current measured is a sum of the capacitive and ionic currents. The latter is due to the finite conductance of the membrane. While it's easy to isolate the ionic contribution, the opposite is not so trivial. One can, for example, change the applied voltage at a constant rate. This would result in constant capacitive currents. Dividing the value of the current by the slope of the voltage, would give the value of the capacitance. However, the finite conductance of the membrane results in a slope of the current response, which is not constant anymore. Applying step-wise changes in the voltage, on the other hand, results in a zero capacitive current, and the total current response for a constant voltage, is purely resistive. Therefore combining this two methods, one should be able to distinguish between the two contributions and estimate the capacitance change. In addition, as already mentioned, the relaxation timescale of lipid membranes are proportional to the heat capacity. Thus measuring the relaxation behaviour in electric experiments could give information about the melting properties of the system. This can be done both with respect to the conductance and the capacitance.

The determination of current-voltage relationships has been shown to be a powerful tool to detect the properties of the system. Further experiments

in this regard, can allow for systematic investigations of the symmetry of the system. In particular they can allow the estimation of the offset potential predicted for curved membranes in the context of flexoelectricity. In this regard, combined measurements of the electrical and mechanical properties of lipid membranes, can be done using the microscopy facilities of the Ionovation Bilayer Explorer.

Finally, measuring the temperature dependence of the membrane relative permittivity with the capacitance method here proposed, would allow to test the theoretical predictions here made, resulting in a better understanding on the dielectric properties of lipid membranes at their phase transition.

Acknowledgments

First of all I would like to thank my supervisor, Thomas Heimburg, for the encouraging support and motivation and for his inspiring way of doing science. Furthermore, I would like to thank him for giving me the chance to listen directly to some of the most notable characters in the biomembrane field, like Helfrich and Evans and to meet prominent scientists like Kuni Iwasa and William Brownell.

A special thank goes to Lars D. Mosgaard, for the inspiring debates on flexoelectricity, for proofreading the thesis and for his incredible helpfulness in every kind of issue.

I would like to thank all the former and present members of the Membrane Biophysics Group at the Niels Bohr Institute: especially Alfredo Gonzalez Perez for the critical proofreading of the thesis and for giving suggestions and advice throughout the experiments, Søren B. Madsen and Katrine Laub for introducing me to the calorimetry and to the droplet method, respectively, and Stanislav Landa for sharing joys and sorrows of the lab life (and for the translations from russian).

The efficiency of the Rockefeller workshop of the Niels Bohr Institute, especially Dennis W. Wistisen, in building the capacitor for the relative permittivity measurements has been very much appreciated. The technical assistance of Roland Hemmler and Niklas Brending with the Ionovation Bilayer Explorer has also been very much appreciated.

I would then like to thank the electrical workshop for the assistance in any electrical related issue and Inger Jensen and Bjarne Bønsøe for being always extremely helpful with any technical issue. I would like also to thank Lisbeth Dilling and Kader Rahman Ahmad of the Niels Bohr Institute Library, for the efficiency with which they fulfill every kind of request and for letting me improve my danish.

A special thank goes to all the members of the Biocomplexity group, especially to Ilaria e Lars, for the "lab meetings" and for the great working environment throughout this year and to the C-room, especially for letting me use my desk as a branch of my house. Thank to Rune for his help with

the images and the nice talks and Pia for the danish translations. I would like to thank Pitt for the stimulating debates on every physical topic and for infinite help in every kind of problems during my master.

A *huge* thank goes to all the incredible people I met in Copenhagen, in particular to the italian community: Virginia, Marco, Lollo, Bello, Raffa, Sara for letting me have a beer every once in a while and for their incredible generosity. Marco and Virginia for adopting me and providing me a house twice. In general, I would like to thank them all for making me feel at home every single day.

To H. for being part of my life. And to all my friends for cheering me up despite the distance.

Last, but definetely not least, I would like to thank my family, for being the anchor in my life and for giving me endless trust and support in every possible way throughout all my choices.

Bibliography

- [1] T. Hianik. Structure and physical properties of biomembranes and model membranes. *Acta Physica Slovaca*, 56:678–806, 2006.
- [2] S. H. Wright. Generation of resting membrane potential. *Advances in Physiology Education*, 28:139–142, 2004.
- [3] A.V. Babakov, L.N. Ermishkin, and E.A. Liberman. Influence of electric field on the capacity of phospholipid membranes. *Nature*, 210(5039):953–955, 1966. cited By (since 1996)13.
- [4] Thomas Heimburg. *Thermal biophysics of membranes*. Wiley-VCH, first edition, 2007.
- [5] J. F. Danielli and H. Davson. A contribution to the theory of permeability of thin films. *Journal of cellular and comparative physiology*, 5(4):495–508, 1935.
- [6] S. J. Singer and Garth L. Nicolson. The fluid mosaic model of the structure of cell membranes. *Science*, 175(4023):720–731, 1972.
- [7] E. Gorter and F. Grendel. On bimolecular layers of lipoids on the chromocytes of the blood. *The Journal of Experimental Medicine*, 41(4):439–443, 1925.
- [8] Andreas Blicher. *Electrical aspects of lipid membranes*. PhD thesis, Niels Bohr Institute, Copenhagen University, 2011.
- [9] T. Heimburg. Lipid ion channels. *Biophysical Chemistry*, 150(1–3):2 – 22, 2010. <ce:title>Special Issue: Membrane Interacting Peptides - Towards the Understanding of Biological Membranes</ce:title>.
- [10] O.G. Mouritsen and M. Bloom. Mattress model of lipid-protein interactions in membranes. *Biophysical Journal*, 46(2):141 – 153, 1984.

- [11] T. L. Sourkes. The discovery of lecithin, the first phospholipid. *Bull. Hist. Chem.*, 29(1), 2004.
- [12] Avanti polar lipids. www.avantilipids.com.
- [13] HGL Coster. The physics of cell membranes. *JOURNAL OF BIOLOGICAL PHYSICS*, 29(4):363–399, 2003.
- [14] Vittorio Luzzati and P. A. Spegel. Polymorphism of lipids. *Nature*, 215:701–704, 1967.
- [15] P.R. Cullis and B. De Kruijff. Lipid polymorphism and the functional roles of lipids in biological membranes. *Biochimica et Biophysica Acta (BBA) - Reviews on Biomembranes*, 559(4):399 – 420, 1979.
- [16] John F. Nagle and Stephanie Tristram-Nagle. Structure of lipid bilayers. *Biochimica et Biophysica Acta (BBA) - Reviews on Biomembranes*, 1469(3):159 – 195, 2000.
- [17] A. L. Hodgkin and A. F. Huxley. A quantitative description of membrane current and its application to conduction and excitation in nerve. *Journal of physiology-London*, 117(4):500–544, 1952.
- [18] F. A. Dodge and B. Frankenhaeuser. Membrane currents in isolated frog nerve fibre under voltage clamp conditions. *Journal of Physiology*, 143, 1958.
- [19] Thomas Heimburg. The capacitance and electromechanical coupling of lipid membranes close to transitions: The effect of electrostriction. *Biophysical Journal*, 103(5):918 – 929, 2012.
- [20] Thomas Heimburg and Andrew D. Jackson. On soliton propagation in biomembranes and nerves. *Proceedings of the National Academy of Sciences of the United States of America*, 102(28), 2005.
- [21] Thomas Heimburg. Mechanical aspects of membrane thermodynamics. estimation of the mechanical properties of lipid membranes close to the chain melting transition from calorimetry. *Biochimica et Biophysica Acta (BBA) - Biomembranes*, 1415(1):147 – 162, 1998.
- [22] M F Schneider and W K Chandler. Effects of membrane potential on the capacitance of skeletal muscle fibers. *The Journal of General Physiology*, 67(2):125–163, 1976.

- [23] Alfred L. Ochs and Robert M. Burton. Electrical response to vibration of a lipid bilayer membrane. *Biophysical Journal*, 14(6):473 – 489, 1974.
- [24] Alan H. Wilson. *Thermodynamics and statistical mechanics*. Cambridge University Press, New York, 1960.
- [25] A. G. Marr and J. L. Ingraham. Effect of temperature on composition of fatty acids in escherichia coli. *Journal of Bacteriology*, 84(6):1260–1267, 1962.
- [26] E. F. DeLong and A. A. Yayanos. Adaptation of the membrane lipids of a deep-sea bacterium to changes in hydrostatic pressure. *Science*, 228(4703):1101–1103, 1985.
- [27] Jeffrey R. Hazel and E. Eugene Williams. The role of alterations in membrane lipid composition in enabling physiological adaptation of organisms to their physical environment. *Progress in Lipid Research*, 29(3):167 – 227, 1990.
- [28] M.J. Janiak, D.M. Small, and G.G. Shipley. Temperature and compositional dependence of the structure of hydrated dimyristoyl lecithin. *Journal of Biological Chemistry*, 254(13):6068–6078, 1979. cited By (since 1996)227.
- [29] J.F. Nagle, R. Zhang, S. Tristram-Nagle, W. Sun, H.I. Petrache, and R.M. Suter. X-ray structure determination of fully hydrated l alpha phase dipalmitoylphosphatidylcholine bilayers. *Biophysical Journal*, 70(3):1419 – 1431, 1996.
- [30] W.J. Sun, S. Tristram-Nagle, R.M. Suter, and J.F. Nagle. Structure of gel phase saturated lecithin bilayers: temperature and chain length dependence. *Biophysical Journal*, 71(2):885 – 891, 1996.
- [31] Thomas Heimburg. A model for the lipid pretransition: Coupling of ripple formation with the chain-melting transition. *Biophysical Journal*, 78(3):1154 – 1165, 2000.
- [32] John F Nagle. Theory of the main lipid bilayer phase transition. *Annual Review of Physical Chemistry*, 31:157–195, 1980.
- [33] Heiko M. Seeger, Marie L. Gudmundsson, and Thomas Heimburg. How anesthetics, neurotransmitters, and antibiotics influence the relaxation processes in lipid membranes. *The Journal of Physical Chemistry B*, 111(49):13858–13866, 2007.

- [34] F.H. Anthony, R.L. Biltonen, and E. Freire. Modification of a vibrating-tube density meter for precise temperature scanning. *Analytical Biochemistry*, 116(1):161 – 167, 1981.
- [35] Holger Ebel, Peter Grabitz, and Thomas Heimburg. Enthalpy and volume changes in lipid membranes. i. the proportionality of heat and volume changes in the lipid melting transition and its implication for the elastic constants. *The Journal of Physical Chemistry B*, 105(30):7353–7360, 2001.
- [36] R. Benz, O. Fröhlich, P. Läger, and M. Montal. Electrical capacity of black lipid films and of lipid bilayers made from monolayers. *Biochimica et Biophysica Acta (BBA) - Biomembranes*, 394(3):323 – 334, 1975.
- [37] RH Adrian, W Almers, and WK Chandler. Membrane capacity measurements on frog skeletal muscle in media of low ion content. with an appendix. *The Journal of physiology*, 237(3):573–605, 1974.
- [38] F.J. Blatt. Gating currents: the role of nonlinear capacitance currents of electrostrictive origin. *Biophysical Journal*, 18(1):43 – 52, 1977.
- [39] S. Duane and C. L.-H. Huang. A quantitative description of the voltage-dependent capacitance in frog skeletal muscle in terms of equilibrium statistical mechanics. *Proceedings of the Royal Society of London. Series B, Biological Sciences*, 215(1198):75–94, 1982.
- [40] Shiro Takashima. Passive electrical properties and voltage dependent membrane capacitance of single skeletal muscle fibers. *Pflügers Archiv*, 403(2):197–204, 1985.
- [41] Gordan Kilic and Manfred Lindau. Voltage-dependent membrane capacitance in rat pituitary nerve terminals due to gating currents. *Biophysical Journal*, 80(3):1220–1229, 3 2001.
- [42] D. Rosen and A.M. Sutton. The effects of a direct current potential bias on the electrical properties of bimolecular lipid membranes. *Biochimica et Biophysica Acta (BBA) - Biomembranes*, 163(2):226 – 233, 1968.
- [43] Darold Wobschall. Voltage dependence of bilayer membrane capacitance. *Journal of Colloid and Interface Science*, 40(3):417 – 423, 1972.
- [44] Stephen H. White. A study of lipid bilayer membrane stability using precise measurements of specific capacitance. *Biophysical Journal*, 10(12):1127 – 1148, 1970.

- [45] Brenda Farrell, Cythnia Do Shope, and William E. Brownell. Voltage-dependent capacitance of human embryonic kidney cells. *Phys. Rev. E*, 73(4):041930, 2006.
- [46] Stephen H. White and T.E. Thompson. Capacitance, area, and thickness variations in thin lipid films. *Biochimica et Biophysica Acta (BBA) - Biomembranes*, 323(1):7 – 22, 1973.
- [47] J. Requena, D.A. Haydon, and S.B. Hladky. Lenses and the compression of black lipid membranes by an electric field. *Biophysical Journal*, 15(1):77 – 81, 1975.
- [48] D.M. Andrews and D.A. Haydon. Electron microscope studies of lipid bilayer membranes. *Journal of Molecular Biology*, 32(1):149 – 150, 1968.
- [49] F.A. Henn and T.E. Thompson. Properties of lipid bilayer membranes separating two aqueous phases: Composition studies. *Journal of Molecular Biology*, 31(2):227 – 235, 1968.
- [50] K. Yoshikawa, T. Fujimoto, T. Shimooka, H. Terada, N. Kumazawa, and T. Ishii. Electrical oscillation and fluctuation in phospholipid membranes: Phospholipids can form a channel without protein. *Biophysical Chemistry*, 29(3):293 – 299, 1988.
- [51] Stephen H. White. Analysis of the torus surrounding planar lipid bilayer membranes. *Biophysical Journal*, 12(4):432 – 445, 1972.
- [52] O. Alvarez and R. Latorre. Voltage-dependent capacitance in lipid bilayers made from monolayers. *Biophysical Journal*, 21(1):1 – 17, 1978.
- [53] K.H. Iwasa. Effect of stress on the membrane capacitance of the auditory outer hair cell. *Biophysical Journal*, 65(1):492 – 498, 1993.
- [54] K.H. Iwasa. A two-state piezoelectric model for outer hair cell motility. *Biophysical Journal*, 81(5):2495 – 2506, 2001.
- [55] Chisako Izumi, Jonathan E. Bird, and Kuni H. Iwasa. Membrane thickness sensitivity of prestin orthologs: The evolution of a piezoelectric protein. *Biophysical Journal*, 100(11):2614 – 2622, 2011.
- [56] R.D. Rabbitt, H.E. Ayliffe, D. Christensen, K. Pamarthy, C. Durney, S. Clifford, and W.E. Brownell. Evidence of piezoelectric resonance in isolated outer hair cells. *Biophysical Journal*, 88(3):2257 – 2265, 2005.

- [57] F. Sachs, W.E. Brownell, and A.G. Petrov. Membrane electromechanics in biology, with a focus on hearing. *MRS Bulletin*, 34(9):665–670, 2009. cited By (since 1996)10.
- [58] William E. Brownell, Feng Qian, and Bahman Anvari. Cell membrane tethers generate mechanical force in response to electrical stimulation. *Biophysical Journal*, 99(3):845 – 852, 2010.
- [59] S. H. White. Thickness changes in lipid bilayer membranes. *Biochimica et Biophysica Acta*, 196(2):354–357, 1970.
- [60] S. H. White. Phase transition in planar bilayer membranes. *Biophysical Journal*, 15(2):95–117, 1975.
- [61] I.A. Bagaveyev, V. V. Petrov, V. S. Zubarev, V. F. Antonov, and P. M Nedozorov. Effect of the phasic transition on the electrical capacitance of flat lipid membranes. *Biofizika*, 26(3):472–474, 1982.
- [62] Wolf Carius. Voltage dependence of bilayer membrane capacitance: Harmonic response to ac excitation with dc bias. *Journal of Colloid and Interface Science*, 57(2):301 – 307, 1976.
- [63] W. Helfrich. Effect of electric fields on the temperature of phase transitions of liquid crystals. *Phys. Rev. Lett.*, 24(5):201–203, 1970.
- [64] A. Jakli, J. Harden, C. Notz, and C. Bailey. Piezoelectricity of phospholipids: a possible mechanism for mechanoreception and magnetoreception in biology. *Liquid Crystals*, 35(4):395–400, 2008.
- [65] David J. Griffiths. *Introduction to Electrodynamics*. Pearson Benjamin Cummings, third edition, 1999.
- [66] E. T. Jaynes. Nonlinear dielectric materials. *Proceedings of the IRE*, 43(12):1733–1737, 1955.
- [67] Robert B. Meyer. Piezoelectric effects in liquid crystals. *Phys. Rev. Lett.*, 22:918–921, May 1969.
- [68] AlexanderG. Petrov. Flexoelectric model for active transport. In JuliaG. Vassileva-Popova, editor, *Physical and Chemical Bases of Biological Information Transfer*, pages 111–125. Springer US, 1975.
- [69] F. C. Frank. I. liquid crystals. on the theory of liquid crystals. *Discuss. Faraday Soc.*, 25:19–28, 1958.

- [70] Alexander G. Petrov. Electricity and mechanics of biomembrane systems: Flexoelectricity in living membranes. *Analytica Chimica Acta*, 568(1-2):70 – 83, 2006. <ce:title>Molecular Electronics and Analytical Chemistry</ce:title>.
- [71] P. G. De Gennes and J. Prost. *The physics of liquid crystals*. Oxford Science Publications, 1974.
- [72] Alexander G Petrov. *The Lyotropic State of Matter: Molecular Physics and Living Matter Physics*. CRC PressI Llc, 1999.
- [73] H. Strey, M. Peterson, and E. Sackmann. Measurement of erythrocyte membrane elasticity by flicker eigenmode decomposition. *Biophysical Journal*, 69(2):478 – 488, 1995.
- [74] P. Méléard, C. Gerbeaud, T. Pott, L. Fernandez-Puente, I. Bivas, M.D. Mitov, J. Dufourcq, and P. Bothorel. Bending elasticities of model membranes: influences of temperature and sterol content. *Biophysical Journal*, 72(6):2616 – 2629, 1997.
- [75] W. Helfrich. Inherent bounds to the elasticity and flexoelectricity of liquid crystals. *Molecular Crystals and Liquid Crystals*, 26(1-2):1–5, 1974.
- [76] W Helfrich. Elastic properties of lipid bilayers: theory and possible experiments. *Zeitschrift fur Naturforschung. Teil C: Biochemie, Biophysik, Biologie, Virologie*, 28(11), 1973.
- [77] E.A. Evans. Bending resistance and chemically induced moments in membrane bilayers. *Biophysical Journal*, 14(12):923 – 931, 1974.
- [78] D. A. Haydon. Functions of the lipid in bilayer ion permeability. *Annals of the New York Academy of Sciences*, 264(1):2–16, 1975.
- [79] A.G. Petrov. Flexoelectricity of lyotropics and biomembranes. *Il Nuovo Cimento D*, 3(1):174–192, 1984.
- [80] Gustav Peinel. Quantum-chemical and empirical calculations on phospholipids: I. the charge distribution of model headgroups of phospholipids obtained by a cndo-apsg procedure. *Chemistry and Physics of Lipids*, 14(3):268 – 273, 1975.
- [81] H. Frischleder. Quantum-chemical and empirical calculations on phospholipids. vii. the conformational behaviour of the phosphatidylcholine

- headgroup in layer systems. *Chemistry and Physics of Lipids*, 27(1):83–92, 1980.
- [82] Alexander G Petrov. Flexoelectricity of model and living membranes. *Biochimica et Biophysica Acta*, 1561(1):1–25, 2002.
- [83] A.G. Petrov and V.S. Sokolov. Curvature-electric effect in black lipid membranes. *European Biophysics Journal*, 13(3):139–155, 1986.
- [84] A. T. Todorov, A. G. Petrov, and J. H. Fendler. First observation of the converse flexoelectric effect in bilayer lipid membranes. *The Journal of Physical Chemistry*, 98(12):3076–3079, 1994.
- [85] Declan A. Doyle, João Morais Cabral, Richard A. Pfuetzner, Anling Kuo, Jacqueline M. Gulbis, Steven L. Cohen, Brian T. Chait, and Roderrick MacKinnon. The structure of the potassium channel: Molecular basis of k^+ conduction and selectivity. *Science*, 280(5360):69–77, 1998.
- [86] E. Neher and B. Sakmann. Single-channel currents recorded from membrane of denervated frog muscle fibres. *Nature*, 250(5554):799–802, 1976.
- [87] O.P. Hamill, A. Marty, E. Neher, B. Sakmann, and F.J. Sigworth. Improved patch-clamp techniques for high-resolution current recording from cells and cell-free membrane patches. *Pflügers Archiv*, 391(2):85–100, 1981.
- [88] D. Papahadjopoulos, K. Jacobson, S. Nir, and I. Isac. Phase transitions in phospholipid vesicles fluorescence polarization and permeability measurements concerning the effect of temperature and cholesterol. *Biochimica et Biophysica Acta (BBA) - Biomembranes*, 311(3):330–348, 1973.
- [89] Masao Yafuso, Stephen J. Kennedy, and Alan R. Freeman. Spontaneous conductance changes, multilevel conductance states and negative differential resistance in oxidized cholesterol black lipid membranes. *The Journal of Membrane Biology*, 17(1):201–212, 1974.
- [90] V. F. Antonov, V. V. Petrov, Molnar A. A., D. A. Predvoditelev, and A. S. Ivanov. The appearance of single-ion channels in unmodified lipid bilayer membranes at the phase transition temperature. *Nature*, 283:585–586, 1980.

- [91] G Boheim, W Hanke, and H Eibl. Lipid phase transition in planar bilayer membrane and its effect on carrier- and pore-mediated ion transport. *Proceedings of the National Academy of Sciences*, 77(6):3403–3407, 1980.
- [92] Konrad Kaufmann and Israel Silman. The induction by protons of ion channels through lipid bilayer membranes. *Biophysical Chemistry*, 18(2):89 – 99, 1983.
- [93] H. Gögelein and H. Koepsell. Channels in planar bilayers made from commercially available lipids. *Pflügers Archiv*, 401(4):433–434, 1984.
- [94] ValerijF. Antonov, AndrejA. Anosov, VladimirP. Norik, and ElenaYu. Smirnova. Soft perforation of planar bilayer lipid membranes of dipalmitoylphosphatidylcholine at the temperature of the phase transition from the liquid crystalline to the gel state. *European Biophysics Journal*, 34(2):155–162, 2005.
- [95] Jill Gallaher, Katarzyna Wodzińska, Thomas Heimburg, and Martin Bier. Ion-channel-like behavior in lipid bilayer membranes at the melting transition. *Phys. Rev. E*, 81(6), 2010.
- [96] V.F. Antonov, E.Yu. Smirnova, and E.V. Shevchenko. Electric field increases the phase transition temperature in the bilayer membrane of phosphatidic acid. *Chemistry and Physics of Lipids*, 52(3–4):251 – 257, 1990.
- [97] K. Jacobson and D. Papahadjopoulos. Phase transitions and phase separations in phospholipid membranes induced by changes in temperature, ph, and concentration of bivalent cations. *Biochemistry*, 14(1):152–161, 1975.
- [98] Katarzyna Wodzinska, Andreas Blicher, and Thomas Heimburg. The thermodynamics of lipid ion channel formation in the absence and presence of anesthetics. blm experiments and simulations. *Soft Matter*, 5:3319–3330, 2009.
- [99] Andreas Blicher and Thomas Heimburg. Voltage-gated lipid ion channels. *ArXiv e-prints*, 2012.
- [100] Ralf W. Glaser, Sergei L. Leikin, Leonid V. Chernomordik, Vasili F. Pastushenko, and Artjom I. Sokirko. Reversible electrical breakdown of lipid bilayers: formation and evolution of pores. *Biochimica et Biophysica Acta (BBA) - Biomembranes*, 940(2):275 – 287, 1988.

- [101] Rainer A. Böckmann, Bert L. de Groot, Sergej Kakorin, Eberhard Neumann, and Helmut Grubmüller. Kinetics, statistics, and energetics of lipid membrane electroporation studied by molecular dynamics simulations. *Biophysical Journal*, 95(4):1837 – 1850, 2008.
- [102] B. Wunderlich, C. Leirer, A.-L. Idzko, U.F. Keyser, A. Wixforth, V.M. Myles, T. Heimburg, and M.F. Schneider. Phase-state dependent current fluctuations in pure lipid membranes. *Biophysical Journal*, 96(11):4592 – 4597, 2009.
- [103] Yoshiaki Kimura and Akira Ikegami. Local dielectric properties around polar region of lipid bilayer membranes. *The Journal of Membrane Biology*, 85(3):225–231, 1985.
- [104] W. Huang and D.G. Levitt. Theoretical calculation of the dielectric constant of a bilayer membrane. *Biophysical Journal*, 17(2):111 – 128, 1977.
- [105] Harry A. Stern and Scott E. Feller. Calculation of the dielectric permittivity profile for a nonuniform system: Application to a lipid bilayer simulation. *Journal of Chemical Physics*, 118(7), 2003.
- [106] István P. Sugár. A theory of the electric field-induced phase transition of phospholipid bilayers. *Biochimica et Biophysica Acta (BBA) - Biomembranes*, 556(1):72 – 85, 1979.
- [107] Debajyoti Bhaumik, Binayak Dutta-Roy, TarunKumar Chaki, and Avijit Lahiri. Electric field dependence of phase transitions in bilayer lipid membranes and possible biological implications. *Bulletin of Mathematical Biology*, 45(1):91–101, 1983.
- [108] R M J Cotterill. Field effects on lipid membrane melting. *Physica Scripta*, 18(3):191, 1978.
- [109] H.P. Duwe and E. Sackmann. Bending elasticity and thermal excitations of lipid bilayer vesicles: Modulation by solutes. *Physica A: Statistical Mechanics and its Applications*, 163(1):410 – 428, 1990.
- [110] R. Dimova, B. Pouligny, and C. Dietrich. Pretransitional effects in dimyristoylphosphatidylcholine vesicle membranes: Optical dynamometry study. *Biophysical Journal*, 79(1):340 – 356, 2000.
- [111] Thomas Heimburg. Monte carlo simulations of lipid bilayers and lipid protein interactions in the light of recent experiments. *Current Opinion in Colloid and Interface Science*, 5(3–4):224 – 231, 2000.

- [112] Hywel Morgan, D. Martin Taylor, and Osvaldo N. Oliveira Jr. Proton transport at the monolayer-water interface. *Biochimica et Biophysica Acta (BBA) - Biomembranes*, 1062(2):149 – 156, 1991.
- [113] H. Trauble and H. Eibl. Electrostatic effects on lipid phase transitions: Membrane structure and ionic environment. *Proceedings of the National Academy of Sciences*, 71(1):214–219, 1976.
- [114] Kerstin Weiß and Jörg Enderlein. Lipid diffusion within black lipid membranes measured with dual-focus fluorescence correlation spectroscopy. *ChemPhysChem*, 13(4):990–1000, 2012.
- [115] V.F. Antonov, E.V. Shevchenko, E.T. Kozhomkulov, A.A. Mol’nar, and E.Yu. Smirnova. Capacitive and ionic currents in {BLM} from phosphatidic acid in Ca^{2+} -induced phase transition. *Biochemical and Biophysical Research Communications*, 133(3):1098 – 1103, 1985.
- [116] W. Hanke, C. Methfessel, U. Wilmsen, and G. Boheim. Ion channel reconstitution into lipid bilayer membranes on glass patch pipettes. *Bioelectrochemistry and Bioenergetics*, 12(3–4):329 – 339, 1984.
- [117] Katrine Rude Laub. Ion channels with and without the presence of proteins. Master’s thesis, Niels Bohr Institute, University of Copenhagen, 2010.
- [118] M. Montal and P. Mueller. Formation of bimolecular membranes from lipid monolayers and a study of their electrical properties. *Proceedings of the National Academy of Sciences*, 69(12):3561–3566, 1972.
- [119] Katarzyna Wodzinska. Pores in lipid membranes and the effect of anaesthetics. Master’s thesis, Niels Bohr Institute, University of Copenhagen, 2008.
- [120] www.ionovation.com.
- [121] Alf Honigmann, Claudius Walter, Frank Erdmann, Christian Eggeling, and Richard Wagner. Characterization of horizontal lipid bilayers as a model system to study lipid phase separation. *Biophysical Journal*, 98(12):2886 – 2894, 2010.
- [122] H. Ti Tien and A. Louise Diana. Bimolecular lipid membranes: A review and a summary of some recent studies. *Chemistry and Physics of Lipids*, 2(1):55 – 101, 1968.

- [123] H. T. Tien and A. Ottova. The bilayer lipid membrane (blm) under electrical fields. *IEEE Transaction on Dielectric and Electrical Insulation*, 10(5):717–727, 2003.
- [124] ValerijF. Antonov, AndrejA. Anosov, VladimirP. Norik, EvgenijaA. Korepanova, and ElenaY. Smirnova. Electrical capacitance of lipid bilayer membranes of hydrogenated egg lecithin at the temperature phase transition. *European Biophysics Journal*, 32(1):55–59, 2003.
- [125] Thomas Heimburg. *Planar lipid bilayers (BLMs) and their applications*, chapter Coupling of chain melting and bilayer structure: domains, rafts, elasticity and fusion., pages 269–293. Elsevier, 2003.
- [126] Emma Werz, Sergei Korneev, Malayko Montilla-Martinez, Richard Wagner, Roland Hemmler, Claudius Walter, Jörg Einfeld, Karsten Gall, and Helmut Rosemeyer. Specific dna duplex formation at an artificial lipid bilayer: towards a new dna biosensor technology. *Chemistry and Biodiversity*, 9(2):272–281, 2012.
- [127] Peter Grabitz, Vesselka P Ivanova, and Thomas Heimburg. Relaxation kinetics of lipid membranes and its relation to the heat capacity. *Biophysical Journal*, 82(1), 2002.
- [128] Carl Johan Friedrich Böttcher. *Theory of electric polarisation*. Elsevier, 1952.